(12)

E.M. 4705

DESIGN AND DEVELOPMENT OF A SEGMENTED MAGNET HOMOPOLAR TORQUE CONVERTER

Semi-Annual Technical Report for
Period Ending May 31, 1975

Submitted to ARPA in July, 1975

Principal Investigator:

C. J. Mole, Mgr.
Superconducting Electric Machinery Systems
Phone (412) 256-3612

Sponsored by:

Advanced Research Projects Agency
ARPA Order No. 2174

This research was supported by the Advanced Research Projects Agency of the Department of Defense under Contract No. DAHC 15-72-C-0229.
Effective date of Contract 10 May 1972.
Contract expiration date 30 August, 1975.
Amount of contract - $2,070,303.

Westinghouse Electric Corporation
Electro-Mechanical Division
P.O. Box 217
Cheswick, PA 15024

The views and conclusions contained in this document are those of the authors and should not be interpreted as necessarily representing the official policies, either expressed or implied, of the Advanced Research Projects Agency or the U. S. Government.

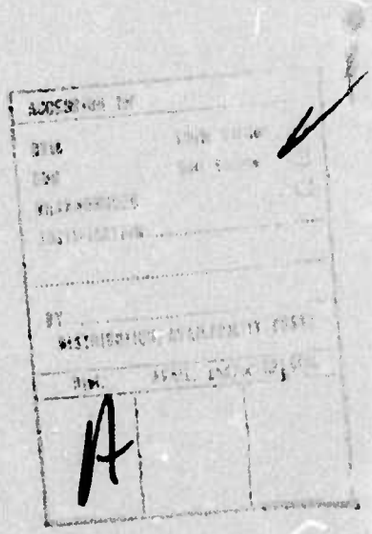

Unclassified

Security Classification

DOCUMENT CONTROL DATA - R & D

(Security classification of title, body of abstract and indexing annotation must be entered when the overall report is classified)

1. ORIGINATING ACTIVITY (Corporate author)
Westinghouse Electric Corporation
Electro-Mechanical Division
Cheswick Avenue, Cheswick, PA 15024

2a. REPORT SECURITY CLASSIFICATION
Unclassified

2b. GROUP

3. REPORT TITLE
DESIGN AND DEVELOPMENT OF A SEGMENTED MAGNET HOMOPOLAR TORQUE CONVERTER

4. DESCRIPTIVE NOTES (Type of report and inclusive dates)
Semi-Annual Technical Report for period ending May 31, 1975

5. AUTHOR(S) (First name, middle initial, last name)
Mole,C.J.; Arcella,F.G.; Berkey,E.; Boes,D.J.; Doshi,V.B.; Feranchak,R.A.; Haller, H.E.III; Johnson,J.L.; Karpathy,S.A.; Keeton,A.R.; Litz,D.C.; Mullan,E.; Reichner,P.; Stillwagon,R.E.; Taylor,O.S.; Tsu,T.C.; Ulke,A.; Wedman,L.N.; Witkowski,R.E.

6. REPORT DATE
July 1975

7a. TOTAL NO. OF PAGES
170 P.

7b. NO. OF REFS
25

8a. CONTRACT OR GRANT NO.
DAHC 15-72-C-0229, ARPA Order-2174

8b. PROJECT NO.

8c.

9a. ORIGINATOR'S REPORT NUMBER(S)
EM-4705

9b. OTHER REPORT NO(S) (Any other numbers that may be assigned this report)

10. DISTRIBUTION STATEMENT
Qualified requesters may obtain copies of this report from Defense Documentation Center, Cameron Station, Alexandria, Virginia 22314

11. SUPPLEMENTARY NOTES

12. SPONSORING MILITARY ACTIVITY
Advanced Research Projects Agency
Department of Defense
1400 Wilson Blvd., Arlington, VA 22209

13. ABSTRACT

This program is for the research and development of a new mechanical power transmission concept: the segmented magnet homopolar torque conve ter. The purpose of this device is to convert unidirectional torque of constant speed (such as from a steam turbine prime mover) into variable speed output torque in either the forward or reverse directions. The concept offers an efficient, lightweight low volume design with potential application over a wide range of speeds and power ratings in the range from hundreds to tens of thousands of horsepower. This machine concept can be applied to commercial and military advanced concept vehicles for both terrain and marine environments.

The program places particular emphasis on the technology of liquid metal current collection systems for the reason this is essential for the success of the homopolar machine concept.

In Phase I the technical problems were reviewed, the machine concepts were studied, and a detailed technical plan was evolved for tne entire program. In Phase II, theoretical, engineering, and experimental tasks were performed to develop a reliable constant speed current collection system which was demonstrated in an actual segmented magnet homopolar generator (SEGMAG). The objectives of Phase III are to extend the technology developed in Phase II for constant speed machines to the case of the torque converter which must operate at variable and reversing speeds.

This report period encompasses a portion of the work performed during Phase III.

DD FORM 1 NOV 65 1473

Unclassified

Security Classification

DN

3903591

14 KEY WORDS	LINK A		LINK B		LINK C	
	ROLE	WT	ROLE	WT	ROLE	WT
alkali metals						
dc motor						
drive						
drive motor						
electric drive						
electric machine						
homopolar						
liquid metals						
motor						
propulsion						
ship propulsion						
torque converter						

TABLE OF CONTENTS

Table of Contents (cont'd)

Table of Contents (cont'd)

REFERENCES

References are listed at the end of each section.

LIST OF FIGURES

List of Figures (cont'd)

LIST OF TABLES

SECTION 1
INTRODUCTION AND SUMMARY

1.0 GENERAL

This is the sixth semi-annual technical report and covers the work performed from December 1, 1974 through May 31, 1975. During this period, Phase III was continued in accordance with the agreed plan.

1.1 BACKGROUND

This program is for the research and development of a Westinghouse-proposed mechanical power transmission concept: the segmented magnet homopolar torque converter (SMHTC). The purpose of this device is to convert unidirectional torque of constant speed (such as from a steam turbine prime mover) into variable speed output torque in either the forward or reverse directions. The concept offers an efficient, light-weight low volume design with potential application over a wide range of speeds and power ratings in the range from hundreds to tens of thousands of horsepower. Initial analysis indicates that this machine concept can be applied to commercial and military advanced concept vehicles for both terrain and marine environments over a wide range of applications with considerable benefit to the U.S. Government, provided the complex current collection, liquid metal technology, and materials problems can be completely solved.

The present contract is part of a proposed three phase program to develop the segmented magnet homopolar torque converter (SMHTC). This program will: a) solve the operational problems relating to current collection systems for segmented magnet machines; b) demonstrate the solution of these problems in a small segmented magnet homopolar machine (SEGMAG); c) utilize the developed technology to design, construct and test a segmented magnet homopolar torque converter (SMHTC).

The program will place particular emphasis on the materials technology of liquid metal current collection systems for the reason that this is essential to the success of the homopolar machine concept for high power density applications.

1.2 OBJECTIVES

1.2.1 Summary of Objectives

In Phase I, completed on January 9, 1973, all of the technical problems were reviewed, the machinery concepts studied, and a detailed technical plan was evolved for Phase II.

Phase II had the primary purpose of providing the necessary theoretical and engineering design work, as well as the supporting experimental tasks, to develop a reliable and efficient current collection system for the successful operation of a segmented magnet (SEGMAG) homopolar generator. Key task areas include: (a) the design, construction, and operation of a SEGMAG generator having sodium-potassium (NaK) current collectors and all necessary support systems for liquid metal handling and purification, cover gas purity maintenance, and shaft seals; and (b) the procurement and testing of a GEC Ltd. homopolar generator with its Gallium-Indium (GaIn) current collector system.

The objectives of Phase III are to extend the technology developed in Phase II for constant speed machines (such as generators) to the case of a torque converter which operates at low speed, zero speed, or reversing conditions, and then to construct and test a demonstration machine.

1.2.2 Summary of Technical Tasks

The technical subtasks for Phase I were described in detail in the first semi-annual technical report (E.M. 4471), and were as follows:

1) Segmented magnet homopolar torque converter (SMHTC) system studies.

2) Application study.

3) Liquid metal current collection systems.

4) Materials study.

5) Segmented magnet homopolar machine design.

6) Seal study.

7) Plan for phase II.

There were five major task areas under Phase II:

(1) Machine Design and Testing

Construct a 3000 HP segmented magnet homopolar machine in order to prove the SEGMAG concept and to provide a test vehicle for the current collectors, seals, and materials which were developed under this program.

Obtain a homopolar generator from the General Electric Co. (GEC) of England in order to obtain operational experience with GaIn as a current collector liquid.

(2) Application Studies

Select the most useful applications for segmented magnet homopolar machines or torque converters.

(3) Current Collection Development

Evolve an effective liquid metal current collection system.

(4) Liquid Metal Support Systems

Develop and fabricate liquid metal and cover gas recirculation systems to protect the liquid metal in the current collectors.

Study the compatibility of all machine materials (insulation, lubricants and structural materials) with the liquid metal current collection fluid.

Conduct a fundamental study of liquid metal technology, including surface wetting, aerosol formation, corrosion reactions, effect of high currents, and chemistry control in liquid metals.

(5) Seal Study

Develop seal systems for unidirectional SEGMAG machines to: (a) confine the liquid metal to the collector zone; and (b) prevent air contamination of the liquid metal and loss of its protective cover gas atmosphere.

To implement the Phase III contructual workscope, the following task areas have been defined:

(1) Machine Design and Testing

SEGMAG demonstration machine development and testing will continue, with the objective of further increasing output power and refining current collector technology.

GEC machine performance will be studied to evaluate GaIn current collection technology.

Torque converter. A conceptual design will be evolved for a prototype torque converter suitable for a military application.

(2) Current Collection Development

The unidirectional SEGMAG current collectors of Phase II will be further refined and extended to higher speed applications. In addition, collectors suitable for reversible and variable speed applications will be developed. The work falls into five categories:

a) SEGMAG Collectors (67 m/s speed), unidirectional constant speed.

b) High Speed Collectors (96 m/s), unidirectional constant speed.

c) Flooded Collectors, for reversing and variable speed, which offer the advantages of design simplicity, and ease of liquid metal containment.

d) Unflooded collectors, for reversing and variable speed, which have the highest efficiency, but difficult containment problems.

e) Hybrid collectors, for reversing and variable speed, which combine the advantages of liquid metal and solid brushes.

(3) Liquid Metal Support Systems

The SEGMAG liquid metal system will be further developed and simplified. Support systems will be developed for use in torque converter and motor applications where reversible and variable speeds are encountered. GaIn technology studies will be pursued with respect to machine requirements.

(4) Seal Study

The seal technology of Phases I and II will be extended to higher speed unidirectional applications. In addition seals for reversible and variable speed applications will be developed, as required for motors and torque converters.

1.3 SUMMARY OF CURRENT PROGRESS

1.3.1 Machine Design and Testing

1.3.1.1 Segmented Magnet Homopolar Generator (SEGMAG)

Based upon analysis of the initial tests of the SEGMAG machine, several minor changes were made in order to increase voltage and current output. The machine was then reassembled and tested with favorable results.

Upon completion of this test series, several additional modifications were made to further improve performance, in preparation for the next series of tests scheduled for the next report period.

The SEGMAG machine is shown in Figs. 2.1.1 and 2.1.2.

1.3.1.2 GEC Machine

No work was scheduled for this report period.

1.3.1.3 Torque Converter

A conceptual design is being prepared for the 8000 HP torque converter of the SEGMAG type.

In addition, a conceptual study of a large (40,000 HP) DISKMAG propulsion motor was performed. However, the inherent low efficiency of this DISKMAG type of machine precludes its use in the applications of interest. Thus, the focus of the conceptual design study will in the future be concentrated on the SEGMAG (drum-type) torque converter configuration.

1.3.2 Application Studies

During this period, effort continued on applying the SEGMAG machine system to tank propulsion. By electrically separating the prime mover and the traction drive, more compact drive systems can be visualized that do not require increasing tank armor weight. Utilizing this principle, an improved performance tank drive system was developed.

1.3.3 Current Collection Development

During this report period, the feasibility of using liquid metal current collectors in homopolar machines of constant high speed (67 m/s) was again demonstrated during retesting of the SEGMAG generator. Improvements in high speed collector performance were found during recent experimental work with the prototypic size test rig. Preliminary analytical evaluations of various types of liquid metal current collectors for torque converter and motor applications were completed, as described below.

1.3.3.1 SEGMAG Collectors

Collector performance during retesting of SEGMAG was essentially the same as in previous runs, with one notable exception. No instability in the annular gap NaK flow was found at 90,000 amperes (as had been previously observed), nor even to a significantly higher level of 110,000 amperes. The theoretical power loss and expulsion pressure expressions for liquid metal current collectors of the SEGMAG type were modified to account for solid-liquid contact resistance. Based on anticipated levels of specific contact resistance, the SEGMAG collector design appears to be near optimum in regard to minimum power loss.

1.3.3.2 High Speed Collectors

Design work and associated drawings which encompass required modifications of the current collector test stand for future tests were completed. Through recent experimentation, plating the solid contact surfaces with nickel imparts very significant beneficial effects to collector performance. The accruing benefits to SEGMAG type machines include improved collector filling capability (collector preheating is no longer required) and lower contact resistance (higher machine efficiency).

1.3.3.3 Flooded Collectors

A study was made to determine if a "flooded gap" motor having a superconducting (SC) excitation magnet may offer an advantage over machines with normal temperature (NT) winding magnets. In the analysis, a 40,000 hp SC machine was compared with a previously designed 8,000 hp NT machine. The SC machine is heavier per unit power output, but does not operate with higher efficiency. Based on this comparison, there does not appear to be an advantage in the use of superconducting magnets in "flooded gap" disk-type homopolar machines.

1.3.3.4 Unflooded Collectors

More than 25 concepts were developed for unflooded reversing current collectors. These were evaluated with the previously defined criteria check list to determine feasibility. Three concepts were selected as feasible and will be further developed. These include a hydrostatically-positioned collector, a collector utilizing hydrostatically-positioned seals, and one utilizing lip-type oil seals. Further study is recommended in the areas of electromagnetic retention and new materials development.

1.3.3.5 Hybrid Collector

Results of a detailed analytical study of the hybrid collector are presented. The hybrid current collector consists of a series of "floating pads" which contain liquid metal and utilize inherently small clearance with the rotor and perimeter labyrinth-buffer gas seals to minimize liquid metal leakage. The study included considerations of supporting liquid metal and gas flow system requirements, pad-rotor hydrostatics, pad geometrical configuration, power losses, and liquid metal expulsion pressures. Analytically, the hybrid collector appears feasible. Areas for concern center around magnitude of hydrostatic liquid metal flow, power losses, and liquid metal leakage. Additional analytical work and an experimental program is required to resolve these concerns.

1.3.4 Liquid Metal Support Systems

Liquid metal support systems performance during the SEGMAG test program was satisfactory. NaK loop, cover gas, material selections, coolant loops, instrumentation, and current collector performance were good.

A method of utilizing a single NaK recirculation and supply loop, for 20 or more current collectors is being analyzed.

The materials compatibility study program of machine materials with NaK and NaK decontamination products has been completed, and optimum material selections noted.

A Ga-In technology review, including property, material compatibility, handling, maintenance, and decontamination and safety practices is being prepared.

1.3.5 Seal Studies

No work was scheduled for this report period.

SECTION 2

MACHINERY

2.1 SEGMENTED MAGNET HOMOPOLAR MACHINE (SEGMAG)

2.1.1 Objectives

The objectives of this program are:

1) To demonstrate the technical and economic feasibility of the Segmented Magnet Homopolar Machine concept, which offers an efficient, lightweight, low volume design with potential applications over a wide range of speeds and power ratings.

2) To provide a test vehicle for evaluation of the current collection systems, containment seals, and liquid metal handling systems developed in previous subassembly testings.

The demonstration SEGMAG unit (rated 3000 HP, 3600 RPM) will subject the current collectors to current densities, leakage flux and other conditions associated with operation in a machine environment. In addition, the unit will provide for long-term testing of current-collectors, their attendant support systems and the machine itself to develop operational data for liquid metal machines.

2.1.2 Prior and Related Work

The SEGMAG concept was developed to provide a high performance DC machine without requiring superconducting magnet excitation. This low reluctance machine, using room temperature excitation, has capability for high output per unit weight and volume. The modular construction allows for higher outputs by using many modules connected in series. The characteristics of this machine have been investigated thoroughly in another U.S. Government Contract (N000 14-72-C-0393).

The demonstration SEGMAG machine design was completed in January 1974. Fabrication of the machine was completed in May 1974. The machine was assembled and installed on the test stand on May 24, 1974. Following connection of the subsystems, machine decontamination and system checkout, the machine technology test program was initiated. The initial portions of the test plan were executed successfully. These tests included slow speed rotor test to insure proper assembly and high speed machine test to develop the vibration signature of the SEGMAG. In addition, the machine friction and windage losses were determined as a function of machine speed.

After disassembly, inspection and minor modifications, the initial series of tests was continued for 140 hours of SEGMAG operation. Short-circuit output of 90,000 amperes and 19 volts oper-circuit was achieved. The testing validated both the SEGMAG machine concept and the liquid metal current collector system.

Following the test run the machine was dissassembled and inspected. Decontamination was rapid and straightforward.

Several modifications were undertaken including:

- Insulation in the collector region to improve NaK containment.
- A strain gauge system on the rotor shaft to improve torque and power measurements.
- Changes in the air gap configuration to improve the machine performance.

2.1.3 Current Progress

After analysis of the data from the initial test series several minor changes were made as follows:

1) The air gap geometry was modified in order to reduce parasitic losses, and

2) The current collectors were silver plated to enhance wetting.

The machine was then assembled and installed on the test stand, and the second test series was initiated in early 1975.

The tests for friction, windage, and NaK viscous loss were repeated for comparison with previous measurements. Series open-circuit and short-circuit tests were then performed with these favorable results:

- Successful operation of SEGMAG and auxiliary machine systems at or near rated design conditions for extended periods. Total running time to date is 215 hours.
- Peak power demonstration of 107,000 amperes and 20.8 volts, corresponding to a rating of 2983 horsepower (versus a program target level of 3000 horsepower).
- Verification that steady state power levels of 90,000 amperes and 20 volts can be maintained, corresponding to a 2413 horsepower rating.

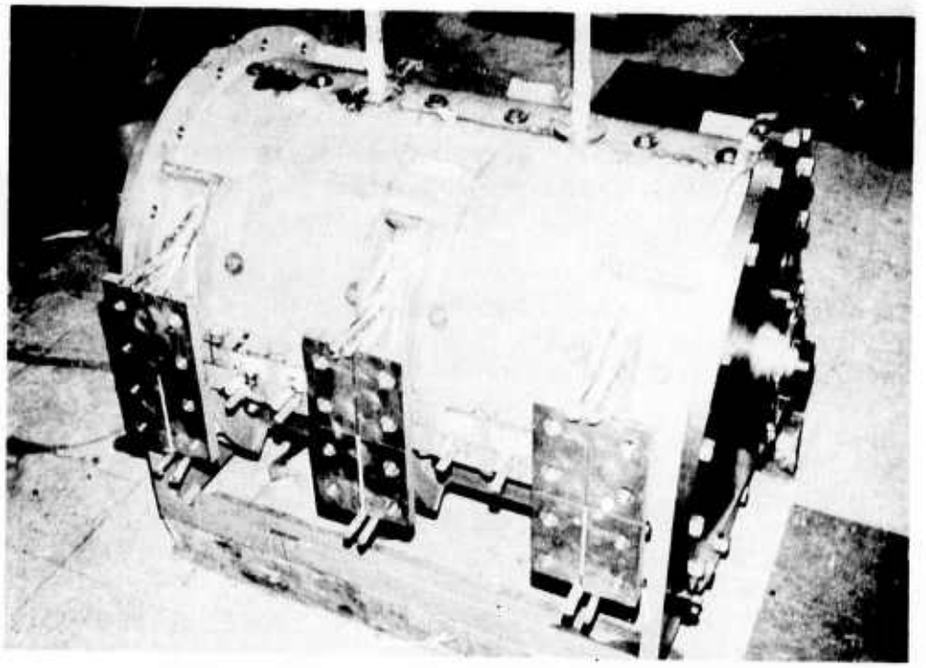

Fig. 2.1.1: SEGMAG Generator - The current collector terminals are shown in the foreground. The leads to the excitation coils are on top.

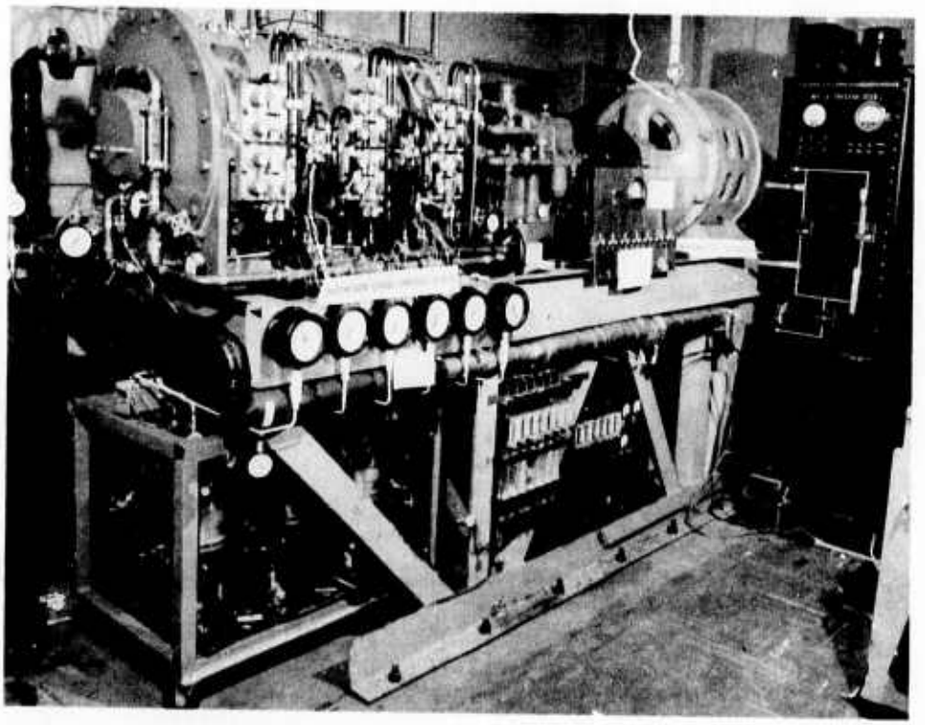

Fig. 2.1.2: SEGMAG Generator on its test stand - The drive system and gas purification system are both on the right. The six NaK purification and supply loops are below. To their right are the gas subsystems for intercollector pressure balancing and shaft sealing.

- Machine efficiency of 92.5%.
- Demonstration that these performance levels are primarily restricted by the capability of the present collector design to confine NaK against the magnetohydrodynamic ejection forces and to operate with low contact resistance.
- Identification of design improvements capable of producing 93,300 amperes at 30 volts (power rating = 3750 horsepower) with 97% efficiency within the volume of the present machine.
- Verification that the technology base developed earlier in the program could be successfully implemented in an operating machine.

2.1.3.1 Detailed Progress Report

The SEGMAG was modified to reduce parasitic losses by increasing the radial gap and by machining circumferential grooves in the stator and rotor active lengths. In addition, the current collector surfaces were silver plated and epoxy insulation was placed on the vertical surfaces of the collector.

Following these minor changes the machine was then re-insulated, baked, assembled, and the performance tests were initiated in January 1975.

Before introducing NaK into the machine viscous and friction losses were determined. Calibrations of instruments to measure shaft torque at operating temperature were completed.

The initial tests followed the previous test programs and consisted of injecting NaK into each collector at zero speed to redefine operating procedures for the NaK supply loops. All NaK supply lines were operated for an extended period following stabilization to insure that all oxides were removed from the lines and the machine internals.

Following successful conclusion of the zero speed NaK supply system tests, the collectors were operated with the rotor rotating to develop filling, operational and withdrawal procedures for the system. These tests were required to insure that the silver plating had not significantly affected the current collector operating characteristics. Each collector was filled, operated and drained individually. The filled collectors were operated at various speeds to the design speed of 3600 rpm to determine the current collector viscous losses as a function of speed. The measured losses, were similar in magnitude to those measured on the current collection test stand. Losses were determined by measuring the power input to the test stand drive motor and subtracting previously measured machine friction and windage losses.

The next series of tests entailed operation of the machine with all current collectors filled. The purpose of this test was to:

- Develop operating procedures for SEGMAG with all collectors filled.
- Develop shutdown procedures from a condition of full speed operation.
- Measure viscous losses of the machine with all collectors functioning.
- Develop operational procedures of the test stand, SEGMAG and all support systems with all collectors filled.

The tests showed that all collectors could be filled and operated successfully at various machine speeds with little or no leakage from the collector area. Collector leakage was measured by collecting NaK that had accumulated in the machine drains located between collectors. Although little or no leakage was measured during extended constant speed runs, some leakage was detected during machine startup and initial current collector filling. As operating procedures were finalized and as personnel became familiar with the operating characteristics of the machine and support system, the collector leakage decreased during transient operation such as filling and withdrawal.

Procedures were developed to fill the collectors with NaK, and to maintain the filled condition with only very minute NaK spillage from the collector area. The most successful technique was to inject NaK at 600 RPM and then increase the speed to 3600 RPM. The collectors were preheated to 85°C prior to filling, in accordance with operational data developed on the current collector test stand. The flow rates used were approximately 250 cc/min. The viscous losses in the collectors were found to be 72 kw for the machine at 3600 RPM. The increased viscous and magnetohydrodynamic losses, compared with earlier test stand experiments were attributed to design differences in the machine environment.

In the open circuit test the three modules were connected in series, with fuses utilized between modules for protection in the event of an accidental internal short circuit. The fuses were never blown, indicating that the insulation which had been applied was adequate to prevent such shorts.

The voltage across each module was monitored, in addition to the full machine voltage.

Two types of short circuit tests were performed. In the first, the center module was shorted and the end modules left open. In the other the end modules were shorted and the center module left open.

The maximum current achieved was 107,000 amperes with a voltage of 20.8 volts.

The collectors performed well during the steady state machine testing at 3600 rpm. During transient operation and at low speed, some NaK

leakage was experienced. A more detailed description of current collector performance during the test will be presented in Section 4.

The mechanical performance of the rotor was excellent over the entire speed range. Vibrations were below 2 mils except at 2700 rpm where a known frame resonance increased them to 5 mils.

Friction and windage losses were measured at various speeds to 3600 rpm where the loss was only about 2 kw.

The cooling system with its associated pre-heaters functioned properly to heat the current collectors above the critical temperature of 75°C prior to filling them with NaK. The collector operating temperatures was 90-100°C at armature currents above 70,000 and 90,000 amperes in the center and end modules respectively, and the collector performance was satisfactory.

The shaft seal performance was excellent during the entire program with no evidence of wear.

The data recorded during the test program was analyzed to determine machine performance.

Table 2.1.1 presents a summary of the losses observed during the open circuit, short circuit, and rotational tests of SEGMAG and compares them with, a) the original design objective, b) the test data obtained during the test program, and c) the capability of the present design with additional modifications.

The losses measured during SEGMAG testing were compared with the design objectives as discussed below:

- Winding Joule Losses. These arise from losses in the armature and excitation winding. The collector temperature required for successful NaK containment (> 75°C) was unexpectedly high, increasing the average winding temperature by about 50°C. This resulted in higher losses of about 10 KW (or 0.56% in machine efficiency) because of the winding temperature coefficient. Higher than expected stray losses, including eddy current and pulsation effects, added an additional 10 KW. The source of these losses is now understood and can be eliminated in future designs.

- Collector Losses. These are a result of viscous drag, magnetohydrodynamic effects, and contact resistance. Their net sum during the test program was about 40 KW higher than expected. The increased viscous and magnetohydrodynamic losses, compared with earlier test stand experiments, amounted to about 19.6 KW (or 1.1% in machine efficiency) and resulted from design differences in the machine environment. Contact resistance loss during the steady state 90,000 ampere test totaled approximately 19 KW, which represents an efficiency penalty of about 1.1%. Previous experimental work

TABLE 2.1.1 - EFFICIENCY TABULATION

Design / Loss, KW	Design Objective 3000HP	Test Run Data 20V, 90,000A 2400HP	Present Design Capability 24V, 93,300A 3000HP
Winding Joule	49.2	70.3	50.3
Collector	32.1	72.4	30.0
Mechanical Friction and Windage	2.6	2.0	2.0
Total, KW	83.9	144.7	82.3
Rating, KW	2240	1800.0	2240.0
Input, KW	2324	1945.0	2322.0
Efficiency, %	96.4%	92.5%	96.5%

during this program indicates that contact resistance losses can be limited to about 6.3 KW under ideal conditions. Additional work is needed to reach these levels in a practical machine. Moreover, known design changes are required to reduce the viscous and magnetohydrodynamic losses to expected levels.

The projected capability of the present SEGMAG machine after incorporating known modifications from the ongoing current collection technology program is given in column 3 of Table 2.1.1. The projected improvements will come mainly from:

- Reduction of current collector operating temperature.
- Elimination of stray losses.
- Reduction of viscous, magnetohydrodynamic, and contact resistance losses.

The test program has identified several areas that require further investigation. These are common to all homopolar machines using liquid metal current collectors. Solutions have been formulated and the necessary experimental investigations are underway:

1) Current Collector Critical Temperature. All of the collectors evaluated in this program show a critical temperature phenomenon directly linked to velocity. Below the critical temperature, the collector is unstable, and it appears that the NaK stream is fragmented in the collector annulus. To overcome this problem, the collectors must at present be preheated to 80-90°C causing the machine cooling system to be derated.

   Potential solutions include:

   - Improved collector configurations to improve NaK stability at low temperatures.
   - Use of direct rotor cooling to control rotor collector temperature and increase the machine current rating.
   - Use of alternate cover gases or reduced pressure to reduce gas entrainment in the NaK.

2) Contact Resistance. Test results have shown that the contact resistance between the collector surface and the NaK represents an electrical loss that can materially affect machine efficiency.

   Potential solutions include:

   - Better understanding of the chemical nature of the interface in NaK current collectors.
   - Reduction of outgassing from constructional materials by alternate materials choices or by application of a sophisticated pre-operation outgassing procedure.
   - Evolution of improved collector surface coatings which do not become adversely absorbed in the NaK.
   - Use of chemical additives in the NaK which do not contaminate the NaK loop system.

3) Machine Current Collector Performance. Distinct differences were noted between the performance of the collectors in SEGMAG and in the test stand - particularly the occurrence of higher viscous losses and random instabilities in the machine which resulted in loss of NaK from the collectors.

   - The continuation of current collection technology development for high speed collectors will provide for more detailed understanding of the collector performance, leading to substantial improvement in NaK containment and reduction of viscous losses.

4) Electrical Insulation. Very small physical defects in the insulation on the conductors and windings, such as pinholes, resulted in shorts and grounds when contaminated with NaK, causing some mal-operation problems.

- Considerable attention must be addressed to this problem in future machines so that some NaK spillage, ejection, or aerosol can be accommodated within the machine because the content of organic insulation must be restricted to limit the potential effect on current collector contact resistance.

Following the completion of this test series, SEGMAG was decontaminated and inspected. Several modifications are underway in preparation for the next series of tests scheduled for mid-1975:

- Parasitic losses. The air gap was redesigned to increase the circumferential reluctance.

- Increased insulation is being provided to prevent pinhole shorts in the machine bore.

- The collector surfaces have been nickel plated to improve wetting of the NaK. Based upon the current collector work described in Section 4, this should eliminate the need to heat the collectors prior to machine operation.

2.2 GEC GENERATOR

2.2.1 Objectives

The General Electric Company, Ltd., of England has developed an experimental homopolar generator which utilizes a GaIn current collection system. This generator employs an electrochemical purification system to maintain the purity of the liquid metal and avoid the "black powder" problems of previous investigators who used this metal. ARPA has approved purchase of this generator for experimental evaluation under the contract. The machine will be used to provide operating and technical experience with GaIn as a current collector liquid and to supplement the main experimental studies which will be conducted with NaK. This experience is expected to be valuable in broadening the scope of the program beyond the alkali metals. The physical design of the machine and its performance will be investigated thoroughly, and the unit may also be employed as a high current dc source in the current collector test program.

2.2.2 Prior and Related Work

Liquid metal current collection systems have a high potential to function efficiently with long, trouble free life in the face of high electrical current loads and high rotational speeds conceived for homopolar machines of the advanced segmented magnet design.

Based on extensive study, NaK-78 was selected as the best liquid metal for current collectors employed in the SEGMAG machine, and GaIn was selected as the alternate choice.

Since GaIn has been identified as the back-up choice to NaK, the ability to work with and study a functioning GaIn unit is expected to be highly instructional in the general sense and also to shorten any subsequent development effort with GaIn.

Based on an extensive search of the market we have concluded that the GEC machine is the best vehicle to provide the GaIn experience needed for this program. No other liquid metal machine in the world, to our knowledge has operated continuously longer than 40 hrs without maintenance. Therefore, this machine, which has operated up to 1000 hours with no problems, represents a unique development.

The GEC generator is a vertical shaft machine utilizing GaIn liquid metal eutectic as the slip ring contactor. The generator is rated at 16,000 amperes, 8 volts when driven at 3400-3600 rpm. Figure 2.2.1 displays schematically the GEC generator vertical shaft concept.

The GaIn purification cell was severely damaged in shipment. A replacement cell was fabricated by Westinghouse using detailed drawings furnished by GEC Company.

The GEC generator test stand was completed in Phase II, and the machine was installed. The test stand is powered by a 50 HP 1750 rpm AC machine, and a drive train provides speeds of 1800 and 3600 rpm.

Installation of the auxiliary equipment was completed, including cover gas, cooling water, and instrumentation. The GEC machine was then successfully tested to verify its performance and to study the GaIn current collector system.

The following are the four basic tests performed on the GEC machine:

1) An open circuit test, to determine no-load voltage and current collection magneto-hydrodynamic losses as a function of field current.

2) A machine short circuit test, to determine the I^2R losses in the machine.

3) A motor test, to measure the vibration levels, magnetohydrodynamic losses, and coastdown time.

4) An endurance test, to confirm the performance capability of the machine and its auxiliaries over a long time period. Liquid metal loss rate, cell performance, argon contamination and seal performance were monitored.

The test results obtained from this program have enabled the machine losses to be segregated into three categories:

- Machine friction and windage losses with GaIn in the collector.
- MHD losses due to leakage flux in the current collector.
- Joule heating losses due to current flow in the machine.

The viscous, friction and windage losses were determined at various speeds and zero excitation by measuring the input power to the coupled drive motor. The difference between this power and the uncoupled drive motor losses at each speed determined the generator losses. The friction and windage losses cannot be separated from the liquid metal viscous losses because gallium indium could not be completely excluded from the collector areas during the test to measure friction and windage losses.

During Phase II, the acceptance tests were successfully performed in England at The General Electric Company, Ltd., and witnessed by Westinghouse personnel. These tests consisted of open circuit, short circuit, generator load, motor and an endurance test. The proper operation and maintenance of the unit were also demonstrated.

Dwg. 6251A96

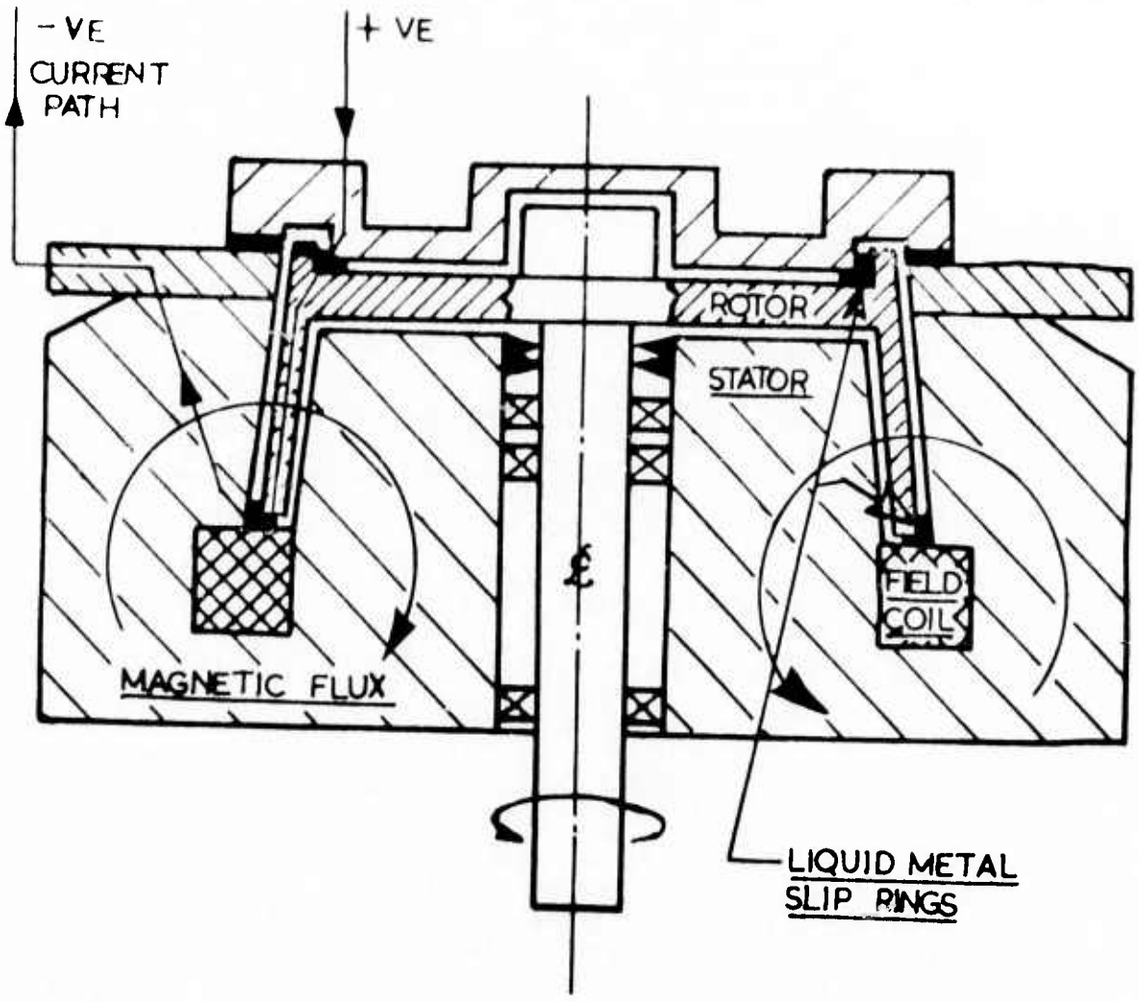

Fig. 2.2.1: GEC vertical shaft homopolar machine schematic

The MHD losses were determined during open circuit tests at various speeds and field currents. The power losses increased with speed due to viscous losses, and with excitation due to the interaction of leakage flux with currents induced in the liquid metal of the collector. These currents induced by the leakage flux resulted in losses that became significant at higher speeds and excitation levels.

The I^2R losses were determined by the short circuit tests. The sum of friction, windage and viscous losses were subtracted from the power losses measured during short circuit to determine joule heating losses in the machine. The MHD losses were neglected because of the low machine flux during short circuit.

The losses measured during the test program at 3600 rpm are:

Viscous, friction, windage	6.2 KW
MHD	1.0 KW
I^2R	7.0 KW
Total losses	14.2 KW

For the 100 KW GEC machine the overall calculated machine efficiency was 85.8%. At lower speeds the efficiency rises to a level approaching 94%.

The GaIn liquid metal was purified by an electrolytic regenerative cell during the entire test. The cell performed well during the entire program with no evidence of GaIn contamination.

2.2.3 Current Progress

No work was scheduled on this program during this period.

2.3 SEGMENTED MAGNET HOMOPOLAR TORQUE CONVERTER (SMHTC)

2.3.1 Objectives

The objective of this program is to investigate the segmented magnet homopolar torque converter (SMHTC), within the framework of some of the more promising applications. This concept will then be demonstrated in a torque converter which will operate at constant input speed (as from a prime mover), and will provide variable output speeds, in both forward and reverse directions, at variable torque up to full power rating.

Our objective in Phase I was to study the various configurations proposed for the SMHTC, and the technical problems involved in developing the prototype machine.

In Phase III a conceptual design is to be evolved for the prototype torque converter.

2.3.2 Prior and Related Work

The SMHTC consists basically of two homopolar machines connected as a generator-motor set. Two basic configurations are being considered: (1) a radial design which uses a generator mounted within a motor; and (2) an axial design which consists of inline generator and motor. At present, the inline configuration is preferred.

Two basic homopolar machine types are being considered: (1) the drum-type (SEGMAG), and (2) the disk-type (DISKMAG).

During Phase I of this contract, electrical analyses of large (30,000 HP) and small (6000 HP) machines were completed.[1] These were of the drum-type (SEGMAG) homopolar machine configuration. Two conceptual designs (radial and axial) were also prepared for the 6000 HP machine, as part of the Phase I effort.

More recent studies (in Phase III) have shown that a rating of 8000 HP, 3600/500 RPM is typical of potential applications to small naval ship drives,[2] and this rating was therefore chosen for the prototype torque converter.

Previously in Phase III, a number of 8000 hp designs for the disk-type "flooded gap" machine (DISKMAG) were investigated.[2] The power losses and internal machine fluid pressures associated with a particular "flooded gap" design were defined. The major areas of concern found for the 8000 HP "flooded gap" design are:

- Complex construction of disks to obtain magnetic circuits with low axial and high circumferential reluctance.

- High machine power losses, attributed mainly to MHD effects in the axial gaps between disks.

- Probability for turbulent rather than laminar flow and high short circuit losses in the liquid along the flat side walls of the machine disks. Reynolds to Hartman number ratios >1000 are calculated for operating conditions down to 30% of rated full load speed. Thus, the assumption of laminar fluid flow employed in the axial gap power loss expression is in doubt except at low speeds.

- A need is recognized for large thrust bearings and high pressure shaft seals to assure a fail safe machine design.

2.3.3 Current Progress

A conceptual design is being prepared for the 8000 HP torque converter of the SEGMAG type. This machine will accept input power from a gas turbine prime mover at 3600 rpm and deliver power to a propeller load at variable speeds to 500 rpm in either forward or reverse directions.

In addition, a conceptual study of a large (40,000 HP) DISKMAG propulsion motor was performed. Electrical design and loss studies were performed to develop optimum configurations for maximum efficiency and power density.

However, the inherent low efficiency of this DISKMAG type of machine precludes its use in the applications of interest. Thus, the focus of the conceptual design study will in the future be concentrated on the SEGMAG (drum-type) torque converter configuration.

2.3.3.1 8000 HP Torque Converter

A parametric study was done to optimize the design of the 8000 HP, 3600/500 RPM torque converter, in terms of low weight and size and high efficiency. Test results from the current collector test stand and the 3000 HP SEGMAG generator were incorporated in the analysis to provide a more realistic assessment of losses than had previously been considered. In particular, provision was made in each design to minimize tooth ripple losses on the rotor and stator surfaces, and to minimize total loss in the collectors, including contact resistance loss.

In a machine of this type, there are a large number of independent variables, and a true optimization was not possible in the time available. To further complicate the situation, the objectives of low

weight and high efficiency are not compatible; i.e., that which tends to decrease weight also decreases efficiency, and vice versa. Therefore, a range of each variable to be considered was defined for both the generator and the motor part of the torque converter. Machines were designed which covered the ranges of variables defined, and appropriate pairings of motors and generators were made to produce torque converters.

The independent variables and their specified ranges were the following:

	Motor	Generator
Rated Current	150,000-400,000 Amps	150,000-500,000 Amps
Current Density	5,000-10,000 Amps/inch^2	5000-10,000 Amps/inch^2
Number of Modules	1-4	1-3
Number of Turns/Module	1-2	1-2
Rotor Diameter	No general specification.	

Because the generator and motor are not constrained to be the same in any of these variables except rated current, the total number of independent variables for a torque converter design is nine.

Current densities in the torque converter conductors of 10,000 amperes per square inch were first considered. However, no designs at this current density were found to have an efficiency greater than about 88%. Therefore, the design current density was reduced to 5000 amperes per square inch.

The weight and losses for typical designs from this study are shown in Table 2.3.1. The weights shown are for the electrical components of the machines, and are not intended to represent the total weight of complete machines; the addition of housings, bearings, shafting, etc. may add 20-50% to the weights shown. In each case, the rotor diameter has already been "optimized", and thus has been removed as an independent variable.

The table shows the difficulty in choosing among the various machines. In some cases the choice is obvious; for example, 2-G is clearly superior to 1-G. However, it is not at all obvious which is superior between 4-M and 5-M.

Various combinations of these SEGMAG motors and generators were combined as torque converters. Table 2.3.2 illustrates a range of typical torque converters resulting from this process. Once again, the choice of an optimum is not obvious. For a particular application, a means could be

TABLE 2.3.1

Weights and Losses of Typical Machines
for an 8000 HP, 3600/500 RPM Torque Converter

Generators

Machine No.	Rated Current-kA	Number Modules	Turns Per Module	Weight, Pounds	Loss, Kilowatts
1-G	150	1	2	3,900	240
2-G	150	2	1	3,800	158
3-G	200	1	1	3,500	147
4-G	200	2	1	3,100	183
5-G	250	1	1	3,000	159
6-G	250	2	1	2,900	207

Motors

1-M	150	1	2	26,700	157
2-M	150	2	2	22,300	209
3-M	150	3	2	21,000	259
4-M	200	2	2	18,000	255
5-M	200	3	1	23,400	172
6-M	250	1	2	17,600	219
7-M	250	2	1	20,600	156
8-M	250	2	2	15,700	312

TABLE 2.3.2

8000 HP, 3600/500 RPM Torque Converter Options

Torque Conv. No.	Rated Current-kA	Generator	Motor	Weight, Pounds	Min. Length, Inches	Motor Dia. Inches	Efficiency
1	150	2-G	1-M	30,500	66	57	94.7%
2	150	2-G	2-M	26,100	82	44	93.9%
3	200	3-G	4-M	21,500	68	41	93.3%
4	200	4-G	4-M	21,100	76	41	92.7%
5	200	4-G	5-M	26,500	75	43	94.1%
6	250	5-G	6-M	20,600	51	49	93.7%
7	250	5-G	7-M	23,600	59	47	94.7%
8	250	5-G	8-M	18,700	88	38	92.1%

determined to relate the benefits of a decrease in size and/or weight to the penalties of a decrease in efficiency. Without having such a relationship in general, objectives were established of an efficiency of about 94%, a weight of about 20,000 pounds, and a size compatible with a space approximately 6 feet long and 4 feet in diameter. Torque converter no. 6 comes closest to meeting these objectives, and thus was chosen for the conceptual design.

2.3.3.2 40,000 hp Disk-Type SC Motor Design (DISKMAG)

An investigation was made to determine if a "flooded gap" motor having a superconducting (SC) excitation magnet may offer any advantages over machines with normal temperature (NT) winding magnets.

The disks of the SC motor were assumed to be of solid copper in order to reduce the complexity of construction as well as reduce electrical resistance. Consequently, without iron in the disks, a greater magnetic induction will appear in the current collector radial gaps. The expected increase in collector radial gap loss due to the larger induction will be compensated to some extent by the reduced ohmic loss in the disks.

The internal fluid pressures and machine power losses were calculated for a disk-type "flooded gap" superconducting 40,000 hp, 180 rpm motor. These characteristics are compared with those of a disk-type "flooded gap" NT design 8,000 hp, 500 rpm motor previously studied.

A number of 40,000 hp disk-type SC "flooded gap" motor designs were considered during the study. The geometrical dimensions and operating conditions for a typical design are listed in Table 2.3.3 and illustrated in Fig. 2.3.1.

A qualitative description of the fluid flow behavior in a "flooded gap" DISKMAG machine was given in the previous Semi-Annual Report, dated Feb. 1975. Governing expressions which permit calculation of the machine seal pressures, rotor bearing thrust forces, and machine power losses, presented in the previous report, were again used during the current period.

For the typical 40,000 hp DISKMAG SC motor under consideration, Table 2.3.4 shows the calculated values of pressure and thrust force which the shaft seals and rotor bearings must withstand under two conditions of liquid metal flow. These pressures and forces are significantly greater than the corresponding ones previously calculated for the 8000 hp NT motor. This difference is attributed mainly to the greater number of disks used in the SC machine, required for the larger power rating.

TABLE 2.3.3

Dimensions and operating conditions for a typical design 40,000 hp disk-type S.C. "flooded gap" (DISKMAG) homopolar motor

A. Operating Conditions

P = machine rated power, 40,000 hp

I = machine full-load current, 100,000A

B_{xi} = axial magnetic induction at inner collector, 1.44T

B_{xo} = axial magnetic induction at outer collector, 1.44T

B_{yi} = radial magnetic induction at inner collector, essentially zero

B_{yo} = radial magnetic induction at outer collector, essentially zero

ω = rotor angular velocity, 18.8 rad/s (180 rpm)

B_x = axial magnetic induction in disks, 1.44T

B. Geometrical Design (rectangular cross-section)

R_s = shaft radius, .206m (8.11 in)

R_i = radius of inner collector, .220m (8.68 in)

R_o = radius of outer collector, .675m (26.6 in)

W_i = width of inner collector, .0140m (.55 in)

W_o = width of outer collector, .0140m (.55 in)

d_i = radial gap of inner collector, 1.27×10^{-3}m (0.05 in)

d_o = radial gap of outer collector, 1.27×10^{-3}m (0.05 in)

N = number of disks, 54

G = axial gap between rotating and stationary disks, 1.40×10^{-3}m (.055 in)

R_5 = outer radius of machine, 0.956m (37.6 in)

L = machine length, 2.14m (84.3 in)

S_p = specific power = 0.63 hp/kg (0.29 hp/lb)

C. Constants and NaK Physical Properties ($\sim$ 100°C)

$f(\delta<1)$ = Fanning friction factor, smooth surface, 0.7×10^{-2}

$f(\delta>1)$ = Fanning friction factor, roughened surface, 1.8×10^{-2}

ρ = mass density, 850 kg/m^3

σ = electrical conductivity, 2.2×10^6 mhos/m

ε_k = specific contact potential (Cu-NaK-Cu), 4.1×10^{-9}Vm^2/A

η = dynamic viscosity, 5.1×10^{-4}N-s/m^2

Dwg. 6252A32

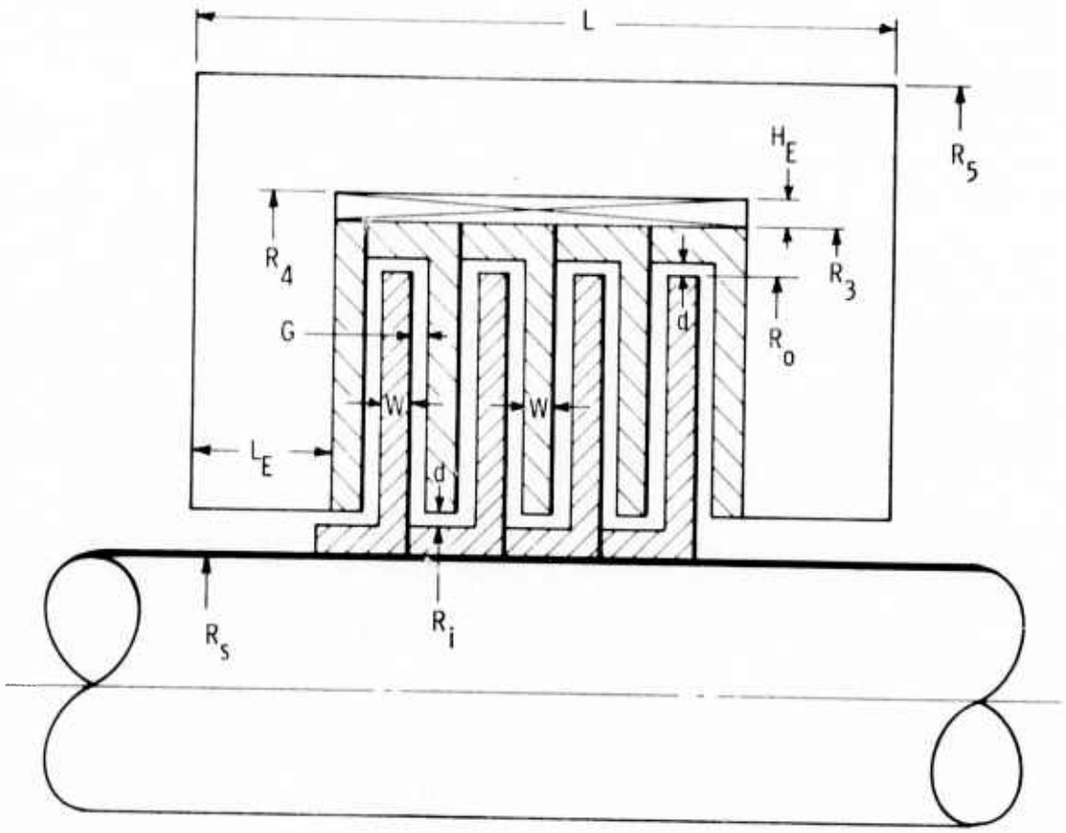

Fig. 2.3.1: Disk-type homopolar machine (DISKMAG)

TABLE 2.3.4

Seal Pressure and Rotor Thrust Forces for a Typical 40,000 hp Disk-type S.C. Motor (DISKMAG)

Condition	Seal Pressure, p_s		Rotor Thrust, F_R	
	N/m^2	(psi)	N	(tons)
No Liquid metal flow through motor	3.32×10^6	*481	2.06×10^6	231.7
Liquid metal circulation by internal centrifugal pressure**	p_i	p_i	6.72×10^5	75.5

*pressure above inlet pressure, p_i

**max. NaK flow rate (assuming no friction), 5.33×10^{-5} m^3/sec (0.845 gal/min)

Table 2.3.5 provides a comparison of calculated power losses for the 40,000 hp SC and 8000 hp NT DISKMAGS. Larger radial gap losses for the SC machine were offset by lower machine losses, but afforded no advantage in reducing the overall loss rating as compared to the NT machine. The corresponding axial gap and collector ohmic losses remained fairly equal (in percent) for both designs considered. The net percentage of all power losses was identical (4.8%) for both designs.

Operating efficiency is generally a function of machine weight, (i.e., higher efficiency can generally be attained by making the machine heavier). The calculated specific power for the 40,000 hp SC design is 0.63 hp/kg compared to 0.69 hp/kg for the 8000 hp NT design. Since it is heavier per unit power output than the 8000 hp NT motor, but does not operate with higher efficiency, there does not appear to be an advantage in the use of a superconducting excitation magnet for "flooded-gap" disk-type homopolar machines.

TABLE 2.3.5

Calculated Power Losses for the 40,000 hp SC and 8000 hp NT DISKMAGS

Power Loss Mode	*40,000 HP Power Loss		**8000 HP Power Loss
	kw	%	%
Radial Gap (P_{rg})	424	30	6
Axial Gap (P_{ag})	597	42	42
Ohmic (P_o)	173	12	11
Machine (conductor + excitation)	237	16	41
Total	1431	100	100
% of Machine Rating	4.8	4.8	4.8

*Superconducting (SC) excitation coil.

**Normal temperature (NT) winding excitation coil.

2.4 REFERENCES

1. C. J. Mole, et. al., "Design and Development of a Segmented Magnet Homopolar Torque Converter," Semi-Annual Technical Report for May 31, 1973, June, 1973, E.M. 4518.

2. C. J. Mole, et. al., "Design and Development of a Segmented Magnet Homopolar Torque Converter," Semi-Annual Technical Report for Nov. 30, 1974, Feb. 1975, E.M. 4648.

SECTION 3
APPLICATION STUDY

3.0 OBJECTIVES

Review and select promising applications for the segmented magnet homopolar machines and torque converters.

Several of the applications resulting from the Phase II application studies will be reviewed in conjunction with ARPA, and the most useful application will be selected.

3.1 PRIOR AND RELATED WORK

Previous Technical Reports discussed a number of applications which are potentially feasible. All of them were contingent upon proper solution of the current collection problem. The problem of using liquid metal to transmit simultaneously large quantities of electrical current and heat from the rotating armature must be solved in a reliable and safe fasnion to realize these applications. In addition many applications require the collection of current at low speed and in both directions of rotation. Considerable progress on the hydraulic and dynamic aspects of the current collecting system has been made during Phase II of this study. The potential success of this current collection system provided encouragement to address the applications study. Prior studies revealed the advantages and disadvantages of segmented magnet homopolar machines in general and torque converters in particular.

3.1.1 Tank Propulsion System

Since one of the advantages of the SEGMAG machine is smaller size for a given capacity, an electric propulsion drive for a military tank was investigated. Electric drives for tanks have another advantage in that they provide a readily controlled independent tractive effort to each track over the entire speed range. The present system uses a hydraulic coupling and a gear unit which has the disadvantages of a fixed number of gear ratios and space constraints due to the mechanically interconnected components. The electric drive, on the other hand, permits smooth control of torque over the entire speed range. Historically, however, electric drives tended to be larger than mechanical drives due primarily to the required motor torque capacity at low speed.

An investigation into utilizing SEGMAG machines for the XM-1 tank was analyzed.

Tractive effort (TE) basically sets the torque and volume of the drive motors. The maximum TE is specified normally as equal to the vehicle weight. The continuous TE or the point for which the transmission cooling system is rated occurs at a coefficient of friction .5 or 50% of the vehicle weight.

For a 60 Ton tank, the maximum TE is 120,000 lbs and the continuous rating is 60,000 lbs. Above 60,000 lbs the duration of the operation is a function of the thermal time constants of the transmission. On hard surface, the continuous rating point corresponds to operation on about a 50% slope. This, of course, is not a condition that exists for long periods in practice. However, extended periods of operation in clay or mud are encountered which require 1000 lbs of TE per ton of vehicle weight - the same loading condition.

The power of the present generation of tanks is selected on the basis of acceleration capability. This is in contrast to earlier criteria when the measure of performance was speed capability on steep grades. Acceleration is the area of greatest concern. Although present day tanks have maximum TE capabilities of 2000 lbs/ton, during an acceleration from zero speed the torque transferred to the drive sprockets does not exceed about 500 lbs per ton. The accelerating tractive effort is reduced by the ability to accelerate the engine under load and again by the energy required to accelerate the rotating parts of the drive.

Therefore, the WK^2 of an electric transmission is a critical area. The generator WK^2 must be considered at the engine shaft and the motor WK^2 must be viewed at the drive sprocket through the output gear. The other parameter affecting acceleration is the load placed on the engine by the transmission at the time the engine is attempting to accelerate.

The XM-1 is a 58 Ton tank which is basically the M-60 with improved performance. The top design speed is 45 mph which could only be used comfortably on hard surfaces.

Continental is providing a 1500 hp diesel engine which drives through a mechanical-hydraulic transmission. It employs a hydraulic torque converter in conjunction with a four speed gear transmission. A certain speed range is covered by each gear ratio. In the lower portion of each speed range the converter is in operation. At, say, the midpoint of the range the converter is locked-up and the system operates as a mechanical drive.

With this type of drive, the power delivered to the drive sprocket peaks at four points. At other speeds the power is reduced either due to the losses in the converter or because the engine is overloaded or both. The peak power is about 85% of rated even at lock-up because of hydraulic spin losses in the transmission.

Considering that the SEGMAG system could achieve efficiencies between 90-95%, the steady state performance is clearly improved over the entire range of vehicle speed.

Several machines were considered for this drive, the pertinent data being presented in the following table:

	Generator	Motor (2 req'd.)
Rating, hp	1500	750
Speed, rpm	3000	450/2880
Dia., in.	27	36
Length, in.	34	35
Wt., lbs	5000	4000

The size of the machinery evolved in these preliminary designs appears to fit into the available space in the XM-1 vehicle. The mechanical arrangement of components, however would have to be scrutinized more closely. The system weight of approximately 16,000 lbs appears to be a slight handicap and would have to be evaluated on the basis of the increased accelerating capabilities of the vehicle. The feasibility of this application can only be evaluated after an intensive analysis of the complete system performance over the required mission profiles and a detailed mechanical layout is completed. These tasks would be outside the scope of the present contract.

3.1.2 Amphibious Vehicles Propulsion Systems

Propulsion systems for several amphibious vehicles were investigated. To gather information on the characteristics of these vehicles and their performance requirements, several visits were made. The first was to the U.S. Marine base at Quantico, Virginia to discuss the requirements of an advanced amphibious vehicle drive.

The present vintage of amphibious vehicles are 25 ton tracked vehicles with 8 knot water speed. They utilize engines with mechanical-hydraulic transmission for land operation and water jets at sea. For the advanced LVA under consideration, the most dramatic performance change desired is to raise the speed to the range of 35 to 70 knots. These high speeds indicate a departure from the displacement type vehicle. Candidate systems include planing hulls, surface effects, etc. In these cases, a drastic reduction in vehicle weight is required to bring the propulsion system within an acceptable power range.

Westinghouse presented a review of the various advanced machines under study and development with special emphasis on the SEGMAG machine concept and the ARPA program objectives.

Also performance characteristics for a typical tracked vehicle were presented and comparisons were drawn between mechanical and mechanical-hydraulic and electric torque converters. The electric drive provides ease of control, high maneuverability and high utilization of the prime-mover rating over a wide range of vehicle speeds. Also, electric drive offers superior acceleration capability.

The need to develop reversing current collectors for the drive motors was identified and a program to define specific machines and the control scheme was suggested.

The vehicle is in the very early stages of idea formulation. Therefore, the needs and the drive systems are too uncertain to permit an evaluation of the advantages that would be derived from an electric drive system.

Due to the limited funds, it appears that the USMC program will be restricted to vehicle concepts based on currently available components or development systems sponsored under a broader program.

A visit was made to the Naval Amphibious Warfare Board at Norfolk, Virginia. They were interested in the present state-of-the-art in electric propulsion systems as they might apply to re-power a range of amphibious vehicles that they operate.

A short Presentation was given of Marine Propulsion Systems utilizing the ARPA developed SEGMAG machine concepts and other electric propulsion arrangements. Interest was indicated by the Navy for several potential applications.

Many questions were generated by these Operations Personnel regarding the application of the SEGMAG drive system. The majority of these questions concerned the liquid metal current collectors, and centered on the following particular categories: 1) The effect of pitch and roll on the liquid metal in the collectors. 2) The types and methods of seals used to maintain the liquid metal in the collectors. 3) The seals required to maintain the nitrogen gas in the machine and the amount of nitrogen required for inventory. 4) The amount of liquid metal discharged from the machine normally and under battle conditions. 5) The effect on safety to personnel in event of liquid metal leakage. 6) Due to the close tolerances in the current collectors, what provisions are incorporated into the machine for thrust absorbtion and thermal growth? 7) Due to the relative high mortility of these small vessels what are the economics of this drive system?

3.2 CURRENT PROGRESS

3.2.1 Tank Propulsion

During this period, effort continued on applying the SEGMAG machine system to tank propulsion. Since the most desired attribute of modern tanks is increased acceleration for more agile mobility, increased horsepower per ton of vehicle weight is obviously the trend to follow. Unfortunately, increasing installed horsepower with present day mechanical drives usually increases the enclosed volume and surface area, thereby requiring more armor weight and more horsepower. Electric drives, although heavy in comparison to mechanical drives, offer one outstanding benefit that breaks this exponentially rising horsepower-weight trend, and that is its freedom in mechanical arrangement. By electrically separating the prime mover and the traction drive, more compact drive systems can be visualized that do not require increasing tank armor weight. Since this separation is accomplished electrically, horsepower increases of the prime mover can be effected by increased speed and thereby increased power density. Utilizing this principle, an improved performance tank drive system was developed. The conceptual system uses modular units of motors, generators and control units. This modularization has distinct advantages for both tracked and wheeled vehicles. It also permits application to many vehicles of varying horsepower requirements utilizing multiple of the modular drive motors with corresponding prime mover sizes.

3.2.2 Ship Propulsion

Another trip was made to the Amphibious Warfare Board at Norfolk, Virginia to inspect ships of the LCU class for possible application of SEGMAG electrical propulsion systems. The present arrangement of diesels, gears and shafting can be modified to accommodate higher horsepower gas turbine-electric drive units without major hull modifications.

SECTION 4

CURRENT COLLECTION SYSTEMS

4.0 OBJECTIVES

The objectives of this task are to study liquid metal current collection technology and to identify the preferred systems for the segmented magnet homopolar machines.

During Phase I the specific objectives were: 1) to review the state-of-the-art of liquid metal current collection system technology; 2) to identify preferred liquid metals and preferred current collector designs under a variety of operating conditions; 3) to identify the operational problem areas which must be resolved for successful performance; 4) to establish the constraints which the liquid metal handling and purification systems must satisfy; and, 5) to establish an experimental program to resolve the problems associated with liquid metal current collectors.

During Phase II the objective was to evolve a liquid metal current collector suitable for unidirectional, constant speed machines of the SEGMAG type and to verify its effectiveness in the 3000 HP demonstration SEGMAG generator.

During Phase III the current collector technology is being extended to: 1) unidirectional high speed (96 m/s collector speed) generator applications; and, 2) reversible and variable speed applications such as motors and torque converters.

4.1 PRIOR AND RELATED WORK

During Phase I of the present ARPA contract, a preferred current collector design was identified for unidirectional homopolar machines, such as the SEGMAG generator. This selection was based on a review study of the complex electromagnetic interactions and forces which will be experienced by functioning collector systems under a variety of operating conditions and liquid metals. The preferred collector design embodies an "unflooded machine gap", with the low density sodium-potassium liquid metal alloy (NaK) confined in narrow circumferential current transfer zones. The liquid metal alloy gallium-indium (GaIn) was selected as an alternative to NaK, especially for homopolar machine applications wherein relatively low speed and high ambient magnetic field operating conditions exist, or in certain situations where liquid metal handling may be considered a problem. The alternative choice of a higher density liquid metal was based on lower calculated power losses when run under the specified operating conditions. Although not as compatible as NaK with most structural and conducting materials, GaIn is quite easy to handle and lends itself to a relatively simple purification process.

Two of the greatest concerns in applying liquid metal current collectors are: a) the magnitude of power losses developed in the fluid; and, b) the confinement of fluid to the current collection zones during all machine operating conditions. A complete discussion of these concerns is contained in the previous reports under this contract.

During Phase II a liquid metal current collector test facility was constructed and an experimental test plan was implemented to resolve recognized problem areas in applying liquid metal current collectors. Part of this effort included an evaluation of collector width effects on the magnitude of the ordinary fluid dynamic power loss. The effect of ambient radial magnetic field and collector width variations on the eddy current power loss was also investigated. The remaining work effort consisted of experimentally evaluating the possible adverse effects which rotor rotational speed, radial magnetic induction, and load current have on liquid metal confinement in the collection zone. This effort culminated in the design and fabrication of the current collectors for the prototypic SEGMAG generator. A complete exposition of this work is contained in the previous reports under this contract.

During Phases II & III the current collector design which was developed was evaluated in a SEGMAG demonstration generator, rated 3000 hp. Tests verified the suitability of this collector for use in homopolar machines of constant speed (to 67 m/s). Concerns include the collector solid-liquid contact resistance, and its influence on machine efficiency, and a collector filling - critical temperature characteristic. Work continued ot extend the unidirectional collector technology to higher speeds for generator applications. Other work centered on development of reversible and variable speed collectors for torque converters and motor applications. Concepts being considered in this development include flooded, unflooded, and hybrid collectors.

4.2 CURRENT PROGRESS

During this report period, the theoretical power loss and expulsion pressure expressions were redeveloped for collectors of the SEGMAG and high speed type to account for the solid-liquid-solid electrical contact resistance. Calculations which illustrate the effects of contact resistance were made and the results are presented in this report. Values of specific contact potential were determined for collectors with copper and nickel plated copper surfaces. These determinations were made with the glove box test rig, using 3000 hp SEGMAG prototypic size liquid metal (NaK) current collectors and typical operating conditions. Changes in the collector filling-critical temperature characteristic were also observed as a function of side wall insulation, cover gas density (nitrogen vs. helium), and contact surface treatment (bare copper vs. nickel plate).

Current collector concepts were developed for the reversing unflooded motor application. Specific configurations were defined and these were evaluated, based upon the previously-established list of criteria, to determine feasibility. Collector concepts which passed this screening procedure were recommended for further development.

An analytical study of the hybrid current collector was made during the period. General expressions derived during the study permit calculation of pertinent collector design parameters and performance characteristics. Incorporating the mathematical expressions in a computer program, quantitative information was obtained for a selected hybrid pad collector. The selected design utilizes circular cross-section pads and they are applied in an axial manner along one flat side wall of the collector rotor.

4.2.1 SEGMAG Collectors

Subsequent to making certain modifications, as discussed in the previous Semi-Annual Report, the demonstration SEGMAG generator was again tested under high voltage-zero current (open-circuit test) and high current-minimum voltage (short-circuit test) conditions. In general, the collector performance characteristics were similar to those determined during the previous run, with one notable exception. Previous running was limited to 90,000 amperes because of an impending instability in the annular gap NaK flow due to suspected MHD effects. However, no hint of flow instability due to the load current-self field MHD expulsion pressure was evident during the recent tests. Stable performance was shown even though the SEGMAG generator test included short circuit current operation to a higher level of 110,000 amperes. This increase in performance capability may be attributed to the recent application of electrical insulation along each collector's rotor and stator flat side walls. Although not considered to be a significant factor in the present test situation, because of the very low induction involved, perturbations to the fluid flow in the annular side channels due to the axial field induced circulating currents will be reduced by the applied electrical insulation.

Based on an analysis of the SEGMAG generator total performance, an otherwise unaccountable machine power loss was attributed to ohmic dissipation in the current collectors. Higher than anticipated collector ohmic power loss would occur if, for example, the solid-liquid-solid specific contact potential, ε_k, and/or if the bulk liquid medium resistivity is greater than predicted. Factors which relate to this situation include initial treatment of the collector solid surfaces and subsequent operating conditions, including creation of foreign surface films and generation of fluid flow instabilities. The existence of a two phase liquid-gas medium, rather than a continuous flowing liquid ring in the annulus, would also result in an increase in bulk resistivity and apparent contact resistance, both causing higher ohmic power loss. Recent efforts to lower the contact resistance through collector surface treatments have been successful. Preliminary results of this work are discussed in Sec. 4.2.2.1.

With a potential for the existence of significant levels of solid-liquid contact resistance, it is deemed necessary to modify the theoretical power loss and expulsion pressure expressions for liquid metal current collectors. The assumptions made and the conditions upon which these modified expressions are based are shown along with the liquid metal current collector model illustrated in Fig. 4.2.1.1.

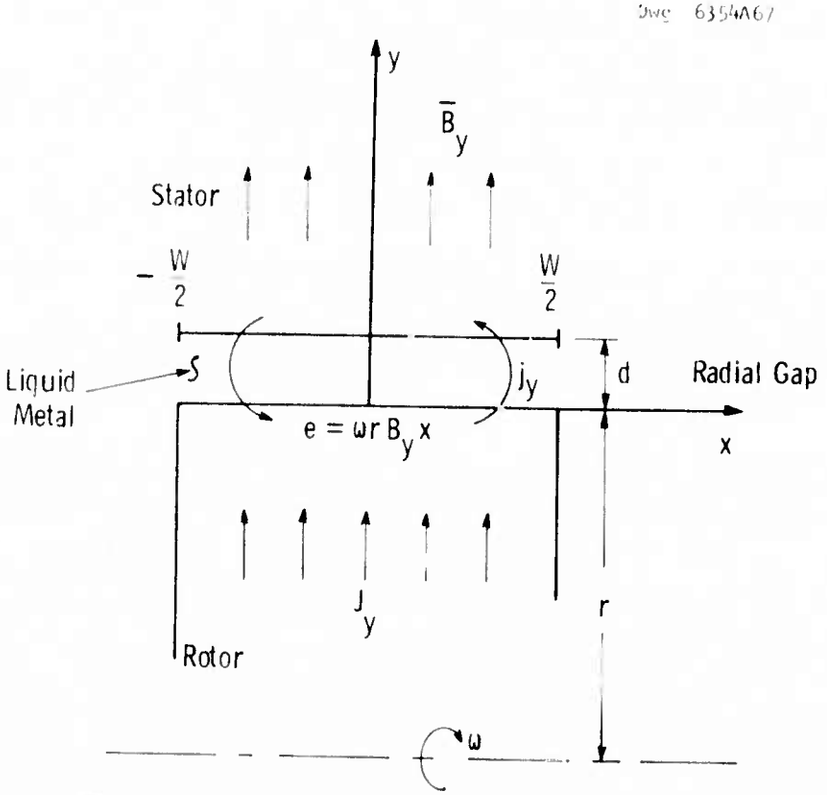

Fig. 4.2.1.1: Model of liquid metal current collector

4.2.1.1 Ohmic Power Loss (P_Ω)

From consideration of the potentials and around any given closed loop we obtain an expression for the circulating current density, j_y, in the liquid metal.

$$2\omega r B_y x = 2(\frac{d}{\sigma} + \varepsilon_k)j_y + (\frac{d}{\sigma} + \varepsilon_k)J_y - (\frac{d}{\sigma} + \varepsilon_k)J_y. \qquad (4.2.1.1)$$

Then

$$j_y = \frac{\sigma\omega r B_y x}{(d+\sigma\varepsilon_k)} \qquad (4.2.1.2)$$

Assumptions:

- Axial component of magnetic field is small (typical for SEGMAG type machines) and neglected.
- Rotor and stator members possess infinite conductivity, but a double contact resistance (ε_k) exists at the solid-liquid-solid interfaces.
- j_y = circulating current density (B_y, ωr effect).
- J_y = load current density (constant across collector width for given value of current, $I/2\pi rw$).
- Current densities (j_y and J_y) in the liquid metal are parallel with the "y" axis.

An expression for the ohmic power loss per unit volume due to electrical resistances of the liquid metal and the solid-liquid-solid interface contacts follows:

$$p_\Omega = (j_y + J_y)^2 \left(\frac{l}{\sigma} + \frac{\varepsilon_k}{d}\right) \qquad (4.2.1.3)$$

Then, the total ohmic power loss is

$$P_\Omega = \int_{vol} p_\Omega = \int_{-\frac{w}{2}}^{\frac{w}{2}} \left(\frac{l}{\sigma} + \frac{\varepsilon_k}{d}\right) (j_y + J_y)^2 \, 2\pi rd \, dx \qquad (4.2.1.4)$$

Substituting Eq. (4.2.1.2) into Eq. (4.2.1.4), performing the integration, and simplifying we obtain the ohmic power loss due to the circulating and load currents.

$$P_\Omega = \frac{\pi}{6} \frac{(\pi B_y)^2 (rw)^3}{\left(\frac{d}{\sigma} + \varepsilon_k\right)} + \frac{I^2 \left(\frac{d}{\sigma} + \varepsilon_k\right)}{2\pi rw}, \text{ watts/collector} \qquad (4.2.1.5)$$

where: P_Ω = total ohmic loss per collector, watts
ω = angular speed of rotor, rad/s
B_y = radial magnetic field, T
r = collector rotor radius, m

w = collector electrical contact width, m

d = collector radial gap dimension, m

σ = electrical conductivity of liquid metal, mhos/m

ε_k = solid-liquid-solid specific contact potential, Vm^2/A

I = collector load current, A

4.2.1.2 Rotor Drag Power Loss (P_{drag})

An expression is developed below for the circulating current in the collector rotor. This current is maximum at the rotor's mid-point and reduces to zero at each edge.

$$i_x = i_{max} - \int_0^x j_y dA, \qquad (4.2.1.6)$$

where

$$i_{max} = \int_0^{w/2} j_y dA$$

From the above expression and Eq. (4.2.1.2)

$$i_{max} = \frac{\pi}{4} \frac{\sigma\omega B_y (rw)^2}{(d+\sigma\varepsilon_k)} \qquad (4.2.1.7)$$

Then, again using Eq. (4.2.1.2) and substituting Eq. (4.2.1.7) into Eq. (4.2.1.6)

$$i_x = \frac{\pi}{4} \frac{\sigma\omega B_y (rw)^2}{(d+\sigma\varepsilon_k)} - \int_0^x \frac{\sigma\omega r B_y}{(d+\sigma\varepsilon_k)} x 2\pi r \, dx$$

Performing the integration and simplifying, we get the rotor current expression below.

$$i_x = \frac{\pi\sigma\omega B_y r^2}{(d+\sigma\varepsilon_k)} \left[\left(\frac{w}{2}\right)^2 - x^2\right] \qquad (4.2.1.8)$$

An MHD interaction between the circulating rotor current, i_x, and the radial field, B_y, causes a rotor drag power loss. An element of this drag loss follows:

$$P_{drag} = \omega r dF = \omega r B_y i_x dx \qquad (4.2.1.9)$$

Substituting Eq. (4.2.1.8) into Eq. (4.2.1.9), the total rotor drag power loss is:

$$P_{drag} = \int_{-\frac{w}{2}}^{\frac{w}{2}} \omega r B_y \frac{\pi\sigma\omega B_y r^2}{(d+\sigma\varepsilon_k)} \left[\left(\frac{w}{2}\right)^2 - x^2\right] dx$$

Performing the integration and simplifying,

$$P_{drag} = \frac{\pi}{6} \frac{(\omega B_y)^2 (rw)^3}{\left(\frac{d}{\sigma} + \varepsilon_k\right)}, \text{ watts/collector,} \qquad (4.2.1.10)$$

where: P_{drag} = rotor drag power loss per collector, watts.

4.2.1.3 Total Power Loss (P_T)

$$P_T = P_\Omega + P_{drag} + P_{vis}, \text{ watts/collector.} \qquad (4.2.1.11)$$

where: P_T = total power loss per collector, watts.

P_{vis} = fluid dynamic (viscous) power loss per collector, watts.

$P_{vis} = \frac{\pi}{4} f\rho (\omega r)^3 r (w + k)$, from Eq. (2) of Semi-Annual Technical Report for period ending May 31, 1974, where the previously undefined terms are:

f = Fanning friction factor

ρ = mass density of liquid metal, kg/m^3

k = additional non-conducting rotor-liquid contact width, m.

4.2.1.4 Calculated Total Power Loss (P_T)

Based on Eq. (4.2.1.11), calculations of collector power loss for a 3000 hp SEGMAG type generator were made, and these represent a wide range of collector widths and specific contact potentials. Pertinent

geometrical parameters, operating conditions, and liquid metal physical properties assumed for the calculations are tabulated below:

$r = 0.178$ m	$I = 10^5$ A
$d = 1.6 \times 10^{-3}$ m	$f = 5.5 \times 10^{-3}$
$k = 6.4 \times 10^{-3}$ m	$\sigma = 2.2 \times 10^6$ mhos/m
$\omega = 377$ rad/s	$\rho = 850$ kg/m^3
$B_y = 0.03$ T	

Results of the power loss calculations are presented in Fig. 4.2.1.2. Rather large losses in power are noted to occur as the specific contact potential, ε_k, is increased, especially for narrow width collectors. This is due to high contact resistance and resulting high ohmic loss associated with transferring the machine load current. Optimum collector widths are indicated (see 'minimum power loss line') for the lower levels of ε_k. If it is assumed that ε_k is near zero, the optimum collector width is 0.5 cm. Further reductions in collector width are undesirable since that would result in an increase in the power loss. If only larger ε_k values can be practically achieved, however, quite high power losses are associated with narrow width collectors. In that case, increasing the collector width will result in lower power loss. Collectors of 1.25 cm width (selected for the 3000 hp SEGMAG demonstration machine) will perform with minimum power loss if the specific contact potential is 4×10^{-9} Vm^2/A. Increases in power loss above the minimum, with wider collectors, is attributed to viscous fluid drag associated with larger contact areas.

4.2.1.5 Expulsion Pressure (P_x)

An axially directed expulsion pressure is created within the collector liquid metal due to a circumferential self-magnetic field associated with both load and circulating currents. The model conditions upon which the governing expression for this pressure is based are shown in Fig. 4.2.1.3.

The circumferentially directed magnetic field induction in the liquid metal gap (B_θ) may be defined as

$$B_\theta = \mu \oint H d\ell \qquad (4.2.1.12)$$

where $\mu = 4\pi\ 10^{-7}$

$$\oint H d\ell = i_{enclosed} = (i_x + I_x)$$

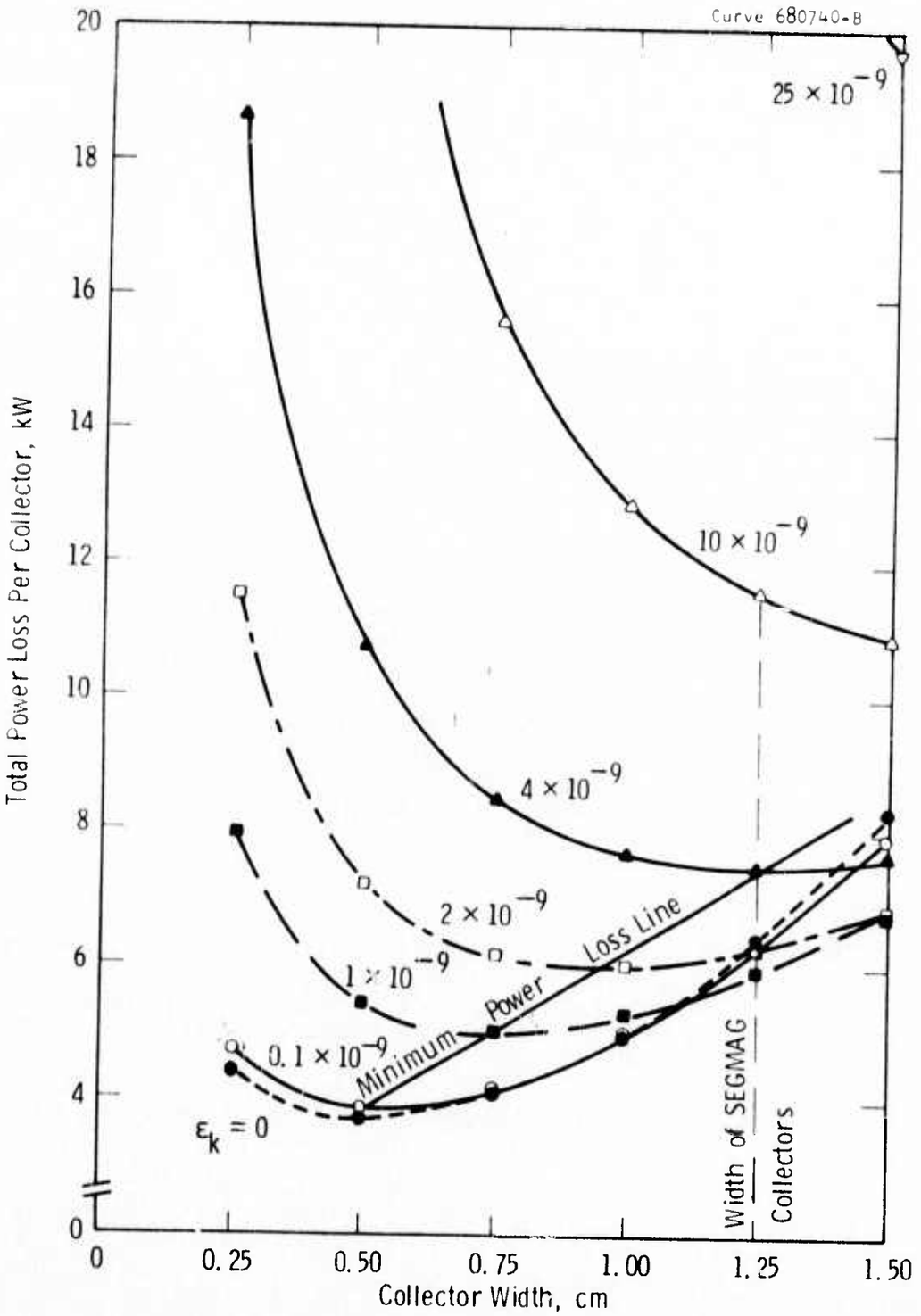

Fig. 4.2.1.2: Calculated power loss for 3000 HP SEGMAG type generator. (Full Load)

Dwg 6354M66

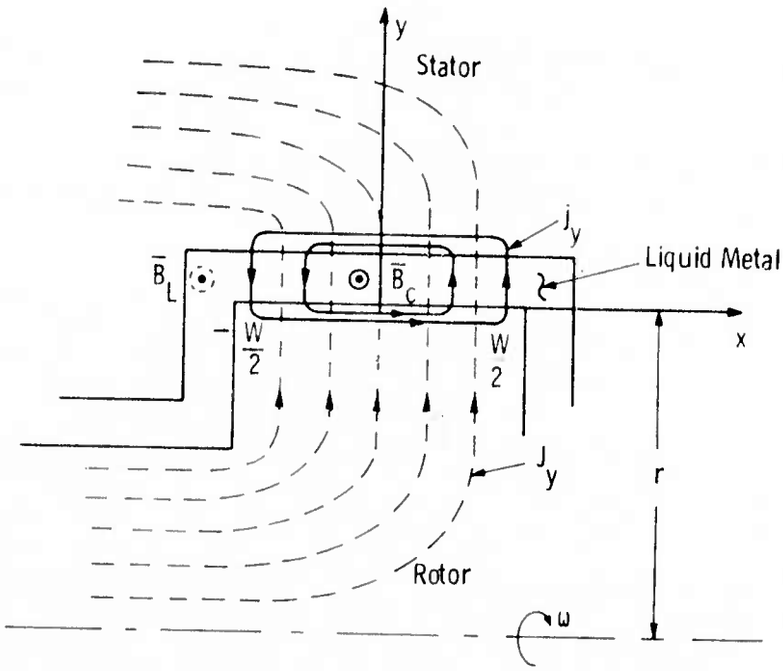

Fig. 4.2.1.3: Model of liquid metal current collector with load and circulating currents

From Eq. (4.2.1.8), the circulating current along the rotor width is

$$i_x = \frac{\pi\sigma\omega B_y r^2}{(d+\sigma\varepsilon_k)} \left[\left(\frac{w}{2}\right)^2 - x^2\right]$$

The axial component of the load current enclosed may be expressed as follows:

$$I_x = 2\pi r J_y \left(\frac{w}{2} - x\right),$$

or

$$I_x = I_L \left(\frac{1}{2} - \frac{x}{w}\right).$$

Then, the field intensity (H) along circumferential loops through the liquid metal gap is

$$\oint H d\ell = H 2\pi r = (i_x + I_x)$$

From the previous expressions developed for i_x and I_x, and employing Eq. (4.2.1.12), we obtain

$$B_\theta = \frac{\mu}{2} \left\{ \frac{I}{\pi r w} \left(\frac{w}{2} - x \right) + \frac{\sigma \omega B_y r}{(d + \sigma \varepsilon_k)} \left[\left(\frac{w}{2} \right)^2 - x^2 \right] \right\} \qquad (4.2.1.13)$$

The radial current density in the liquid metal is

$$J = J_y + j_y \qquad (4.2.1.14)$$

Utilizing Eq. (4.2.1.2) the above expression becomes

$$J = \frac{I}{2\pi r w} + \frac{\sigma \omega r B_y}{(d + \sigma \varepsilon_k)} x \qquad (4.2.1.15)$$

An element of axial expulsion pressure due to the MHD interaction between B_θ and J is

$$p_x = B_\theta J \, dx$$

The resulting pressure in the liquid metal along the rotor width, with respect to the left-hand edge, is

$$P(x) = \int_{-\frac{w}{2}}^{x} B_\theta J \, dx, \qquad (4.2.1.16)$$

where $-\frac{w}{2} \leq x \leq \frac{w}{2}$

Substituting Eqs. (4.2.1.13) and (4.1.2.15) into Eq. (4.2.1.16), letting

$$\alpha = \frac{I}{\pi r w}$$

$$\beta = \frac{\sigma \omega B_y r}{(d + \sigma \varepsilon_k)}$$

$$\gamma = \frac{\mu}{2},$$

performing the integration and simplifying we obtain the following expressions for the expulsion pressure due to the load and circulating currents:

$$P(x) = \frac{\gamma}{2}\{(\frac{\alpha^2 W}{2} + \frac{\alpha\beta W^2}{4})(\frac{W}{2} + x)$$

$$- (-\frac{\alpha^2}{2} + \frac{\alpha\beta W}{2} + \frac{\beta^2 W^2}{4})[(\frac{W}{2})^2 - x^2]$$

$$-\alpha\beta[(\frac{W}{2})^3 + x^3] + \frac{\beta^2}{2}[(\frac{W}{2})^4 - x^4]\} \qquad (4.2.1.17)$$

4.2.1.6 Calculated Axial Expulsion Pressure, (P_x)

Based on Eq. (4.2.1.17), calculations of the axial expulsion pressure in the liquid metal for a fully loaded 3000 hp SEGMAG type generator were made. In addition to the parameters previously tabulated in Sec. 4.2.1.4, the present pressure calculations involved a collector width of 1.27×10^{-3} cm and an ε_k value of 3×10^{-9} Vm^2/A. Results of the calculations are presented in Figs. 4.2.1.4 and 4.2.1.5.

The expulsion pressure caused by the combined load and circulating currents is noted to increase axially from one edge of the collector gap width to the other for load currents greater than 25 kA. The initial reversal in the direction of expulsion pressure noted at relatively low load current is attributed to predominance of the circulating current. Relatively large pressures appear across the collector gap width at higher load current levels. All pressures, of course, must be counterbalanced in order to prevent gross loss of liquid metal from the collector. This is accomplished in the SEGMAG generator through self adjusting asymmetric extensions of liquid metal along the collector's flat side walls.

Influence of collector contact resistance on the expulsion pressure is indicated by the contrasting sets of curves in Fig. 4.2.1.5. As ε_k increases from zero to 3×10^{-9} Vm^2/A, the circulating current is obviously reduced to such an extent that it has smaller and smaller effects on the basic load current-self field interaction. Very low values of ε_k cause axial pressures in both directions in the liquid metal, placing the fluid in a state of tension. This effect tends to cause axial separation of liquid metal in the annulus, which is undesirable. If too severe, this action would cause gross loss of liquid metal from the current transfer zone, high bulk and contact resistance, and high ohmic power loss. If present, a varying ε_k would likely cause sloshing action of the liquid metal leading, again, to less efficient current collection and fluid spillage from the collection zone.

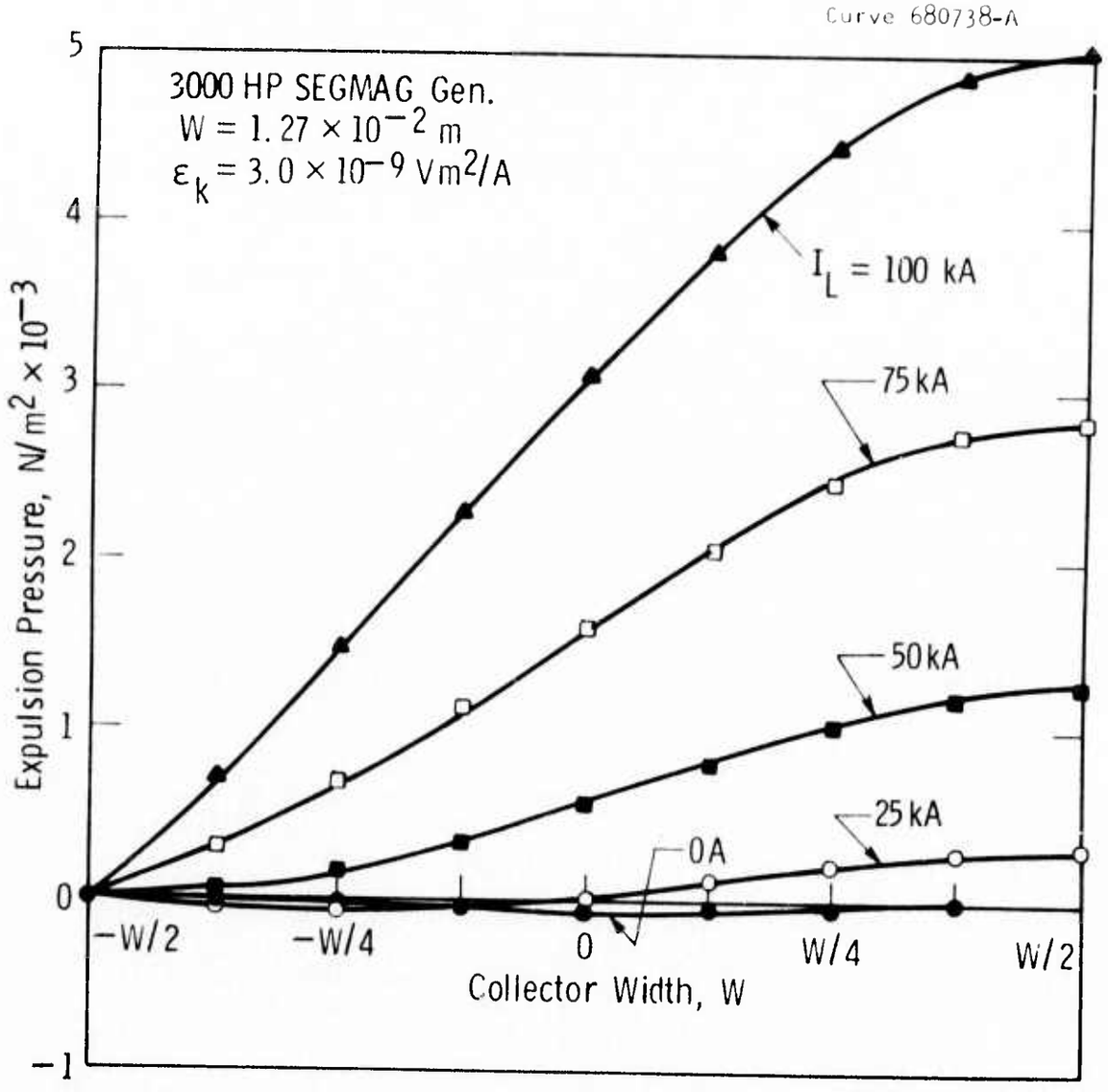

Fig. 4.2.1.4: Calculated axial expulsion pressure caused by load and circulating currents

E.M. 4705

Curve 680739-A

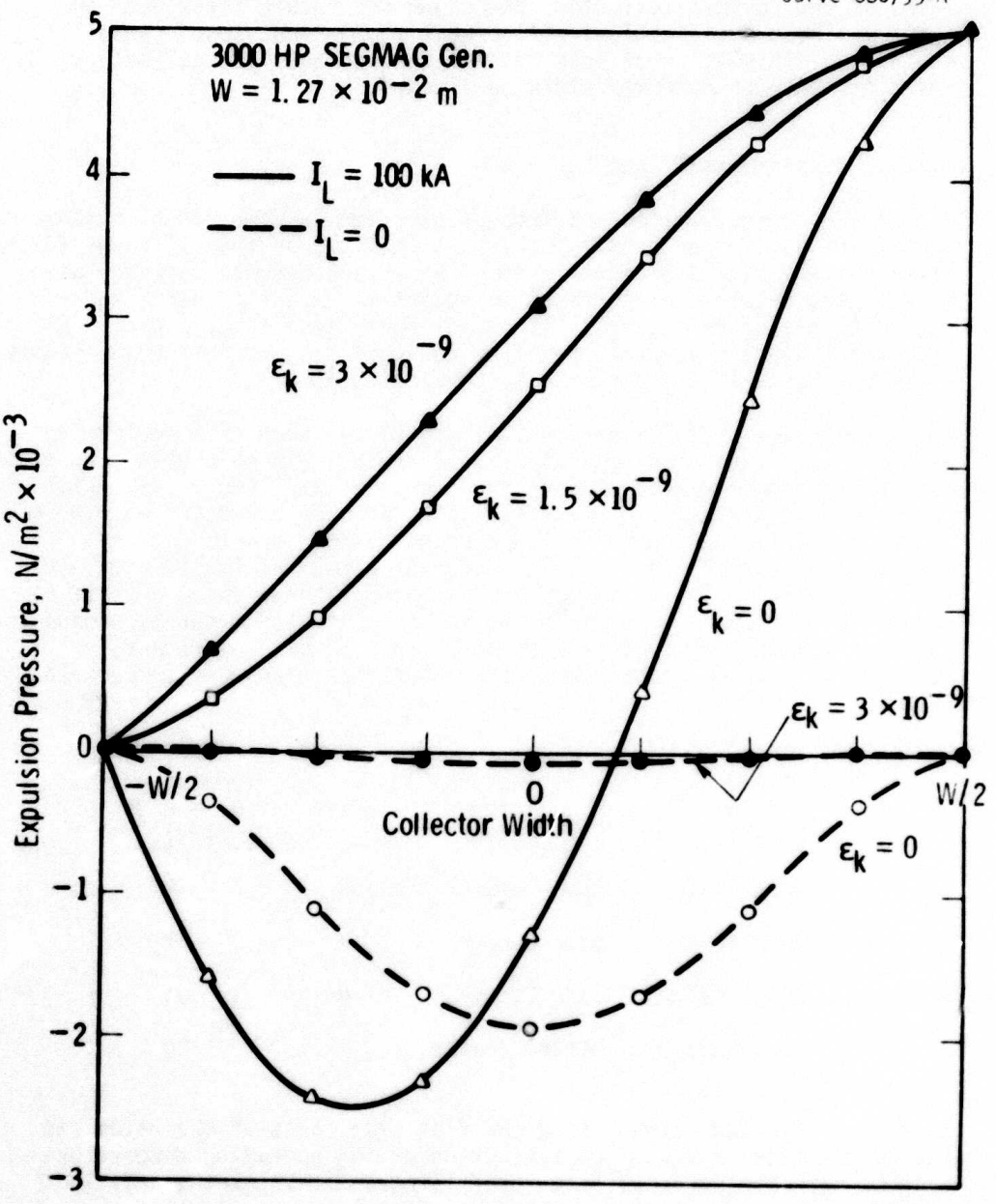

Fig. 4.2.1.5: Effect of ε_k on axial expulsion pressure caused by load and circulating currents

4.2.2 High Speed Collectors

Design work and associated drawings which encompass required modifications of the current collector test stand for future tests were completed. These modifications will permit higher test speed capability, controlled circulation of load current through the test collectors, and acceptance of narrower width collectors.

4.2.2.1 Experimental Test Results

During the current period a number of experiments were run to evaluate the effect of a lower density cover gas (helium) on the collector filling-critical temperature characteristic. Other experiments were run with nickel plated collector surfaces to ascertain potential benefits in regard to easier collector filling and lower contact resistance. All experiments were made with the glove box test rig, using 3000 hp SEGMAG prototypic size liquid metal (NaK) current collectors.

It is desirable that the current collectors be capable of performing at the lowest possible temperature so that the machine cooling capacity will not be compromised. During the course of previous experimental work, current collector performance in a nitrogen cover gas was found to be critically dependent on temperature. Good performance was observed, in terms of gap filling and confinement of liquid metal to the collector, if operation occurred at temperatures above a critical level for each speed. Operation below the critical temperature caused an adverse effect on collector performance. Results of recent collector filling-critical temperature determinations are summarized below:

Collector Side Walls	Collector Contact Surfaces	Cover Gas	Critical Temperature @ 60 r/s, (°C)
Uninsulated	Bare Copper	N_2	78
Insulated	Bare Copper	N_2	62
Insulated	Bare Copper	He	51
Insulated	Nickel Plated	N_2	≤ 28

From the above data, insulating the flat side walls of the rotor and stator permitted a significant lowering of the operating temperature without sacrificing capability for filling and maintaining a filled collector when operating in nitrogen. Additional lowering of the critical temperature (to 51°C) was demonstrated when the 60 r/s

collector ran in a helium environment. Finally, temperature was not found to be critical in regard to liquid metal filling of the collector, down to 28°C, when the contact surfaces were plated with nickel and operation was again in a cover gas of nitrogen.

Although beneficial results were shown experimentally for the above noted collector design changes and cover gases, a complete physical understanding of their effects is incomplete at this time. Conjecture as to the mechanisms which explains the improved collector filling ability will likely include gas-liquid flow dynamics as well as foreign surface films and solid-liquid wetting.

Previous experimental and theoretical work point up a concern for the effect of solid-liquid contact resistance on collector performance. A knowledge of the magnitude of the specific contact potential is necessary to the design of a collector for minimum power loss. Recent experiments were run wherein the contact resistance of collectors with bare and nickel plated copper surfaces was calculable. Calculations of the specific contact potential for the collectors were possible utilizing experimentally determined values of power loss associated with circulating currents induced by radial directed magnetic fields in the liquid metal. The difference between measured drive shaft power with and without an applied radial magnetic field, less a correction for previously determined stray power loss, is taken as the circulating current power loss. An expression for that loss in terms of ε_k and the known operating conditions is obtained from the sum of Eqs. (4.2.1.5) and (4.2.1.10), realizing in this case that the load current, I, is zero.

$$P_{circ} = \frac{\pi}{3} \frac{(\omega B_y)^2 (rw)^3}{\left(\frac{d}{\sigma} + \varepsilon_k\right)}, \text{ or rearranging terms} \qquad (4.2.2.1)$$

$$\varepsilon_k = \frac{\pi}{3} \frac{(\omega B_y)^2 (rw)^3}{P_{circ}} - \frac{d}{\sigma} \qquad (4.2.2.2)$$

Utilizing the above technique, specific contact potentials were determined for collectors with copper and nickel plated copper surfaces and these are plotted as a function of temperature in Fig. 4.2.2.1. Despite scatter in the data, a tendency is shown for the contact resistance of both collectors to decrease with increasing temperature. This characteristic is possibly related to another experimental observation, namely, an increasing fluid flow stability with rising temperature. Lower resistance is thus attributed to a larger solid-liquid contact area and to improved wetting at higher temperatures.

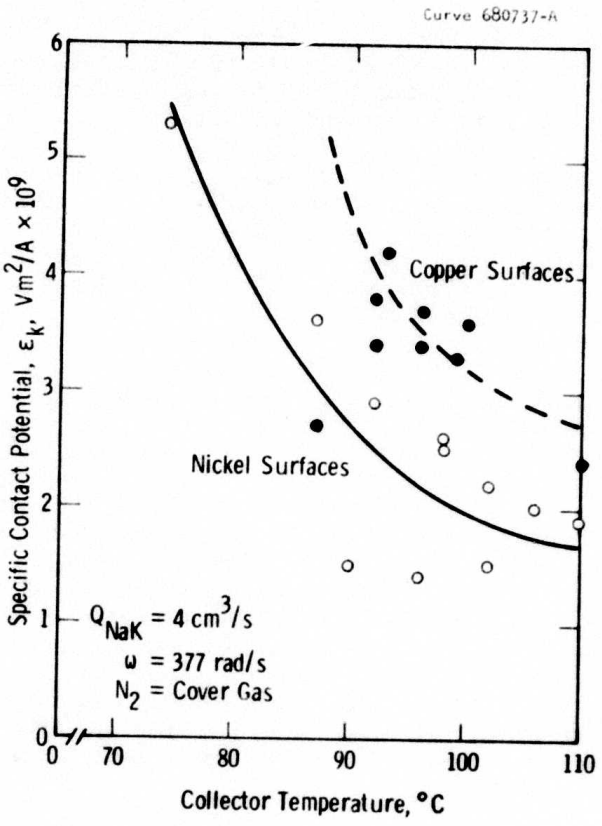

Fig. 4.2.2.1: ε_k values determined from test rig-radial field experiments.

The average specific contact potential is reduced by about 40% when the copper collector contact surfaces are plated with nickel. This characteristic is probably related to the expected existence of thinner and less continuous tarnish films on surfaces of nickel. If that premise is true, constriction of the current will be less, leading to lower contact resistance. Nickel, unlike silver and gold, is essentially insoluble in NaK. Upon disassembly and decontamination of the test collector following eight days of testing and exposure to NaK, the 0.005 mm thick nickel plate was intact and bright.

Thus, it appears that through nickel plating a more chemically clean NaK compatible collector surface is assured as a function of time. The accruing benefits include improved collector filling capability (temperature independent) and lower contact resistance (greater machine efficiency).

4.2.3 Flooded Collectors

Work during the period on flooded collectors is covered in the Machinery Section (2.3.3.2) of this report.

4.2.4 Unflooded Collectors

In a horizontally mounted machine with an unflooded active length, the collector design problem becomes one of confinement of the liquid to the annular collector gap. For a motor, the confinement technique must be independent of rotor speed and direction of rotation. Use of centrifugal forces induced by disk rotation, as in the case of high speed generators, cannot be used as the sole device for achieving containment of the liquid metal. The objective of this study is to develop new concepts for the current collectors in an "unflooded" motor application, to evaluate these, and to select the most promising ones for more detailed investigation.

During this reporting period, collector concepts were developed, using the classification list (Table 4.2.4.2) as a guide, and these were evaluated using the list of criteria (Table 4.2.4.3) as a feasibility check-list.

4.2.4.1 Reference Unflooded Motor Design-Collector Requirements

The "reference" motor design (Table 4.2.4.1 of the previous Semi-Annual Report), which was defined to establish approximate parameters as requirement guides for the current collector design, was modified slightly. The axial field through the collector was changed to 0.1 Tesla, a minimum axial clearance requirement of 0.15 cm (0.06 in.) was established, and the change in radial gap due to machine operation was introduced as 0.11 cm (0.045 in.) minimum. These changes have been incorporated in the revised Table 4.2.4.1 of this report.

The radial clearance in a journal bearing of a size adequate to transfer the machine torque, has been estimated to be about 0.030 cm (0.012 in.), which is the amount of additional eccentricity that can occur due to changes in the shaft position with varying speed. An additional change in radial gap will be caused by any differential thermal growth of the rotor and the stator. For example, if the rotor and stator expansion rates are based upon the properties of iron (expansion coefficient $\approx$ 11.7 x 10^{-6} m/m°C, 6.5 x 10^{-6} in/in°F) then the differential thermal radial growth will be:

$$\delta_p = R \alpha \Delta T \qquad (4.2.4.1)$$

$$\delta_p = 1.07 \times 10^{-5} \text{ m/°C } (0.234 \times 10^{-3} \text{ in/°F}),$$

for a radius, R = 0.914 m (36 in), and for a 28°C (50°F) temperature difference:

$$\delta_p \approx 3.05 \times 10^{-4} \text{m } (0.012 \text{ in})$$

TABLE 4.2.4.1

Unflooded Motor Reference Design-Collector Requirements (Revised)

1. Power Rating - 40,000 hp
2. Maximum Speed - 180 rpm (18.9 rad/sec)
3. Collector Diameters: outer - 72 in. (1.83 m), for drum (SEGMAG and disk-type machines (DISKMAG)
   inner - 32 in. (0.81 m), for disk-type machines
4. Axial and Radial Dimensions Allocated for Current Collector Cross-section - 1.5 in. (3.81×10^{-2}m)
5. Maximum Permissible Current Density - 16,000 amps/in^2 (2.48×10^7 A/m^2)
6. Maximum Collector Current - 300,000 amps
7. Axial Field through Collector - 1000 gauss (0.1 Tesla)
8. Maximum Radial Field through Collector - 500 gauss (0.05 Tesla)
9. Liquid Metal Leakage from Collector - near zero
10. Maximum Power Loss per Collector Pair - 65 hp (4.85×10^4 w)

The above values were used to establish the following related parameters:

11. Tip Speeds (from 2 and 3): outer - 57 ft/sec (17.2 meter/sec)
    inner - 25 ft/sec (7.7 meters/sec), for disk-type machine
12. Bearing Radial Clearance 0.012 in. (3.05×10^{-4}m) (based on 1 mil/in. (1 mm/m) diametral clearance and a 24 in. (0.61 m) shaft dia., necessary for 3 per unit torque at 15,000 psi (1.03×10^8 N/m^2) shear design strength)
13. Minimum Width of Liquid Metal Contact: outer - 0.083 in. (2.11×10^{-3}m)
    inner - 0.187 in. (4.74×10^{-3}m), for disk-type machine

ADDITIONAL REQUIREMENTS

1. Collector must pass 150% rated current at zero speed for 10 secs.
2. Collector must be operable cold without pre-heating.
3. Collectors for a machine must be supplied from a common liquid metal source.
4. Collector must be capable of deceleration from full speed forward to full speed reverse in several seconds.
5. Collector shall be designed for sudden stops.
6. Collector shall be designed for sudden load changes.
7. Collector shall be designed to provide for axisymmetric current flow.

The following assumptions will be made, but will be re-evaluated, if necessary, when more specific machine and collector designs are available:

1. Relative axial movement between the rotor and stator will be a minimum of 0.06 in. (0.15 cm).
2. Coolant channels or other cooling techniques will not interfere with the current collection design.
3. Joining of any required conductor bars to collector rings will not interfere with collector design.
4. Any mechanical strengthening rings will be outside of the current collector envelope (i.e., the collector will not have to support the loading of other components, due to centrifugal force or relative thermal growth).
5. Changes in radial gap, due to operation, will be assumed to be a minimum of 0.045 in. (0.11 cm).
6. Insulation requirements will not interfere with collector design.

If the thermally-induced dimensional changes are based upon the expansion coefficient of copper (α = 17.5 x 10^{-6} m/m°C, 9.7 x 10^{-6} in/in°F), then the change in radial gap would be:

$$\delta_p = 4.3 \times 10^{-4} m \ (0.017 \text{ in.})$$

Rotor growth due to rotational stresses, should be negligible at the expected tip speed. Therefore, the cumulative gap change that must be accommodated by the seal, including an additional 3.8 x 10^{-4}m (0.015 in) for dimensional tolerances, would be about 11 x 10^{-4}m (0.045 in) (for a 28°C, 50°F maximum temperature difference).

Table 4.2.4.2

Classification of Unflooded Reversing Collector Concepts

A. Sealed Annular Chamber (Seal Types)

1. Rubbing - lip seal, face, radial
2. hydrostatic - face, radial, floating
3. hydrodynamic - face, radial, floating
4. labyrinth - clearance, knife/groove, slinger, transverse gas flow, adjustable
5. buffer fluid - liquid, gas, grease, wax
6. electromagnetic retention - special field/current source
7. absorbent (wick) - labyrinth, slinger/wick
8. low-speed only - centrifugal, electromagnetic
9. magnetic fluid
10. surface tension - wetted/non-wetted surfaces
11. solidification - thermal, chemical

B. Conducting Seal

1. conducting wick - stationary/rotating, fiber, foam
2. hydrodynamic/hydrostatic
3. flooded (alternately) labyrinth

C. Low-Speed Flooding or Low-Speed Brush Contacts

1. pressure-controlled volume
2. pump/control system
3. gas injection

D. Axial Injection (or Radial Ejection)

1. inertial containment
2. venturi effect

E. Zero Pressure (free-fall)

F. Constant-Speed Seal-Rotor

TABLE 4.2.4.3
Evaluation Criteria for Current Collectors

1. Containment (Leakage)
   a) aerosol
   b) liquid

      [free-surface stability, gravity force, acceleration/deceleration (angular/transverse), momentum changes (coriolis)]

2. Power Loss
   a) viscous
   b) ohmic (bulk & contact)
   c) MHD
   d) friction (rubbing)

3. Circulation System Requirements
   a) pressure/flow control
   b) purification/separation

4. Radial/Axial Clearance
   a) bearing clearances
   b) dimensional tolerance
   c) thermal growth
   d) centrifugal growth

5. Mechanical Adequacy
   a) thermal stress
   b) rotational (torque) loading
   c) hydraulic load (static/dynamic)
   d) centrifugal loading/stresses
   e) MHD forces (radial, tangential, axial)
   f) wear (rubbing, erosion)
   g) vibration/oscillation stability
   h) load rate (shock)

6. Temperatures (cooling)
   a) heat generation (see power loss)
   b) temperature distribution (collector and rotor conductors)

7. Electrical Adequacy
   a) voltage drops
   b) recirculating currents
   c) asymmetry effects (including variable NaK thickness/area)

8. Material Compatibility
   a) chemical
   b) mechanical (e.g., rubbing surfaces)

9. Assembly

10. Fabricability

11. Maintenance

4.2.4.2 Collector Concepts and Evaluation

A. Sealed Annular Chamber

A1. Rubbing Seal

The peripheral speed of the "reference" design (17.2 m/s, 3380 ft/min) approaches the upper limit of about 17.8 to 25.4 m/s (3500 to 5000 ft/min) typically recommended for lip-type elastomeric oil seals.[1,2] Maximum pressure differential capability recommended for this type of seal is about 69,000 N/m^2 (10 psi). In small quantities, the cost of relatively standard Buna-"N" seals, which generally use garter springs to generate lip pressure, is about $1 per inch of diameter, or about $72 for the "reference" machine. Catalog listed seals of this diameter are about 1.91×10^{-2}m (3/4 in) wide and an inch or less in radial thickness. Split seals are available to simplify installation. (Special configurations can be made to order.) Shaft eccentricities greater than 2.36×10^{-3}m (0.093 in) can be accommodated. Standard "Axial Clamp Seals," which provide an axial sealing lip, are also available. These have an axial length of 3.18×10^{-2}m (1-1/4 in) and a radial height of about 1.27×10^{-2}m (1/2 in), with an operating deformation of about 2.39×10^{-3}m (0.094 in).

Figure 4.2.4.1 shows an arrangement of lip-seals which provide isolation of adjacent collectors in a multi-turn motor. The chambers formed between collectors may be used to introduce oil droplets to lubricate the seals and to drain any NaK leakage that might occur. Alternatively, they may be filled with oil to balance the gravity-induced pressure drop across the seal, which would otherwise increase from top to bottom. In addition, it may be possible to circulate the oil between the collectors at a rate great enough to cool the collectors.

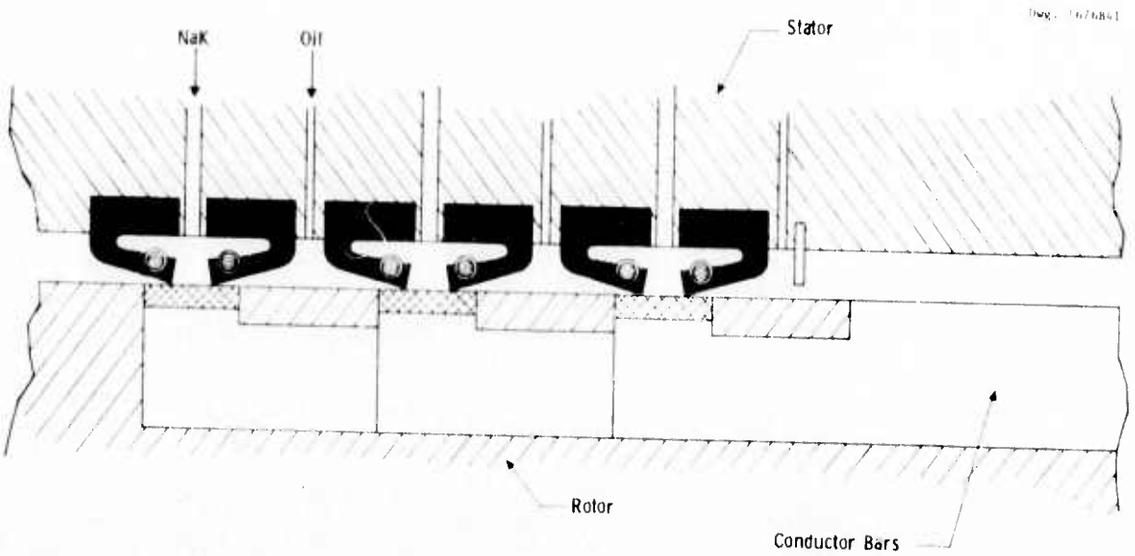

Fig. 4.2.4.1: Lip-Seal Collector Configuration

A rubbing seal, which may ride on a very thin ($\sim 2.54 \times 10^{-6}$ m, 1×10^{-4} in) film of oil or liquid metal, should provide excellent containment. Even without pressure balancing techniques, these seals should be adequate for the expected ejection pressure of about 20,700 N/m^2 (3 lb/in^2) in the "reference" machine. Since there is no free surface of the liquid metal, aerosol formation should not be a problem unless there is significant leakage.

The power loss in a rubbing-lip-seal is difficult to estimate, but one supplier provided a rough estimate of radial sealing force at the lip, as 131 N per meter (3/4 lb/in) of circumference. If this value is used with an effective friction coefficient of 0.125, then the estimated power loss for the "reference" motor design becomes:

$$P_s = \pi\ D\ \mu\ m\ V = 1.63\ kW \qquad (4.2.4.2)$$

where: D = diameter of seal

μ = friction coefficient

m = radial contact force

V = rubbing velocity of the seal

Another estimate of power loss may be made by calculating the viscous loss in a thin supporting film of oil, using the following expression for power loss:

$$P'_s = (\mu V/h)(\pi DL)V,$$

$$P'_s = \pi DL\ \mu V^2/h \qquad (4.2.4.3)$$

where in this case:

P'_s = power loss

μ = absolute viscosity

D = diameter

L = length of seal lip contact film

V = seal velocity

h = film thickness

If an oil film 2.54×10^{-6}m (1×10^{-4}in) thick[1] is assumed, with a viscosity, $\mu = 8.07 \times 10^{-3}$N sec/m^2 ($1.17 \times 10^{-6}$ lb sec/in^2), the power loss becomes:

$$P_s = 5310 \text{ kW per meter (135 kW per inch) of contact length}$$

If the contact length is assumed to be 7.62×10^{-4}m (0.030 in.), then the estimated power loss for each seal would be:

$$P_s = 4.05 \text{ kW}$$

The power loss can be reduced by using a lower-viscosity fluid. For example, if NaK is assumed to be the lubricating film ($\mu = 5.2 \times 10^{-4}$ N-sec/m^2, 7.55×10^{-8} lb-s/in^2), then

$$P_s = 0.261 \text{ kW}$$

In addition to the seal lip loss, there will be the viscous and ohmic losses in the liquid metal annulus (~ 6 kW for a 1 in. collector width). The combination of these losses must not exceed the maximum permissible (~ 20 kW per collector) based on machine efficiency objectives.

Liquid metal circulation requirements are expected to be quite flexible for this concept. Minimum flow rate would be based on purification requirements and replacement of any leakage that might occur. A "batch" loading system may be feasible. An oil separation system may be necessary, but contamination (oil-in-NaK or NaK-in-oil) should be small and simple gravity separation techniques may be applicable.

A smooth rotor with axial insertion into the stator appears feasible with this design. This may greatly simplify assembly, and axial movements should not be a problem. Simple components and perhaps off-the-shelf components can be used for sealing. This would result in minimal fabrication and component costs. No compatibility problems are foreseen, however, "aging" (loss of elasticity) of Buna-"N" or other possible seal materials should be investigated.

Although seal life should be long, once a satisfactory design has been established, it is possible that contaminants (such as oxides) would reduce the operating life of the seals. On-site seal replacement appears to be impractical, unless a scheme is devised for use in conjunction with a split stator. However, seal replacement should be a relatively simple operation, if the motor is taken out of service.

The use of simple lip-type oil seal appears to be feasible for large motor applications where the tip speeds are about 17.8 m/s (3500 f/min) or less. The low cost of these seals makes the experimental evaluation of this concept a relatively simple task. Initial tests, to evaluate tip-speed limits, oxide-induced wear, and "aging" effects, can be run on a simple shaft and smaller diameter seals (at increased rpm). Subsequent evaluation of large-diameter seals would also be inexpensive because the seal cost would add little to the cost of the test set-up required for any full-size concept evaluation.

A2. Hydrostatically-Positioned Seal

A hydrostatically-positioned seal uses gas or liquid pressure differences to control the size of a small gap between the rotor and the stationary seal. An increase in the seal gap tends to increase the leakage flow from a chamber; this reduces the chamber pressure, thus creating a force which brings the seal closer to the rotor and maintains the small gap. The seal may be positioned either axially, against the face of a disk or ring, or radially, in which case the seal ring must be segmented or otherwise flexible enough to permit the changes in diameter required to follow rotor thermal expansion and dimensional tolerance variations.

Two important considerations in the seal design are the selection of fluid used in the seal, and the pressure in the seal chamber. Three fluid types may be considered: the cover gas, an oil, or the liquid metal itself. For the large circumference, even a very small seal clearance would result in a significant leakage into the machine if NaK were used. Therefore, use of NaK requires an added drain chamber; otherwise, it would not satisfy the objective of near-zero leakage into the machine. An added drain chamber is also required with an oil or gas buffer fluid (Figure 4.2.4.2), unless the buffer pressure is higher than the collector pressure (Figure 4.2.4.3). In that case, however, buffer fluid will enter the collector, and it must be demonstrated that there is no resulting deterioration of collector performance. Another consideration is the possibility that MHD-induced forces will upset the pressure balance if the liquid metal is used for this purpose.

It may be desirable to segment an axial seal (as well as the radial seal) if dimensional controls, such as flatness, become difficult for rings of such large diameter. In this manner, or by making the seal ring very flexible, the seal clearance can be kept small at all points along the circumference. In any event, it will probably be necessary to provide local pockets (chambers) along the seal circumference so that an angular shift of the ring axis would provide a restoring moment. This restoring force might not exist for a complete annular pressure pocket.

Seal clearances of about 2.54×10^{-5} m (1×10^{-3} in) or less should be achievable with hydrostatically-positioned seals. Fluid leakage through such a narrow annular gap would be approximately:[3]

$$q = \frac{\pi D h^3 \Delta p}{12 \mu L}, \qquad (4.2.4.4)$$

where: q = leakage flow

D = seal diameter

h = seal clearance

Δp = pressure drop across seal

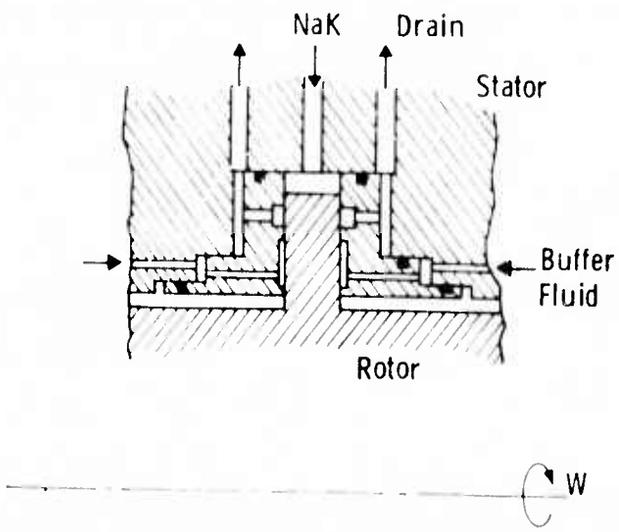

Fig. 4.2.4.2: Hydrostatically-Positioned Seal (Sealed Drain)

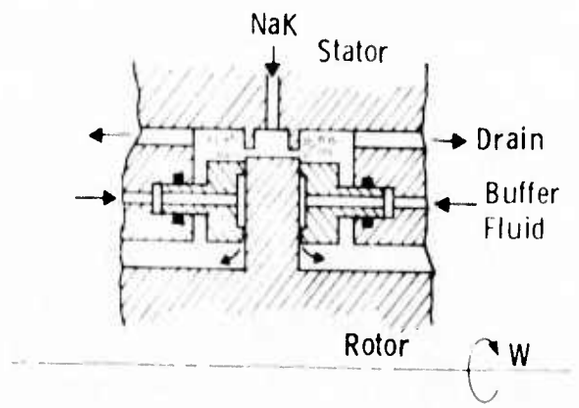

Fig. 4.2.4.3: Hydrostatically-Positioned Seal

μ = absolute viscosity

L = width of seal land, in the direction of leakage flow

As in the previous section, viscous power loss associated with this seal land would be:

$$P'_s = \pi D L \mu V^2/h, \qquad (4.2.4.3)$$

Equations (4.2.4.3) and (4.2.4.4) may be combined to find:

$$P'_s\, q = \frac{\pi^2 D^2 V^2 \Delta p\, h^2}{12}. \qquad (4.2.4.5)$$

Based upon estimated liquid-metal ejection pressures of roughly 6,890 N/m^2 (1 psi) (at the top) to 20,700 N/m^2 (3 psi) (at the bottom), an average of at least 13,800 N/m^2 (2 psi) can be assumed to induce leakage from the collector. (The gravity head could possibly be balanced by a buffer liquid.) To provide some margin, a pressure difference of 20,700 N/m^2 (3 psi) will be used in the leakage calculation.

For the specific case where:

D = 1.83m (72 in).

V = 17.2 m/s (57 ft/s)

Δp = 20,700 N/m^2 (3 psi),

and if the units for "P_s" are (kW), h(m) and those for "q" are (cc/min), then:

$$P'_s\, q = 1.01 \times 10^{12} h^2.$$

This relationship (which is independent of μ and L) is plotted in Fig. 4.2.4.4 which permits the selection of a seal gap that provides both acceptable power loss and acceptable leakage.

Equations (4.2.4.3) and (4.2.4.4) may also be combined in a manner which eliminates the variable clearance "h" to find:

μL	L		
N - s/m	NaK (m) (in)	Oil (m) (in)	Nitrogen (m) (in)
1.50×10^{-4}	2.87×10^{-1}	1.27×10^{-2}	7.72
	11.3	0.500	304
7.45×10^{-5}	1.43×10^{-1}	6.35×10^{-3}	3.86
	5.63	0.250	152
1.32×10^{-5}	2.54×10^{-2}	1.13×10^{-3}	6.85×10^{-1}
	1.00	4.44×10^{-2}	27.0
6.62×10^{-6}	1.27×10^{-2}	5.65×10^{-4}	3.43×10^{-1}
	0.500	2.22×10^{-2}	13.5
3.31×10^{-6}	6.35×10^{-3}	2.83×10^{-4}	1.71×10^{-1}
	0.250	1.11×10^{-2}	6.74
1.32×10^{-6}	2.54×10^{-3}	1.13×10^{-4}	6.85×10^{-2}
	0.100	4.44×10^{-3}	2.70
3.97×10^{-7}	7.62×10^{-4}	3.30×10^{-5}	2.05×10^{-2}
	0.030	1.33×10^{-3}	0.809

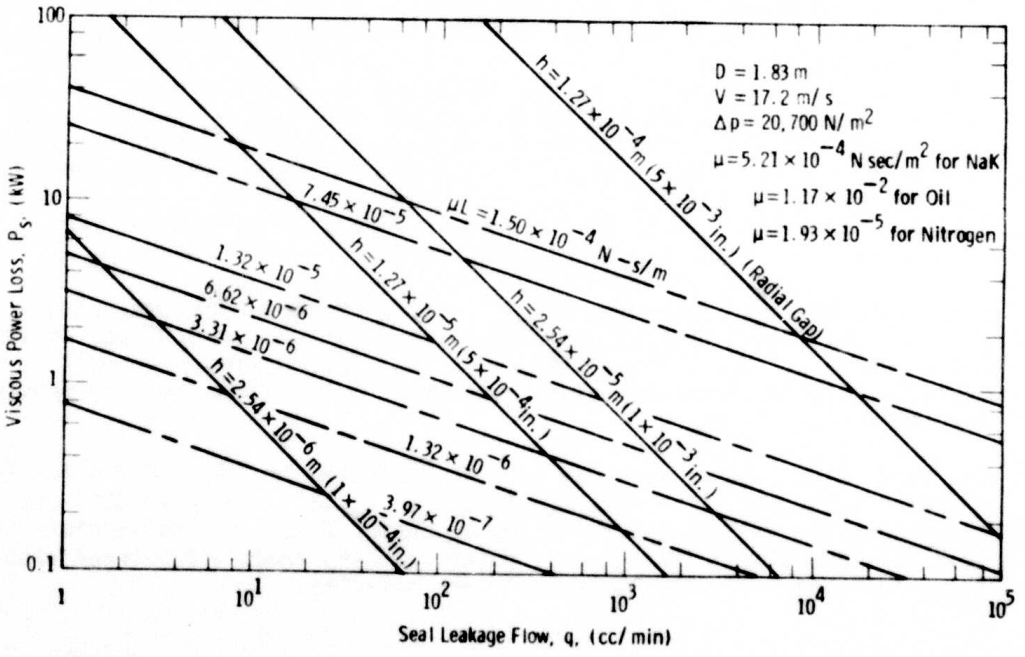

Fig. 4.2.4.4: Power-leakage relationship for a single annular seal lip (at Δp = 20,700 N/m², 3 psi).

$$(P'_s)^3 q = \frac{\pi^4 D^{10} \omega^6 \Delta p}{12} (\mu L)^2. \qquad (4.2.4.6)$$

With the selected values for D, V, and Δp, this expression is also presented in Fig. 4.2.4.4 with the parametric lines of constant (μL) also identified in terms of corresponding values of L for NaK, oil, and nitrogen viscosities. (It should be noted that the equations used for Fig. 4.2.4.4 apply only in the laminar regime and should be reviewed when a specific design is selected.)

To avoid the situation where a known leakage of liquid metal is inherent in the design, hydrostatic support of the seals by the liquid metal itself has been ruled-out unless an additional drain is incorporated. This leaves designs such as those shown in Figs. 4.2.4.2 and 4.2.4.3 where a buffer fluid prevents leakage of the liquid metal, but instead the buffer gas or liquid leaks into the machine space. These designs are expected to provide excellent containment of the liquid metal, provided that a stable operating condition can be maintained.

Leakage flow of the buffer fluid can be estimated from Fig. 4.2.4.4, and will depend upon the selected pressure in the position-control pocket. If, for simplicity, a buffer pressure difference of 20,700 N/m^2 (3 psi) is assumed with the configuration of Fig. 4.2.4.2, then with 1.27×10^{-5}m (0.0005 in) as a seal clearance, a seal lip of 1.14×10^{-3}m (0.045 in) thickness would permit about 4(92) = 368 cc/min of buffer oil leakage per collector, with half of this entering the machine and the other half entering the seal drain chamber. If a gas buffer (N_2) is used, a wider seal would be desirable. In this case, a seal length of 1.27×10^{-2}m (0.5 in) would permit about 4(4960) = 19,840 cc/min (0.7 cfm) of buffer gas leakage. It is difficult to estimate these leakages, however, before a detailed design of the seal is completed and the pressure drop and the seal clearance can be determined. For example, a change in clearance from 1.27 to 1.02×10^{-5}m (0.0005 to 0.0004 in) would just about cut the leakage rates to half the values shown above.

The effect of acceleration loading (inertial forces on the seal ring) should be evaluated when the application environment and seal design are better defined. The inertial forces on the seal ring must be small compared with the pressure-balance restoring force of the seal to prevent rubbing or seal leakage.

The seal viscous power loss may also be estimated from Fig. 4.2.4.4. In a design such as that in Fig. 4.2.4.2, with a 1.27×10^{-5}m (0.0005 in) clearance, the following table shows the power loss for a particular seal configuration. It should be noted that the trade-off between viscous power loss and seal leakage has not been optimized.

Buffer	Buffer Seal Length	Buffer Power Loss	NaK Power Loss (6.37×10^{-3}m, 0.25 in. long seal)	Total Seal Power Loss
oil	1.14×10^{-3}m (0.045 in)	4x1.77 kW	2 x 0.443 kW	7.97 kW
N_2	1.27×10^{-2}m (0.50 in)	4x0.033 kW	2 x 0.443 kW	1.02 kW

For the configuration shown in Fig. 4.2.4.3, the NaK power loss (in the seal) would be eliminated and the losses would become:

Buffer	Buffer Seal Length	Total Seal Power Loss
oil	1.14×10^{-3}m (0.045 in)	7.08 kW
N_2	1.27×10^{-2}m (0.50 in)	0.13 kW

The viscous and ohmic losses in the liquid metal annulus of the current collector must be added to the above values before comparing them with the permissible total power loss for each collector.

If the design of Fig. 4.2.4.2 is used, and if we assume a seal clearance of 1.27×10^{-5}m (0.0005 in), then with the design value of 20,700 N/m^2 (3 lb/in^2) pressure difference the recirculating NaK leakage from the seal would be about 36.2 cc/min per cm of seal length (for each of the two seals), see Fig. 4.2.4.4. A seal length of 6.37×10^{-3}m (0.25 in), for example, would permit a total leakage of 736 cc/min for each collector and a recirculation system of at least this capacity must be provided.

Additionally, a system must be provided to circulate the buffer fluid. Coarse estimates of circulation flow rates, based upon the configurations assumed in this evaluation, were given previously as about 368 cc/min of oil or 19,840 cc/min (0.7 cfm) of nitrogen per collector.

Consideration must be given to prevention of plugging of the orifices or capillary inlet lines that are used to establish the clearance-flow-pressure relationships for the hydrostatically-positioned seals. This is another reason to select oil or gas instead of NaK to establish the pressure-balance since Nak oxide formation could alter the restriction characteristics. Even with gas or oil, however, it may be desirable to add inlet screens to filter the fluid before it enters the restriction.

An oil/NaK separation system would be required if an oil buffer fluid is used. A high percentage ($\sim$ 33%) of oil may be expected in the mixture, however, simple gravity-separation techniques probably can be used with a large reservoir.

For an axially-applied seal, radial thermal expansion will not affect operation although there must be sufficient clearance in the stator to permit relative radial expansion without creating binding or friction forces that would interfere with axial motion. The 3.05×10^{-4}m (0.012 in) potential radial shift of the rotor due to bearing clearance is negligible compared with the 9.15×10^{-1}m (36 in) collector radius. There also should be no problem in accommodating large relative axial movements 7.62×10^{-4} to 1.52×10^{-3}m (0.030-0.060 in) if the static seal ("O"-ring) friction force is made negligible relative to the hydrostatic restoring force of the seal.

A radially-applied seal, however, would have to be segmented to permit relative thermal expansion and in addition must be designed to make the static seal friction negligible relative to the restoring force to accept movement due to rotor bearing clearance. In this case axial rotor movement would cause no problem.

A detailed examination of thermal gradients in the seal ring will be required to assure that distortion of the sealing surface does not occur. The seal rings will require a key to prevent rotation due to viscous forces. The magnitude of the viscous torque can be determined from the power losses defined earlier:

$$T = P_s/\omega, \qquad (4.2.4.7)$$

where: P_s = viscous power loss

ω = rotor angular velocity

T = viscous torque

The force on a key or keys at the seal diameter would be:

$$F_k = T/R \qquad (4.2.4.8)$$

where: F_k = tangential force on key

R = seal radius

For the present case, with:

$R = 9.15 \times 10^{-1}$m (3 ft)

ω = 18.9 rad/s (180 rpm)

P = 4 kW/seal,

F_k = 231 N (52 lb) per seal (max)

Additional areas of concern which should be investigated when a more definite design is established are the stability of the seal in relation to oscillation of the ring (both parallel movement and tilting of the ring) and in response to acceleration loading. The possibility of particulate oxide material reaching the seal/rotor interface and causing abrasive wear should also be considered. The possible "aging" (loss of elasticity) of the static seals should be investigated if a material such as Buna-"N" is used for this application. However, minor leakage at these sealing points should not be critical.

A radial application, which results in a more complex seal, might permit a continuous rotor (free of projections) and therefore a simpler assembly. Axially-positioned seals probably require a horizontally-split stator as well as split seal rings. Additional design effort is required to establish an assembly procedure.

Since very small seal clearances are necessary, machining requirements may be affected. The ability of the seal to follow movements of the rotor will establish permissible run-out tolerances, and this must be determined through further design and perhaps experimentation. Flatness of an axially-applied seal (or circularity of a radially-applied seal) may be a manufacturing problem due to the small clearance ($\sim$ 0.0127 mm, $\sim$ 0.0005 in) and large diameter ($\sim$ 1.83m, $\sim$ 72 in), unless the seal ring is made sufficiently flexible so that it conforms to the rotor. Fabrication cost should be investigated when a more definite design is established.

Under ideal operating conditions, no seal wear would be expected since no mechanical contact occurs, unless contaminants seriously block the flow restrictions, forcing the seal against the rotor, or oxide particles result in abrasive wear. Seal replacement or repair would probably be difficult and expensive.

In summary hydrostatically-positioned seals appear to be feasible, although the ability to maintain the small clearances on large diameter rings must be demonstrated. Conformity of a large-diameter ring to the mating rotor surface may be a problem unless the ring is segmented or is flexible. Design and analysis of the pressure-balance system remains to be completed. It has the advantage that the collector annulus may be circumferentially continuous, and it has only one pair of solid-liquid contact surfaces. The seal rings will probably have to be segmented for assembly purposes (for an axial seal) or to accommodate relative thermal expansion.

This concept has problems and advantages that are similar to those of the "Hydrostatically-Positioned Collector" (B2, below), and these design studies will be continued in parallel so that an early selection between the two may be made.

A3. Hydrodynamically-Positioned Seal

A hydrodynamically-spaced seal has the advantage (over hydrostatics) that a significant chamber pressure is not required. This could reduce the liquid-metal recirculation or leakage from the collector. However, the capability of continuous operation at speeds between zero and ±17.2 m/s (3380 ft/min), is a severe requirement for a dynamic fluid film lubricated seal.

An estimate of the feasibility of low-speed operation may be based upon semi-dry friction induced power loss.

$$P = F_f V = \mu \Delta p (\pi D L) V \quad , \qquad (4.2.4.9)$$

where

P = power loss

F_f = circumferential friction force

V = seal velocity

μ = friction coefficient

Δp = average pressure difference across seal

D = seal diameter

L = seal face width

If a friction coefficient of 0.15 is assumed, with a maximum (worst case) pressure difference of 27,600 N/m^2 (4 psi), the full-speed power loss may be calculated as:

P = 414 kW/m (10.5 kW/in.) of seal face width

If about 5 kW maximum loss per seal is permitted, the speed at which the hydrodynamic film becomes effective must be less than:

$$\omega = (5/10.5)\ 180 \text{ r/min} \approx 86 \text{ r/min} \ ,$$

for a 2.54×10^{-2} m (1 in.) seal face width.

If, for simplicity, a Rayleigh stepped bearing is assumed, the optimum load carrying capacity would be:[4]

$$W = \frac{6\mu V L B^2}{h^2} (0.03438) \ , \qquad (4.2.4.10)$$

where

W = load

μ = absolute viscosity

V = velocity of rotor

L = bearing length normal to motion

B = bearing length in direction of motion

h = minimum film thickness

The bearing load pressure is defined as:

$$P = W/LB = \frac{6\mu VB}{h^2}(0.03438). \qquad (4.2.4.11)$$

With $B = 1.27 \times 10^{-2}$ m (0.5 in.) and if an effective support area of 40% is assumed (due to the reversing requirement), to give the required effective load pressure as $27{,}600\ N/m^2 \div 0.40 = 69{,}000\ N/m^2$ (10 psi), then for a NaK lubricant ($\mu = 5.21 \times 10^{-4}$ N-sec/m^2, 7.55×10^{-8} lb-sec/in.^{2}) eq. 4.2.4.11 gives

$$h = 1.85 \times 10^{-5}\ m\ (0.730 \times 10^{-3}\ in.),\ \text{at full speed (180 r/min).}$$

At 86 r/min:

$$h = 1.85 \times 10^{-5}\ m\ (86/180)^{1/2}$$

$$h = 1.28 \times 10^{-5}\ m\ (0.505 \times 10^{-3}\ in.)$$

This adequate film thickness indicates that a hydrodynamically-spaced seal is probably feasible, although low-speed losses will probably be high, when compared to a hydrostatically-positioned seal. (Power limits for low-speed operation have not yet been established).

Two configuration alternatives are shown in Fig. 4.2.4.5. In configuration (a), the gap of the two independent seals (and therefore the leakage) will increase with increasing speed. In configuration (b), the sum of the two gaps is controlled by machining (or shimming at assembly) the space between two joined seals, and the hydrodynamic forces (and the pressurized NaK) tend to center the seal assembly around the rotor collector. The rotational effect on the fluid film would also tend to prevent leakage in configuration (b). However, it may not be possible

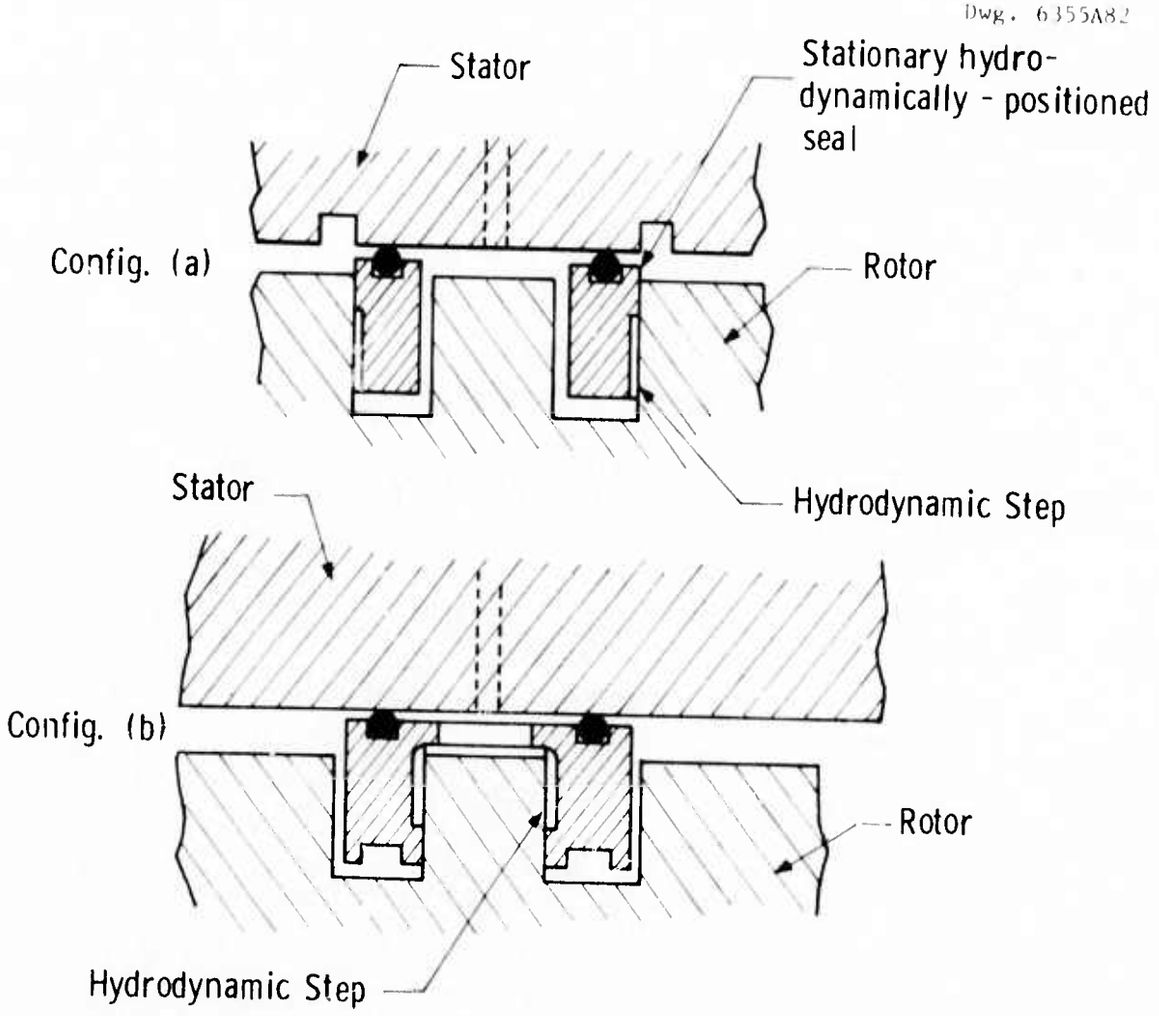

FIG. 4.2.4.5. Hydrodynamically-Positioned Seals.

to achieve the very close tolerances necessary for the seal interface, and an externally-pressurized or spring-loaded face may be required.

Since an axial seal is used, radial clearance is a possible problem only for the static seal between the collector seal and the stator housing, which must accommodate relative thermal growth. This seal also must permit relative axial movement due to axial shifts of the rotor. Thermal distortion of the sealing surface could be a problem. Keying of the seal to the housing probably will be necessary to prevent seal rotation. The effect of acceleration loading will have to be determined when a specific application is defined.

Machining tolerances for the large-diameter seal ring will be very tight, to maintain the small gap and to achieve the proper hydrodynamic wedge effect. Possible "aging" (loss of elasticity) of the static seal material should be investigated. It would probably be desirable to have a hard surface or a removable bearing face applied to the rotor so that damage or wear will not destroy the rotor. Rotor face and seal materials must be selected to minimize wear. Circulation system requirements will depend primarily on purification.

The axially-applied seal will probably have to be split and rigidly joined again after assembly on the rotor. Once this is accomplished, it may be possible to install the rotor axially into a smooth stator bore, as shown in Fig. 4.2.4.5, thus eliminating the need for a split stator and simplifying the design. If the rotor can be pulled out axially, the sealing system can be easily repaired or replaced, providing that consideration is given to the use of a hardened or removable collector rotor bearing face as noted above.

The use of an Oilite-type porous bearing may be considered, but the path of recirculation of lubricant must be defined for the required face-type bearing, as opposed to the conventional journal bearing application of that material. (A continuous radial seal cannot be used because of the potentially large relative thermal growth which could reduce the radial clearance).

Although this concept appears to be feasible it is probably best considered as part of the hydrostatically-positioned seal.

A4. Deep-Groove Labyrinth

Since the groove depth must be small in comparison with the collector diameter, a deep-groove labyrinth will still have to contain, as a minimum, the gravity-induced pressure head of about 15,170 N/m^2 (2.2 $lb/in.^2$) for a filled collector annulus. Since the leakage would be large for the required seal clearance of about 1.02-1.52 mm (0.040-0.060 in.), even for an extensive seal length, the concept might be feasible only if the expulsion pressure is minimized. The major pressure component, due to gravity, may be minimized by establishing a liquid metal flow rate such that the frictional drag at the collector wall is just equal to the gravitational body force.

For a static rotor and a uniform-thickness annular collector groove, and if no leakage of liquid metal occurs, the recirculating liquid metal introduced at the top will be split equally between the two collector paths and will join again at the bottom of the collector. In each path the flow velocity will be constant at:

$$v = Q/2A \ , \qquad (4.2.4.12)$$

where:

Q = liquid metal flow rate

A = collector area

Including the frictional drag loss in head, Bernoulli's equation may be written as:

$$P_1/\gamma + v_1^2/2g + Z_1 = P_2/\gamma + v_2^2/2g + Z_2 + h_f, \qquad (4.2.4.13)$$

where:

P = pressure

γ = density

v = velocity

h_f = head loss due to wall friction drag

Z = height (location) relative to bottom of collector, and the subscripts relate as follows:

1. inlet (at top of machine)
2. variable point between top and bottom.

Since the velocity will be constant:

$v_1 = v_2$, and

$$h_f = f(\ell/d)v^2/2g \ , \qquad (4.2.4.14)$$

where:

f = friction factor
ℓ = length of circumferential path
d = hydraulic diameter.

Then, Bernoulli's equation may be re-written as:

$$(P_2-P_1)/\gamma = (Z_1-Z_2)-f(\ell/d)(v^2/2g),$$

$$\Delta P = D\gamma - f(\ell/d)(v^2/2g)\gamma. \qquad (4.2.4.15)$$

For a rectangular collector channel, the hydraulic diameter is:

$$d = 4(cw)/2(c+w), \qquad (4.2.4.16)$$

$$d = 2c/(1+c/w)$$

where:

c = radial collector gap

w = collector width

If the radial dimension is small in comparison with the width, the hydraulic diameter is approximately:

$$d = 2c.$$

For a value of $\Delta P = 0$, from top to bottom, equation (4.2.4.16) gives:

$$f(\pi D/2)(v^2/2g) = D(2c).$$

$$v^2 = 8gc/\pi f. \qquad (4.2.4.17)$$

The Reynolds number for flow in this annulus is:

$$R_e = \frac{vd}{\nu} = \frac{2vc}{\nu}, \qquad (4.2.4.18)$$

where:

ν = kinetic viscosity.

If the radial collector gap is selected as 3.18×10^{-3} m (0.125 in.), the above relationships may be combined (for NaK, $\nu = 2.32 \times 10^3$ m^2/hr, 6.95×10^{-6} ft^2/sec) to find:

$$f = 32gc^3/\pi\nu^2 R_e^2$$

$$f = 7.68 \times 10^6/R_e^2 \qquad (4.2.4.19)$$

This expression may be used with the curves of friction factor vs "R_e" for very smooth pipes to find:

$$f \approx 0.027$$

$$R_e \approx 16{,}900$$

$$v \approx 1.72 \text{ m/s } (5.64 \text{ ft/s})$$

The corresponding liquid metal flow rate (in two parallel paths), for each cm of collector width would be:

$$Q = 6{,}530 \text{ cc/min, per cm of width}$$
$$(16.9 \text{ in.}^3\text{/s, per inch}).$$

The above values seem possible to achieve. Some pressure inequality will exist along the flow path due to the fact that the friction drop is linear along the angular (circumferential) path while the gravity head is linear with vertical height, but this deviation is probably small. More important will be the effect of rotation and surface conditions on the friction factor, and changes of properties with temperature.

In any event, some pressure will probably be necessary to assure low contact resistance, or will be caused by magnetic or acceleration forces. Rotor eccentricity due to bearing clearance is another source of pressure build-up and velocity variation due to the varying gap thickness. Therefore this technique is not recommended for use alone but may be considered for incorporation into another system in order to reduce the expulsion pressure.

A5. Variable Viscosity Buffer Material

This concept would utilize a seal made of a material with a low viscosity in the rotational direction (perhaps at a local radial position) but with sufficient strength to prevent extrusion in the axial direction. It could also consist of a slurry of solids larger than the leakage gap ($\sim$1.52 x 10^{-3} m, 0.060 in.) in an adhering liquid retained by the particles.

Since no material of this nature is presently available, the concept could not be fully evaluated and therefore it was dropped from further consideration.

A6. Electromagnetic Retention

Electromagnetic retention utilizes the forces generated between magnetic fields and electrical current flow in the liquid metal, to counter the various expulsion forces. Although this technique may be used in combination with a small-clearance hydrostatically-positioned seal or collector, it is probably not required for those designs. Therefore, this concept will be evaluated for the case of the relatively large seal clearance required to accommodate thermal expansion, bearing clearance, and dimensional tolerances. The sum of these requirements to prevent seal rubbing, is dependent upon the specific design configuration, materials, and operating procedures, but an estimated minimum clearance of 1.02 to 1.52 x 10^{-3}m (0.040 to 0.060 in) will be assumed for the present evaluation.

Because of the gravity effect on expulsion pressure, and for other reasons, a uniformly-filled seal gap cannot be assumed. That is, the retention technique must also function with only a locally-filled or partially-filled annulus, and must prevent droplets and aerosol from escaping.

General Relationships

In general, the retention body force on an element of the liquid metal will be:

$$F = J \times B,$$

where: F = retention body force (N/m^3)

B = flux density (T)

J = uniform current density through the element (A/m^2)

and where "B" and "J" are normal to each other and also normal to the resulting force "F". The maximum containment pressure (N/m^2) will be:

$$p = J \times B\ (\ell), \qquad (4.2.4.20)$$

where: ℓ = length of element in the direction normal to "B" and "J" (meters).

Neglecting contact resistance, the corresponding ohmic power losses would be:

$$P = I^2R = I^2\rho(b/\ell t) = J^2\ (\ell t)^2\ \rho b/\ell t$$

$$P = \rho J^2\ (vol), \qquad (4.2.4.21)$$

where: P = ohmic power loss (watts)

b = length of element in direction of current flow (m)

t = length of element in direction of magnetic flux (m)

$(vol) = b\ell t$ = volume of element

ρ = liquid metal resistivity (Ω-m)

As a specific example, to establish the order of magnitude of pressure build-up and power loss that might be obtained, we may select:

$1/\rho = 2.20 \times 10^6$ mhos/m (NaK)

$J = 6.20 \times 10^6$ A/m^2 (4,000 A/in^2)

$B = 1$ T

$p/\ell = 6.20 \times 10^6$ N/m^3 (22.8 lb/in^3)

$$P/vol = \frac{(6.20 \times 10^6)^2 \text{ A}^2/\text{m}^4}{2.2 \times 10^6 \text{ mhos/m}} = 17.5 \times 10^6 \text{ W/m}^3 \text{ (286 W/in}^3\text{)}.$$

If in addition, we select a radial gap of 1.27×10^{-3}m (0.05 in), and a 27,600 N/m^2 (4 psi) containment pressure, then for a 1.83 m (72 in) collector diameter:

$\ell = 27{,}600/6.20 \times 10^6 = 4.45 \times 10^{-3}$m (0.175 in).

$P = 17.5 \times 10^6 \ (1.27 \times 10^{-3}) \ (4.45 \times 10^{-3}) = 98.8$ W/m (2.50 W/in) of circumference

$P = 98.8 \times \pi(1.83) = 568$ W

For a full seal annulus at 27,600 N/m^2 (4 lb/in^2) and 4.45×10^{-3}m (0.175 in) length, the required current and voltage (for radial current flow and circumferential flux) would be:

$I = 6.20 \times 10^6$ A/m^2 x π(1.83 m) $(4.45 \times 10^{-3}$m) = 159,000 A

$V = P/I = 568/159{,}000 = 3.57 \times 10^{-3}$ volts

(An additional voltage drop would be introduced due to contact resistance.)

For circumferential current flow and radial flux:

$$I = 6.2 \times 10^{6}\ A/m^2 \times 1.27 \times 10^{-3}\ m \times 4.45 \times 10^{-3}\ m = 35\ A$$

$$V = P/I = 568/35 = 16.2 \text{ volts (neglecting contact drops)}$$

Therefore, the use of a radial flux with annular current flow permits more reasonable values of required voltage and current for containment, if a satisfactory configuration can be defined.

Self-Field Concept

One possible electromagnetic containment technique which would not require an externally imposed magnetic field is shown in Fig. 4.2.4.6. This concept uses the ejection pressure resulting from current flow in a separate electrical path provided for containment. As shown in the figure, axial conductor bars are embedded along the stator bore, and these are alternately connected to the positive and negative terminals of the retention system power source. When liquid metal enters the rotor/stator gap and contacts two or more conductors, a current flows through the liquid metal and the self-field provides a body-force which drives the liquid metal back toward the collector. A shoulder is provided on the rotor to eliminate a direct leakage path and assure liquid metal contact with the embedded conductors.

A simplified analysis of this concept shows the following relationship for containment pressure:[5]

$$p = (5/6)\ \mu\ \ell^2\ J^2, \tag{4.2.4.22}$$

where: μ = gap permeability ($\sim 4\pi \times 10^{-7}$ hy/m)

ℓ = axial length of liquid metal extension into the containment system (m) (see Fig. 4.2.4.6).

The ohmic power loss was found (as above) to be:

$$P = \rho J^2\ (\text{vol}) = \rho J^2 (\pi D \ell t), \tag{4.2.4.23}$$

with:

$$J = V/\rho b, \tag{4.2.4.24}$$

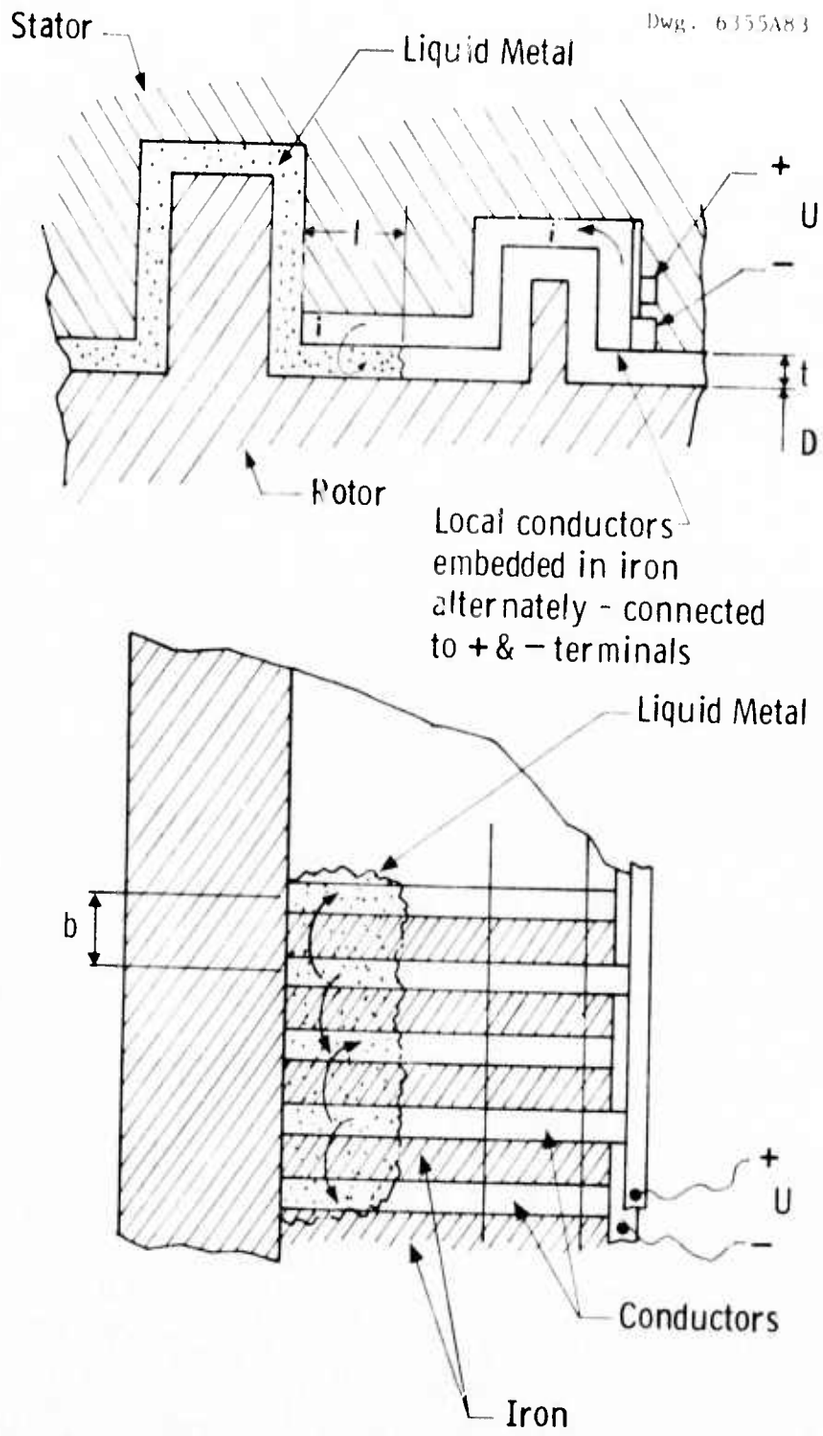

Fig. 4.2.4.6: Self-field electromagnetic (E.M.) containment

where: V = applied voltage between conductors

b = circumferential spacing of conductors

D = collector diameter (1.83 m)

Equations (4.2.4.22) and (4.2.4.23) above, may be combined to find:

$$P = 6\pi D t p_\rho / 5\mu\ell. \qquad (4.2.4.25)$$

For a radial gap (t) of 1.27×10^{-3}m (0.05 in) and a pressure of 27,600 N/m^2 (4 psi):

$$P = 87.5/\ell. \qquad (4.2.4.26)$$

For an acceptable power loss limit of 5 kW, the minimum length of liquid metal extension into the gap, would be:

$$\ell = 87.5/5{,}000 = 0.0175 \text{ m } (0.688 \text{ in})$$

Equations (4.2.4.23) and (4.2.4.24) may be combined to show:

$$V/b = (P_\rho/\pi D\ell t)^{\frac{1}{2}} \qquad (4.2.4.27)$$

For the 5 kW condition, above, the resulting value becomes:

$$V/b = 4.21 \text{ volts/m } (0.107 \text{ volts/in}).* \qquad (4.2.4.28)$$

It can be seen from Equations (4.2.4.26) and (4.2.4.27), that the length "ℓ" cannot be reduced without increasing the power loss, and that increasing "ℓ" (and reducing "P") results in even lower values of (V/b). Therefore, equation (4.2.4.28) shows the maximum acceptable value for (V/b).

The spacing of conductor bars must be selected to minimize the probability of a droplet escaping without "shorting" of two adjacent bars. If a spacing of 3.18×10^{-3}m (0.125 in), is selected, the supply voltage would be only:

$$V \quad 4.21 \times 3.18 \times 10^{-3} = 0.0134 \text{ volts},$$

and the corresponding current (for a full ring) would be:

$$I = 5{,}000/0.0134 = 373{,}000 \text{ A}.$$

*Contact resistance would increase the required supply voltage, but would also increase the power loss.

A power source of this type does not appear to be feasible. If a higher-voltage source is used, with the same bar spacing, Equation (4.2.4.24) shows that the current density would increase proportionally; Equation (4.2.4.22) shows that the axial length of the liquid metal along the bars would decrease in inverse proportion; and Equation (4.2.4.25) shows that the power loss would then increase in proportion to the increased voltage. Therefore this concept does not appear feasible for containment of small droplets, which requires close spacing of conductors and an extremely high-current power source.

External-Field Concept

A practical configuration which will provide either a continuous (uni-directional) circumferential current or a continuous circumferential magnetic flux (independent of load current), has not been found. Therefore, a modification of the self-field concept (Fig. 4.2.4.6) was considered, with magnetic poles of alternate polarity added between the local conductors. A preliminary review of techniques to provide the localized magnetic field, either electromagnetically or with permanent magnets, indicates that the large radial gap and the required small spacing of opposite magnetic poles make it impractical to achieve a sufficiently high field within the specified geometric constraints.

Rotational Force Concepts

Because of the difficulty in providing either circumferential flux or current in the seal annulus, it may be preferable to produce a circumferential force due to field and current in the other two orthogonal directions. The resultant circumferential motion of the liquid metal can then be converted to an axial pressure gradient by the use of angled vanes, such as a "wind-back" seal, or by using a "manometer effect" due to centrifugal force. These concepts have not yet been fully evaluated, but justify additional analysis.

Considering the many possible configurations, it is recommended that further study be made in this category, although no satisfactory arrangement has been found thus far.

A7. Absorbent Wick

The use of an absorbent wick as a seal has the advantage of improved energy absorption for particles of liquid metal, and it also may be used to directly drain the captured material. However, it is not expected that a wick will reduce leakage from a filled annulus of large radial thickness, other than by perhaps improving the wetting action. It may prove advantageous, however, if a flexible material can be found which will fill the radial gap and still permit relative expansion and movement of the rotor. The material then becomes, in essence, a rubbing seal and should be considered as an alternative to the lip-seal or hydrodynamic seal discussed in (A1) and (A3) above. Materials such as "Foametal" or "Feltmetal", elastomer sponge, or other fibrous configurations could be considered. Since experimentation would be necessary to establish flexibility, wear characteristics, and containment adequacy, feasibility cannot be established at this time.

A8. Low-Speed Seal

This concept would include a seal that could be applied when the centrifugal effects could no longer retain the liquid metal against the force of gravity. Neglecting MHD expulsion effects, this "dropout" speed is expected to be about 60 rpm for the rotor.

The power loss for this type of seal will probably be acceptable if the seal area is made small. The complication and added cost of the retraction mechanism suggests that this concept be considered only if simpler rubbing seals (A1 and A3 above) are not acceptable.

A9. Magnetic Fluid

The technology involved in the suspension of a solid electromagnetic filler in a liquid for use as a seal, has been under development by Ferrofluidics Corp. and has resulted in their "Ferrometic" rotary seal. A cartridge seal of this type is presently being tested at the Westinghouse Research Labs. The peripheral velocity limit for this sample is about 7.11 m/s (1400 ft/min), 3.81×10^{-2}m (1.5 in) dia. at 3600 r/min due to temperature rise from the viscous power loss, without cooling. The supplier's literature gives a temperature limit of 107°C (225°F) for continuous operation, probably based on fluid vapor loss. The sales literature gives rpm limits for various shaft diameters which indicate a similar maximum peripheral speed for modular seals. With cooling and fluid replenishment, peripheral speeds as high as 56 m/s (11,000 ft/min) are claimed.

The radial gap in the commercial units, is typically 5.08×10^{-5} to 1.27×10^{-4}m (0.002 to 0.005 in), but the company states that this value can be much larger if required, apparently by increasing the mmf of the magnet and by scaling up the geometry and fluid volume. (The viscous shear area and power loss also would be scaled up.) The pressure capability per seal land, for this radial gap, is about 20,700 N/m^2 (3 lb/in^2). If the present pitch (between lands) of about 1.57×10^{-3}m (0.062 in) is scaled up to a desired radial gap of 1.02×10^{-3}m, it would become:

$$L = (1.02 \times 10^{-3}/1.27 \times 10^{-4})\ 1.57 \times 10^{-3} = 1.26 \times 10^{-2}\text{m}\ (\sim 0.5\ \text{in})$$

This might be reduced with a modified configuration, so that two of these seals could be fit within the collector space allocation.

Present cost of a 3.81×10^{-2}m (1.5 in) dia. cartridge seal is about $750, but the components are relatively simple and the cost of some of the presently used fluids is only about 10 cents per cc. (probably less than $10/seal point). Present fluids have a very high start-up torque (viscosity) at low temperature and may not be compatible with the liquid metal, and a search for a better fluid such as a silicone oil may be necessary. The use of a mineral oil carrier is presently being considered in a Navy program, which utilizes liquid metal current collectors.

A visit to the Ferrofluidics Corporation was made in November of 1972 by Ⓦ personnel primarily to evaluate the feasibility of developing a metallic (liquid metal) magnetic-fluid shaft-seal for large turbine-generators. It was concluded that the magnetic liquid metal, necessary to improve thermal conduction for the high-speed (~ 10.2 m/s, 20,000 ft/min) shaft application, would require a research and development effort, and a program of that nature is under consideration. (Design with a conductive magnetic fluid must also consider the possibility of circulating current losses due to radial field.)

Both of the above approaches, magnetic fluid seal and matnetic fluid conductor, require two steps in the development program; materials (fluid) development, and configuration development. Fluid properties (including magnetic characteristics) are necessary to complete a design study. Presently, it appears that magnetic saturation due to the high circumferential flux of the load current could greatly reduce if not eliminate the effectiveness of a magnetic seal within the current loop. Therefore, although some additional study would be required to verify that the problem cannot be overcome, it appears that these concepts have low probability of success for a short-range program, and have been eliminated from consideration as primary contenders.

A10. Surface Tension/Wetting

The feasibility of retaining the liquid metal in the current collector through the use of surface tension, is strongly related to gap width (rotor/stator) and shear energy input at the surface. The maximum retention capacity can be determined by examining the case of perfect wetting in the sealing zone, and complete non-wetting external to that zone, along an annular gap. For this configuration, the surface tension angle will be zero or parallel to the gap surface.

The annular gap configuration may be approximated by that between two parallel plates, and the retention force would be:

$$F = 2\sigma, \qquad (4.2.4.29)$$

where "σ" is the surface tension of the sealing fluid. The maximum pressure that can be retained will then be:

$$\Delta P_{max} = 2\sigma/h, \qquad (4.2.4.30)$$

where h is the radial (or axial)gap width.

For NaK, the surface tension would be about 1.05×10^{-1} N/m (6.00×10^{-4} lb/in), and the maximum pressure capability for a radial gap of 1.02×10^{-3}m (0.040 in) would be:

$$\Delta P_{max} = 206 \text{ N/m}^2 \ (3.0 \times 10^{-2} \text{ lb/in}^2)$$

The surface tension of NaK is high. By comparison, oils have values of only 2.0 to 6.5×10^{-2}N/m, and water has a value of 7.5×10^{-2}. Mercury has a surface tension of almost 5×10^{-1} N/m, but even this would retain only 980 N/m^2 (1.42×10^{-1} psi) pressure difference. To contain 27,600 N/m^2 (4 psi), the gap width would have to be reduced to 3.62×10^{-5}m (1.4×10^{-3}in) for mercury or 7.61×10^{-6}m (3×10^{-4} in) for NaK. In addition, even these gaps would not be adequate during rotation, with shear energy disruption of the surface.

It is apparent that surface tension cannot sustain any significant pressure difference and therefore cannot be utilized as a primary seal. It is probably possible, although not easy, to place a number of these interfaces in series, with another fluid between them, to increase the pressure capacity. However, the large number required and the shear effect of rotation makes this alternative infeasible. Therefore this concept has been dropped from further consideration.

A11. Solidification

The concept which involves sealing with a locally solidified region of the liquid metal would require a complex thermal or chemical control system. Additionally, the shear area of the seal would have to be made very small because of the increase in viscosity (by a factor of 2 or 3) as the liquid metal approaches the solidification point. Also, the seal could freeze when the rotor is stationary and no viscous heat is generated, greatly increasing start-up torque. Since no simple configuration has been found which would eliminate these problems, no further effort is planned for this concept.

B. CONDUCTING SEAL

B1. Conducting Wick

In the use of a conducting wick as a current collector, the large gap and the need to wet both rotor and stator elements to assure good electrical contact eliminates any improvement in liquid metal retention. Improvement in retention can result only if the effective gap is made smaller or is eliminated. This may be possible by providing a wick which is flexible and will deform as the rotor expands or shifts. As in the case of the wick-type seal, the possible materials would be "Foametal", "Feltmetal", elastomer sponge, or other fibrous materials.

The wick could be divided into a central feed zone and two adjacent drain zones, all made up of the same material, with a small radial gap to prevent aerosol generation. Gas flow may be used to assist drainage and to improve containment.

Since the lip-seal and the hydrodynamic seal (A1 and A3 above) were found to be marginally feasible, the conducting wick applied in a similar manner may also prove to be adequate. However, since material properties such as flexibility, wear rate, and permeability are not established, a complete evaluation of feasibility cannot be made at this time. An experimental program to evaluate various candidate materials is planned. An important consideration to be evaluated during a test program, is the tendency of the wick material to be wiped over the pores at the rubbing interface and possibly interfering with the flow of liquid metal.

B2. Hydrostatically-Positioned Collector

The hydrostatic positioning technique described for the seals (above) can also be applied to the complete collector/seal assembly. The collector may be positioned either axially or radially. If radially applied, the collector ring must be segmented or otherwise flexible enough to permit the changes in diameter required to follow rotor thermal expansion and dimensional tolerance variations. In comparison to the separate seals, this configuration has only one floating member instead of two, but introduces two NaK/copper contact-resistance interfaces in place of one. (It might be feasible to join the two seals to form one floating assembly, and to provide a conducting flexible bellows or spring support of the collector to eliminate a second liquid-metal contact-resistance interface, but this would complicate the designs.)

Many design configurations are possible. Some of the alternatives are listed below:

1) Use of liquid metal, oil, or gas as the positioning fluid.

2) Either annular channels or localized pockets for the liquid metal, for the second fluid, and for the drain chambers.

3) Pressure of a buffer fluid less than, equal to or greater than that of the liquid metal.

Local pockets are expected to improve the stability of the collector ring by providing a restoring moment (or centering force) when the ring is tilted (or radially displaced). An annular ring would permit circumferential flow to equalize the pressures and thereby reduce the restoring force. A configuration containing local pockets, adapted from the "hybrid" pad design, is shown in Fig. 4.2.4.7.

The alternative of an annular groove has the advantage (over pockets) that an increase in the relative motion (angular velocity) of the rotor would probably not increase the liquid metal recirculation requirement, although detailed concepts of both would be required for an adequate comparison. The required collector width to produce 2.48×10^7 A/m^2 (16,000 A/in^2) would be less than 2.11×10^{-3}m (0.083 in) for an annular groove at 1.83m (72 in) diameter.

The use of oil or a gas to provide the collector positioning force would make this independent of magnetic forces that might otherwise alter the operation if the conducting liquid metal is used for this purpose. Gas is probably preferable to oil because of the much lower viscous power loss, although an evaluation of damping requirements should be made, and because separation from the liquid metal does not appear to be a problem with gas. However, the design sealing requirements may be more complicated if a separate system is required for the gas. The permissible pressure of a gas pocket, relative to that of the liquid metal, would be related to the pocket size and geometry.

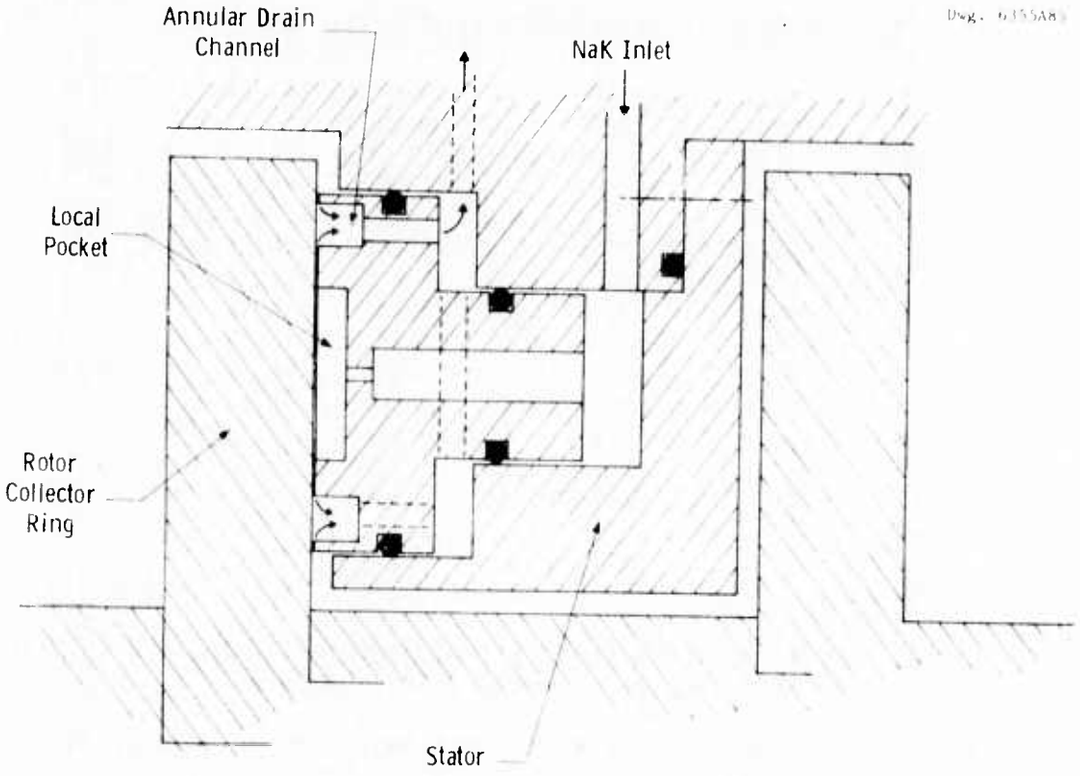

Fig. 4.2.4.7: Adaptation of pad design to annular collector ring

For the present evaluation, a configuration will be assumed, which uses the liquid metal to provide positioning force, and which has dimensions similar to those now being considered for the "hybrid" pad.

Good containment of liquid metal within the collector ring pocket is expected. This is due to the small seal gap, and the gas flow into the annular drain chambers from the machine gap. (The required gas flow velocity and corresponding pressure drop must be determined.) Since the drain grooves are annular, a step or projection could be provided so that the gas seal lips would overlap the rotor and not be directly in-line with the liquid metal seal gap.

The drain channels should be evaluated to assure that they can adequately handle the liquid metal flow without filling or significant accumulation at the bottom of the annular channel. Assembly requirements will probably necessitate a split seal ring, and two or more segments may be preferable to a rotationally symmetric design to prevent leakage at the split. (Sealing of the stator split may still be required.)

For power loss calculations, it will be assumed that the collector ring is insulated to prevent current flow except in the area of the local

pressure pockets. This reduces the MHD-induced viscous power loss, and also reduces the recirculating (eddy) current which produces a power loss and an ejection pressure.

Since the MHD force occurs only in the pocket, where the tangential flow is blocked, the viscous losses will be primarily in the narrow seal gap. This can be estimated from Fig. 4.2.4.4 of concept A2, as less than 1.5 kW for a radial length of 2.1×10^{-2}m (0.825 in) and a liquid metal gap of 1.27×10^{-5}m (0.0005 in).

The load current ohmic loss due to bulk resistivity of the liquid metal in a cylindrical volume was previously defined as

$$P_B = J^2(\text{vol})/\sigma,$$

where: σ = conductivity of the liquid metal (2.20×10^6 mhos/m for NaK).

For 2.48×10^7 A/m^2 (16,000 A/in^2) current density and a pocket cross-sectional area of 1.73×10^{-4}m^2 (0.268 in^2), the power loss becomes

P_B = 48.4 kW per meter (1.23 kW/in) of pocket depth (for each pocket).

For 70 pockets with a depth of 1.52×10^{-3}m (0.06 in), the total power loss due to bulk resistivity would be.

P_B = 5.16 kW.

It will probably be necessary to add dams or otherwise design to prevent MHD-induced viscous losses in the liquid-metal supply annulus behind the collector ring. The load current ohmic loss in this annulus will depend on final dimensions, but a rough estimate will be made based on the assumptions that the radial width is the same as the pocket diameter, 1.48×10^{-2}m (0.583 in), the depth is 3.18×10^{-3}m (0.125 in), and that the full area is uninsulated. The conduction area and current density are

$$A = 1.83\pi(1.48 \times 10^{-2}) = 8.5 \times 10^{-2}\text{m}^2 \ (132 \text{ in}^2)$$

$$J = 300{,}000/8.5 \times 10^{-2} = 3.53 \times 10^6 \text{A/m}^2 \ (2{,}270 \text{ A/in}^2)$$

The power loss becomes:

$$P_B = (3.53 \times 10^6)^2(8.5 \times 10^{-2})(3.18 \times 10^{-3})/2.2 \times 10^6$$

$$P_B = 1.53 \text{ kW}.$$

The contact resistance loss for each interface pair due to load current will be:

$$P_C = \epsilon_k JI, \qquad (4.2.4.31)$$

where: ε_k = specific contact potential (4.1×10^{-9} Vm^2/A). The total for the pockets and the annular supply ring would be

$$P_C = 4.1 \times 10^{-9} (300{,}000)(2.48 \times 10^7 + 3.53 \times 10^6)$$

$$P_C = 30.5 \text{ kW} + 4.33 \text{ kW} = 34.8 \text{ kW}.$$

Due to the larger area, it is seen that only about 15% of the contact loss is associated with the annular supply channel.

The eddy-current ohmic power loss per unit area, without laminations and assuming $\varepsilon_k = 0$, would be

$$P = \frac{B^2 V^2 L^2 \sigma}{12\, d} = 79.6 \text{ kW/m}^2 \text{ (51.4 W/in}^2\text{)} \qquad (4.2.4.32)$$

where: B = flux density normal to collector (0.1 T)

V = linear velocity of collector (17.3 m/s)

L = collector width (1.48×10^{-2}m, max)

σ = liquid metal conductivity (2.2×10^6 mhos/m)

d = conducting gap thickness (1.52×10^{-3}m)

The power loss would be less than that shown above, since the conduction pocket area is circular rather than rectangular. The total eddy-current power loss for the 70 pockets would be less than

$$P = 79.6(70)(1.73 \times 10^{-4}) = 0.964 \text{ kW}$$

The following table summarizes the power loss approximations. These are meant only to establish the relative significance of each type of loss, since the values may change greatly as a collector design is developed.

Type of Loss	Power Loss (kW)
Viscous	Less than 1.5
Bulk Resistance	
Pockets	5.16
Supply Ring	1.52
Contact Resistance	
Pockets	30.5
Supply Ring	4.33
Eddy Current	0.96
Total	44.0

Review of the table leads to the conclusion that a reduction in current density to reduce contact losses, should be made by increasing the number of pockets or by increasing the pocket area.

The leakage of a circular pad (hybrid design, Eq. 4.2.5.5) would be:

$$Q_p = \frac{\pi c^3 P_1}{6\mu \ln(D_2/D_1)} \qquad (4.2.4.33)$$

where: Q_p = leakage flow
c = seal clearance
μ = absolute viscosity
D_2 = outer diameter of seal
D_1 = inner diameter of seal
P_1 = pocket pressure

For the pad presently under consideration, the following values may be assumed:

$c = 1.27 \times 10^{-5}$m (5×10^{-4}in)

$\mu = 5.2 \times 10^{-4}$ N-s/m^2 (7.55×10^{-8}lb-s/in^2)

$D_2 = 2.1 \times 10^{-2}$m (0.825 in)

$D_1 = 1.48 \times 10^{-2}$m (0.583 in)

$P_1 = 137{,}900$ N/m^2 (20 lb/in^2)

$A_C = 1.73 \times 10^{-4}$m^2 (0.268 in^2)(conduction area)

This results in a leakage flow of:

$Q_p =$ 50 cc/min (0.051 in^3/s).

For 300,000 amperes and 2.48×10^7A/m^2 (16,000 A/in^2), the required area for all the pads on a single collector is 1.21 m^2 (18.75 in^2), and therefore 70 pads will be required (this would give about 8.13×10^{-2}m (3.2 in) of circumference per pad), and the total leakage would be:

$Q_p =$ 3,500 cc/min (0.356 in^3/s).

For comparison, from Eq. (4.2.4.4), an annular gap would have a leakage flow (inward and outward) of approximately:

$$Q = 2 \times \frac{\pi c^3 P_o}{12\mu L/D}, \qquad (4.2.4.34)$$

where: D = collector diameter

L = seal length

If the seal length is taken to be the same as that for the pad ($\frac{D_2-D_1}{2}$), the flow may be calculated as:

$$Q = 10{,}100 \text{ cc/min } (10.3 \text{ in}^3/\text{s}).$$

This is almost three times as great as that for the pads.

It is possible, however, to machine local pockets in a collector ring, in which case the leakage will be less than or equal to that for the pads. (The viscous power loss would be greater if the seal area is greater than that for the pads.)

The effect of gravity head (about 15,170 N/m^2, 2.2 lb/in^2, for an annular ring) is relatively small, but should be considered when a firm design is established.

Ejection pressure built-up by rotational forces may be evaluated (approximately) on the basis of a model consisting of a thin annular liquid-metal ring of radial thickness "L". If the rotational velocity of the liquid ring is assumed to be half that of the rotor, the pressure at the outside diameter, required to constrain this fluid, would be:

p = rotational force/area

$$p = \frac{(2\pi RwL\rho)R(\omega/2)^2}{2\pi Rw} = L\rho R\omega^2/4, \qquad (4.2.4.35)$$

where: w = ring width

L = radial thickness

ρ = mass density of liquid metal

R = radius of thin ring

ω = angular velocity of rotor.

The pressure may be evaluated with the following values used in the above equation

$L = 2.54 \times 10^{-2}$m (1.0 in)

$\rho = 865$ N-s^2/m^4 (1.68 lb-s^2/ft^4)

$R = 9.15 \times 10^{-1}$m (36 in)

$\omega = 18.8$ rad/ s (180 r/min)

The result is the small pressure:

$p = 1790$ N/m^2 (0.259 psi), for 2.54×10^{-2}m (1.0 in) radial thickness.

The ejection pressure resulting from load-current, assuming a single-turn module, would be:

$$P_L = 6.28 \times 10^{-7} I_p^2, \qquad (4.2.4.36)$$

where: I_p = load current per unit circumference (A/m)

P_L = ejection pressure (N/m^2).

For the assumed current density of 2.48×10^7A/m^2 (16,000 A/in^2), and an effective pad diameter of 1.48×10^{-2}m (0.583 in), the current per unit of collector circumference would vary from zero at each end to a peak at the central line (of maximum radial height) of I_p = 367,000 A/m (9,330 A/in). This is equivalent to a peak pressure of:

$$P_{L_{max}} = 84{,}600 \text{ N/m}^2 \text{ (12.3 lb/in}^2\text{)}.$$

This value is sufficiently large, that a more detailed analysis of the load-current influence on positioning (gap) and flow rate is required.

The interaction of radial field "B" and axial current density "J" (for an axially-applied collector ring) results in a circumferential body force which is similar to a gravitationally-induced pressure head. The peak pressure, at one circumferential point, will be:

$$P_{max} = (J \times B)d, \qquad (4.2.4.37)$$

where: $d = 14.8 \times 10^{-3}$ m (0.583 in. pocket diameter)

$J = 2.48 \times 10^{7}$ A/m^2 (16,000 A/in^2)

$B = 0.05$ T

$P_{max} = 18{,}300$ N/m^2 (2.66 lb/in^2).

For a radially-applied collector the result would be similar except that an axial field would be used in the computation. For an axial field of 0.1 Tesla, the maximum pressure would be:

$$P_{max} = 36{,}600 \text{ N/m}^2 \text{ (5.32 lb/in}^2\text{)}.$$

For an axially-applied collector ring, radial thermal expansion relative to the rotor, and the rotor shift due to the 0.012 in. radial bearing clearance, should not affect operation. However, expansion of the collector ring relative to the stator could cause binding or increased friction and prevent axial movement. Sufficient clearance must be allowed to accommodate this relative growth, or the ring should be segmented. A radially-applied collector would also have to be segmented to permit relative thermal expansion. In both cases, static seal friction must be made negligible relative to the restoring force which positions the collector ring.

The force required to oppose the torque and prevent rotation due to viscous drag would be small (unless a rub occurs). From Eqs. (4.2.4.8) and the previously determined viscous drag power loss of less than 1.5 kW, this force will not exceed:

$$F_K = 87.2 \text{ N (19.6 lb)}$$

A detailed examination of thermal gradients in the collector ring will be required to assure that distortion of the sealing surface does not occur. Additional areas of concern which should be investigated when a more definite design is established are the stability of the seal, in relation to oscillation of the ring or segments (both parallel movement and tilting of the ring) and in response to acceleration loading. The possibility of oxide material reaching the seal/rotor interface and causing abrasive wear should also be considered.

Heat transfer to remove the viscous and electrically-induced losses from the collector ring will depend on the cooling techniques used in the rotor and stator. The temperature does influence the seal gap and flow rate of the liquid metal, but if the operating temperature is held below about 93°C (200°F), the variation is expected to be less than 15%. This effect should be reviewed again when a more-definite design is selected.

The acceptability, from an electromagnetic point of view, of local conduction paths at each pocket, as opposed to a rotationally symmetric collector, should be verified. The pocket width used in this sample analysis subtends an angle of 0.927° with a spacing (pitch) of 5.15°, and covers 18% of the circumference. For a multiple-turn machine, the possible effect of this lack of rotational symmetry on the magnetic forces in the liquid metal should also be investigated.

The possible "aging" (loss of elasticity) of the static seals should be investigated if a material such as Buna-"N" is used for this application. However, minor leakage at these sealing points should not be critical.

A radial application of the collector segments might permit a smooth cylindrical rotor and therefore a simpler assembly. An axially-applied collector would probably also be split at least on the horizontal centerline, for assembly purposes. The collector ring can be pushed back to increase the clearance for assembly. Additional design effort is required before an assembly procedure is established.

The ability of the collector to follow movements of the rotor will establish permissible run-out tolerances, and this must be determined through further design and perhaps experimentation. Flatness of an axially-applied collector (or circularity of a radially-applied seal) may be a manufacturing problem due to the small clearance ($\sim 1.27 \times 10^{-5}$m, 5×10^{-4}in) and large diameter ($\sim$ 1.83m, 72 in), unless the collector is segmented or made sufficiently flexible so that it conforms to the rotor. Fabrication cost should be investigated when a more definite design is established.

Under ideal operating conditions, no collector wear would be expected since no mechanical contact occurs, unless contaminants block the restrictions or oxide particles result in abrasive wear. Seal replacement or repair would probably be difficult and expensive.

In summary, the hydrostatically-positioned collector ring is very similar to the hybrid pad design. It has the advantage, however, that collector rotation does not tend to drag liquid metal from the sealed area. Also, more design flexibility is provided since gas-pressured positioning pockets may be interspersed along the circumference. This is particularly important if contact resistance is a significant factor, since the number of contact pairs can be reduced from two to one. (The hybrid pad can probably be extended circumferentially to provide an intermediate configuration with similar advantages.) Conformity of a large-diameter ring to the mating rotor may be a problem unless the ring is segmented or flexible. The concept appears to be feasible but its success is dependent upon the maintenance of a very small clearance without rubbing.

The design study will be continued to evaluate alternative configurations, to optimize the positioning stability, and to establish an experimental program to demonstrate feasibility.

B3. Flooded Labyrinth

A (semi-) flooded labyrinth will not be effective with the large radial clearance necessary to prevent rubbing and the low leakage velocity for reasonable recirculation rates. It may be used as a retractable or hydrostatic/hydrodynamically-positioned device, but these are covered in other sections of this report. Another alternative is the addition of solid material particles between labyrinth seal strips. If the particles are sized or shaped such that they cannot escape through the seal gap, and if the material is selected so that the liquid metal readily wets the particles, then it may be possible to retain the liquid metal within the conducting seal. This concept then becomes similar to the Variable-Viscosity Buffer Material (A5 above), which has more flexibility in material selection since either the liquid metal or another fluid may be used. Therefore the Flooded-Labyrinth concept will not be considered further.

B4. Conducting Bearing

A roller or ball bearing may be used to maintain concentricity between the stator (outer race) and the rotor (inner race), to improve the performance of a lip-type seal. A sealed bearing might be used, eliminating the need for a separate sealing device. If the sealed bearing is filled with liquid metal, then the rolling elements will be lubricated by the liquid metal and an electrical conduction path would be provided between the rotating and stationary parts. (Provisions must be made for relative expansion in the radial and axial directions). A preliminary survey shows no bearings available which are intended for operation as high as 180 rpm for diameters of about 1.83 m (72 in.). Therefore this concept will not be investigated further at this time.

C. LOW-SPEED FLOODING OR LOW-SPEED BRUSH CONTACTS

C1. Pressure-Controlled Liquid Volume

If the machine is initially flooded with liquid metal, then as the rotor is brought up to speed, projecting collector rings will act as viscous pumps tending to increase the fluid pressure in the collector region. If the liquid metal supply system is designed to maintain a constant pressure in the collector, and if this pressure corresponds to a semi-filled collector (the outermost, conducting region of the collector would be completely filled) at full speed, then the fluid in the machine gap will flow toward the collector as the speed is increased and will be drained into the recirculation system until the proper fluid level is reached in the collector. As the speed is reduced and the centrifugal pressure reduced, the fluid will be pumped back into the collector and eventually into the gap, flooding the machine at standstill. In this manner, an acceptable viscous power loss may be achieved.

The part-speed power loss of this system would have to be evaluated and the effect of MHD pumping of the liquid metal must be included. However, since the machine insulation would have to be designed for flooded operation, and since the objective of this study is to develop collectors for an unflooded machine, this concept will not be carried further.

C2. Low-Speed Brush/High-Speed Liquid

The use of solid brushes at low speed which are retracted at high speed after injection of liquid metal permits the use of liquid metal only at the high speeds where brush wear and power loss would be high and where centrifugal containment of the liquid is effective. However, the cost of a dual system will be large, periodic replacement of brushes will be required (and this requires removal of the liquid metal and decontamination of the machine), the brush material would probably have to be compatible with the liquid metal, and the brush wear debris must be contained. Total size of the dual system may also be a problem.

Although this concept appears to be technically feasible, it does not seem to be a practical solution to the collector problem and will not be considered further, in the present study.

C3. Gas Injection

An alternative way to reduce viscous power loss in a flooded machine is the injection of cover gas to displace the liquid metal at the rotating or stationary surfaces (or both). Injection of gas may be local or through porous walls, and may be continuous or only at high speeds. However, as in concept C1 above, the machine insulation must be designed for flooded operation. Also, since the objective of this study is the development of unflooded machine collectors, this concept will not be evaluated further.

D. Axial Injection (or Radial Ejection)

D1. Inertial Containment

Inertial containment would utilize the kinetic energy of the liquid metal, as it enters the collector, to contain or rotate the fluid within the collector annulus. Probably the most effective configuration would be tangential inlet ports at both sides of the collector, causing unidirectional rotation of the liquid metal annulus, with tangential exit ports near the center of the collector width. Wind-back type grooves between the inlet and exit ports may assist in preventing leakage flow out of the collector region. Analysis of the velocity distribution in such an annulus would be difficult when the viscous drag at the collector surfaces are considered. At present, it is felt that the probability of developing a feasible configuration of this concept is small, and therefore a detailed analysis is not justified.

D2. Venturi Effect

Proper orientation of the liquid metal inlet flow and the shaping of the annular passage to minimize disturbance and to guide the liquid directly toward the exit, would reduce the tendency for aerosol formation and leakage from the collector. The liquid metal inlet could be either in the rotor or the stator, but rotation of the rotor should be designed to encourage flow along the normal path rather than oppose it. However, due to the large annular gap area, the flow rate in the axial or radial direction would have to be very large to provide sufficiently high velocity to create a venturi effect for containment. Therefore, this concept will not be pursued further.

E. Zero-Pressure (Free Fall)

E1. Variable-Area Annulus

This technique is similar to the "Deep-Groove Labyrinth" system (A4) described above, except that the cross-sectional area of the collector annulus is varied to permit a matching of inertial head with gravitation head to prevent a pressure rise from the liquid metal inlet at the top, to the exit at the bottom of the annulus. The area variation could be obtained either by tapering the radial gap thickness from the top to a smaller value at the bottom, or by varying the width in a similar manner. The possible advantage of this technique is a lower liquid metal recirculation flow rate, since the wall friction drag is not required (and will be assumed equal to zero for the initial computation). Bernoulli's equation, for constant pressure and negligible friction factor, becomes:

$$v_1^2/2g + Z_1 = v_2^2/2g + Z_2 \qquad (4.2.4.38)$$

Examining this expression from inlet to exit gives:

$$\Delta(v^2) = 2g\Delta Z = 2gD = 35.9\ m^2/s^2\ (386\ ft^2/s^2)$$

For example, if $v_1 \approx 0$, then $v_2 \approx 5.99$ m/s (19.7 ft/s), or:

$v_1 = 1.52$ m/s (5 ft/s); $v_2 = 7.10$ m/s (20.4 ft/s)

$v_1 = 3.05$ m/s (10 ft/s); $v_2 = 7.66$ m/s (22.0 ft/s)

Since the inlet and exit flow rates must be equal, the annulus cross-sectional area must vary inversely with the velocity. If the channel at the exit is 3.18×10^{-3}m (0.125 in.) radially and 6.35×10^{-3}m (0.25 in.) wide, since the exit velocity is relatively constant at ~6.10 m/s (20 ft/s), the flow rate through two parallel paths would be:

$$Q = Av \approx 14{,}750\ cc/min\ (15.0\ in.^3/s)$$

The inlet width could be varied depending on the selected velocity. For an inlet velocity of 1.52 m/s (5 ft/s), the width of a 3.18×10^{-3}m (0.125 in.) radial gap would be:

$$w = (6.10/1.52)\ 6.35 \times 10^{-3} = 2.54 \times 10^{-2}\text{m}\ (1.00\ \text{in.})$$

The calculated velocities were not negligible in terms of wall-friction pressure drop (even for a zero inlet value), and therefore this approach, at best, must be a combination with that of concept A4. For simplicity, then the concept of concept A4 should be preferred, since the annulus is then of uniform cross-section. The variable-area concept should therefore be dropped from further consideration.

F. Constant-Speed Seal Rotor

Rotation of liquid metal in the collector annulus may be achieved by electromagnetic or injection inertial forces as described above, or through mechanical or viscous shear forces induced by a separately rotating ring. In one possible form, this ring could be the collector well itself, as a rotating "U"-shaped channel with both a rotor and stator collector ring projecting into the liquid-metal filled well. The ring (well) could be hydrostatically floated on its outside diameter to provide the bearing function, and if cover gas were used as the hydrostatic fluid, it might also be allowed to escape in a tangential direction to provide a rotational reaction force. In addition to machining complexity, assembly and liquid metal supply and drainage would be difficult. Therefore, a detailed analysis of this design will not be made.

4.2.4.3 Summary of Results

Of the 25 to 30 concepts that were studied, three have been selected for continued development. Two of these are hydrostatically-positioned (the seal A1, and the collector ring B2) and have similar advantages. The ability to maintain a very small clearance gap, between the large-diameter rings and their mating rotor surfaces, is the primary area of concern. The rings will probably be segmented or made flexible to improve conformity to the rotor surface.

The third selected concept uses a simple, inexpensive lip-type oil seal for the large-motor applications with tip speeds of about 3500 fpm or less. Experimental evaluation of this concept should be relatively simple.

Further study of concepts utilizing electromagnetic retention forces will be pursued in order to achieve a practical configuration. Analysis shows that adequate forces can be achieved with reasonable current and flux densities, and acceptable size and power loss.

A number of concepts are dependent upon the development of new materials, and further effort in this area is expected to be productive; in particular, the characterization and evaluation of presently available felt-, foam-, and wick-type materials for sealing or impregnation with liquid metal.

4.2.5 Hybrid Collectors

The hybrid collector is in general a cross between a solid brush and a liquid metal annulus current collector. Specifically the hybrid collector consists of hydrostatically positioned pads which utilize liquid metal for hydrostatic support as well as current transfer. Each hybrid pad is designed such that the liquid metal is confined to sealed flow paths.

The present objectives are: 1) to establish collector geometry for a typical application, 2) to define problem areas for future study, and 3) to establish collector feasibility.

Table 4.2.5.1 is a list of general requirements that are used to evaluate operational feasibility for the hybrid collector. These general requirements apply to any homopolar machine that would use a hybrid current collector. Table 4.2.5.2 is a list of specific requirements for a hybrid current collector when applied to a chosen application, which in this case is an 8000 horsepower, 500 rpm motor.

A schematic of the hybrid current collector is shown in Figure 4.2.5.1. The stator, represented by the shaded portion, houses and provides support for the hybrid pads. By design, movement of the pads is restricted to reciprocating motions along their axial centerlines. Current is transferred from the rotor to the stator or vice versa through the pads. Liquid metal flows into and out of the pad through holes in the stator. The confinement buffer gas flows toward the pad from the inside of the machine (i.e., the inside of the machine is pressurized with buffer gas). Figure 4.2.5.2 shows a typical hybrid pad, revealing current transfer and supporting fluid flow paths. A detailed description and analysis of the current transfer and fluid flow for the hybrid pad will be covered in a later section on theory.

Figures 4.2.5.1 and 4.2.5.2 show axially mounted hybrid pads. Location of the pads on one of the rotating ring's flat sides, rather than on its curved circumference (radially mounted pad), was selected here because:

1) The machining costs associated with matching flat surfaces are expected to be less than the costs associated with matching curved surfaces.

2) The general theory for the flat surface type collector is applicable to the rounded surface. If a distinct advantage is found for the radially mounted over the axially mounted collector, the analysis would remain valid.

TABLE 4.2.5.1 - General Requirements for Reversing Collectors

1. Horizontally mounted machine.
2. Variable speed with reversing capability.
3. Max. current = 300,000 A.
4. Max. collector current density = 2.48×10^7 A/m^2 (16000 A/in^2).
5. Max. collector cross-sectional space 0.038 m axially by 0.038 m radially (1.5 in x 1.5 in).
6. Max. allowable collector loss = 2% total power.
7. Liquid metal leakage to be near zero.
8. Collector must pass 150% rated current at zero speed for 10 secs.
9. Collector must be operable cold without pre-heating.
10. Collectors for a machine must be supplied from a common liquid metal source.
11. Collector must be capable of deceleration from full speed forward to full speed reverse in several seconds.
12. Collector shall be designed for sudden stops.
13. Collector shall be designed for sudden load changes.

TABLE 4.2.5.2 - Specific Requirements for Typical Application

1. Type machine = motor for a torque converter.
2. Power = 5966 kw (8000 hp).
3. Speed = 8.3 r/s (500 rpm).
4. Collector dia. = 0.864 m (34 in).
5. Current = 250,000 A.
6. Collector radial flux = 0.05 T.
7. Collector axial flux = 0.1 T.
8. Number of collectors = 8.
9. Number of turns = 2.

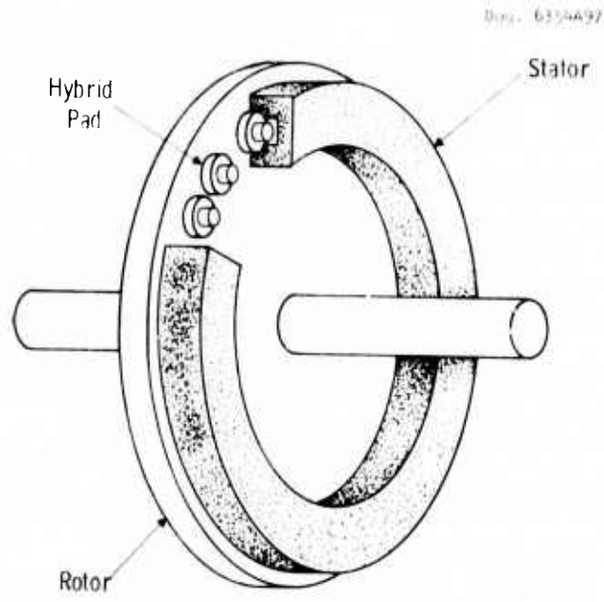

Fig. 4.2.5.1: Hybrid pad current collector schematic

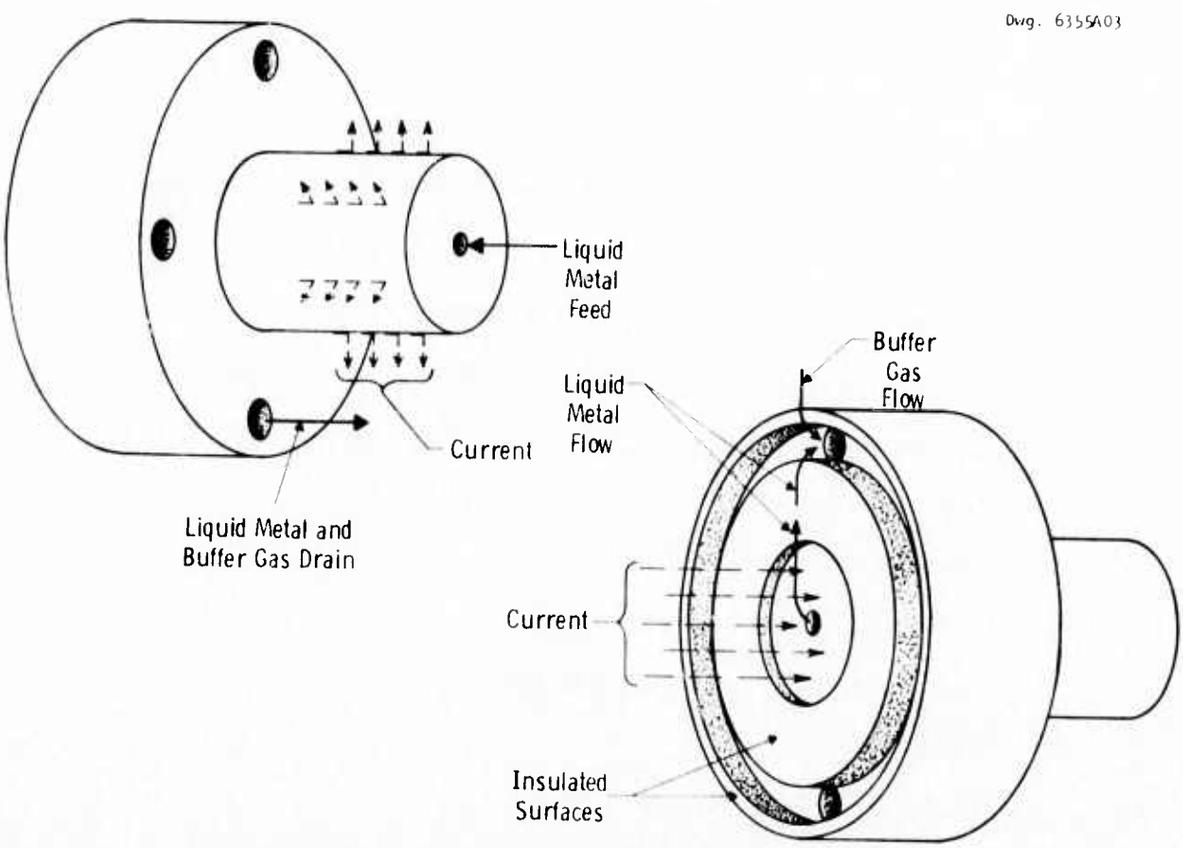

Fig. 4.2.5.2: Typical hybrid pad

3) For some or all of the radially mounted collectors, the MHD force is always in the direction of rotation which tends to encourage leakage. The axially mounted collector can be applied such that the MHD force is either with or against the direction of rotation.

Typical current collectors are illustrated schematically in Figure 4.2.5.3. In all cases, the current (I) is the useful load current being transmitted out of the rotor and the magnetic field (B) is a stray field from the excitation coil. For the axially mounted collector the MHD force due to the interaction of the load current and the magnetic field can be directed either in the same direction (Figure 4.2.5.3a) or opposite direction (Figure 4.2.5.3b) to the rotor viscous drag force. These forces act on the liquid metal which is contained between the hybrid pad and the rotor.

The direction of the MHD force for the radially mounted collector can likewise be in either direction as shown in Figure 4.2.5.3c and 4.2.5.3d. A similar analysis can be made regarding the load current loop ejection force direction for both axial and radial pad placements. Because of construction and assembly complications, the design depicted by Figure 4.2.5.3c is not considered to be practically feasible.

Figure 4.2.5.4 is a schematic of the homopolar motor which is being used as a typical application for the hybrid collector. The collectors are distributed in four regions of the motor with the current and flux directions defined for each region. For convenience, the current collectors are assumed to be placed on the rings such that the MHD force opposes the viscous drag force. Such force opposition will likely aid in confining the liquid metal, but this must be proven. With axial pad placement, as assumed, the load current loop ejection force is always directed radially outward. Figure 4.2.5.5 depicts the four machine collector regions, each complete with directions of the load current, ambient magnetic field, and associated pressure forces acting on the liquid metal. Power loss and confinement pressure relationships based on the forces displayed in Figure 4.2.5.5 are derived in the following section on theory.

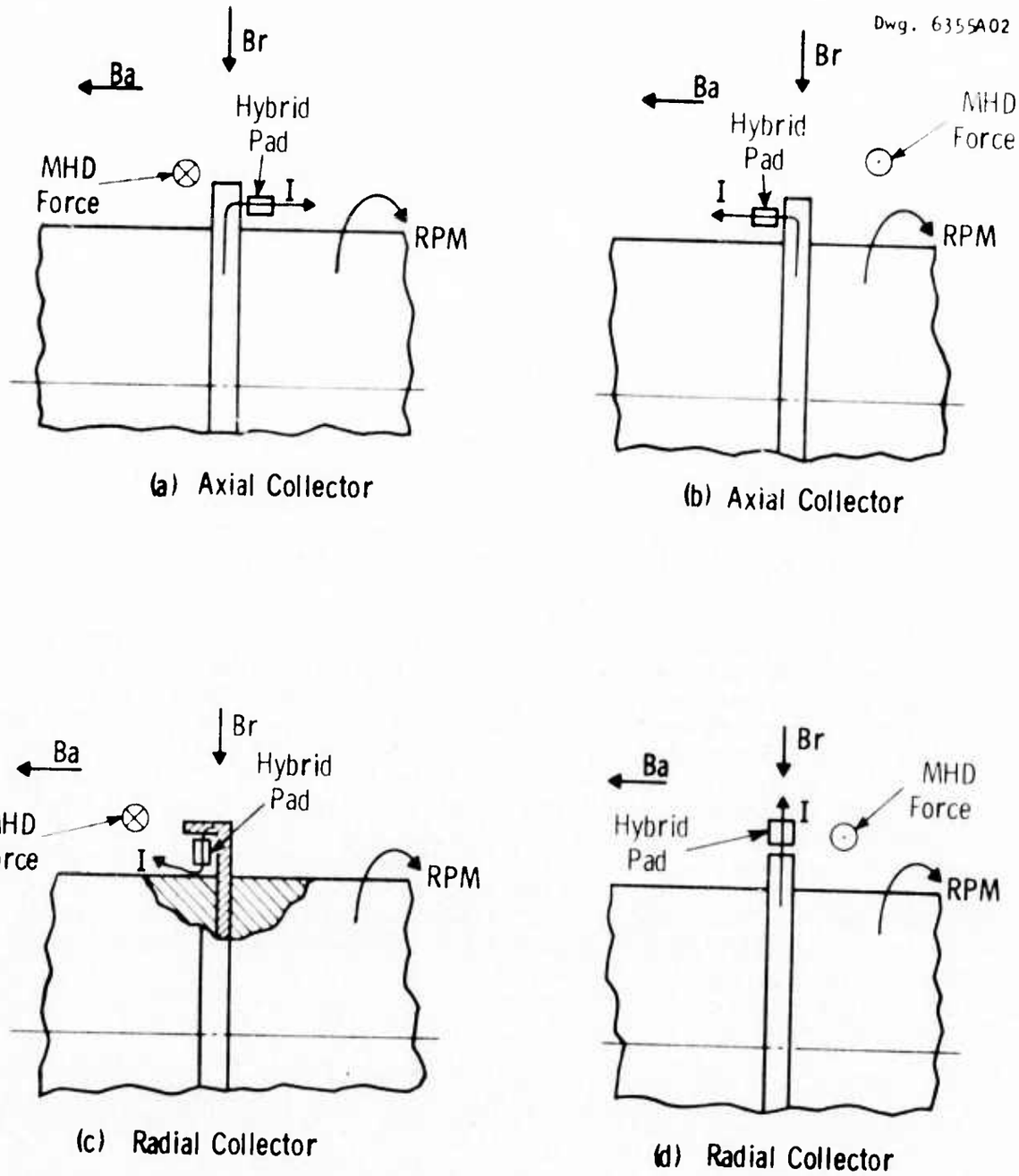

Fig. 4.2.5.3: Axial and radial current collector schematic

Dwg. 6354A98

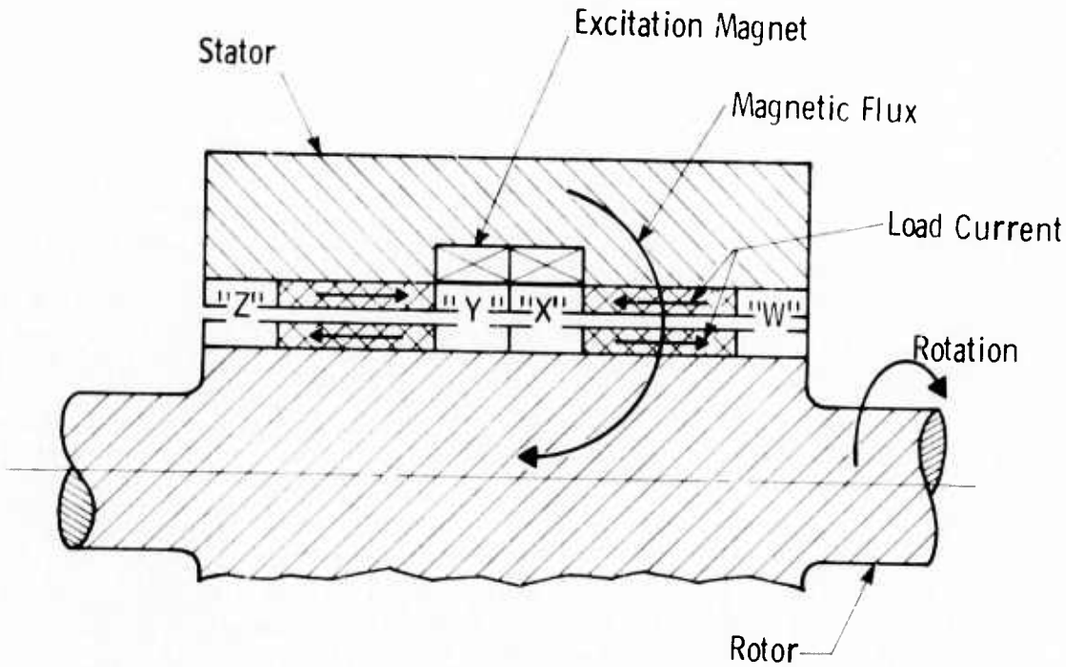

Collector Region	Rotor Current	Axial Flux	Radial Flux
W	Out of Rotor	←	↓
X	Into Rotor	←	↓
Y	Into Rotor	←	↑
Z	Out of Rotor	←	↑

Fig. 4.2.5.4: Homopolar motor schematic

Dwg. 2570272

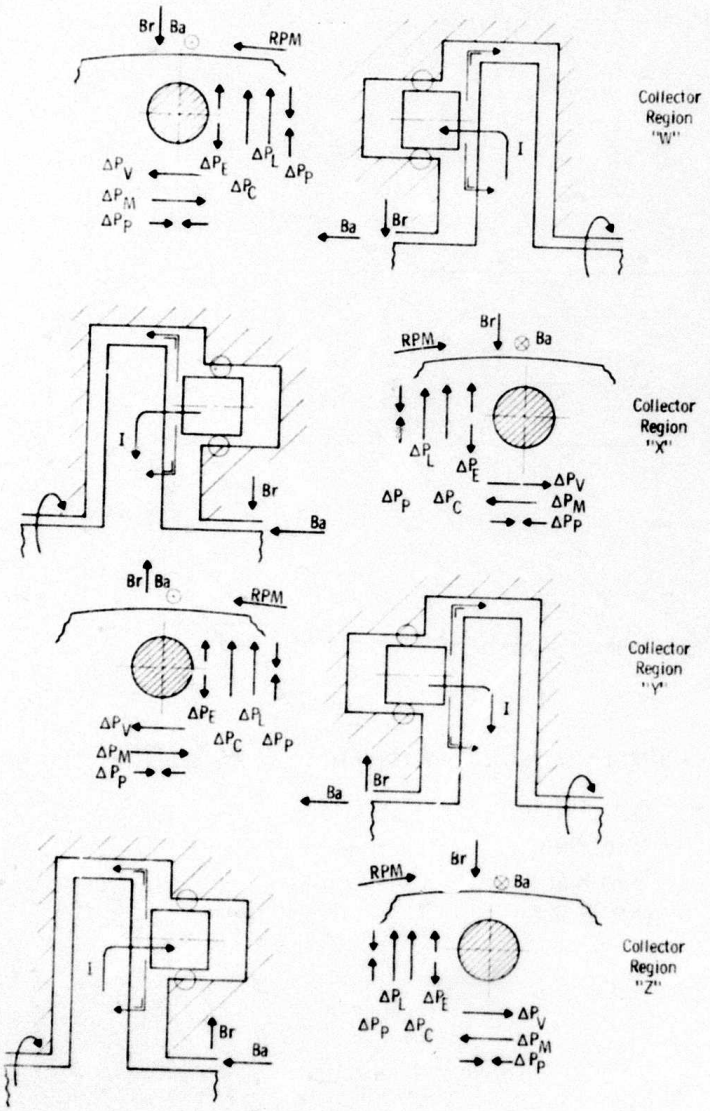

All pressures are acting on the liquid metal that is confined between the hybrid pad and the rotor.

ΔP_V = Viscous drag pressure due to fluid shear

ΔP_M = Electro-magnetic pressure due to the load current crossed into the radial magnetic field

ΔP_L = Load current loop pressure due to the current loop made by the rotor and stator bars

ΔP_C = Centrifugal pressure

ΔP_E = Eddy current ejection pressure due to the eddy current loop self-induced field

ΔP_P = Pinch confinement pressure due to the load current crossed into the load current induced azimuthal magnetic field

I = Load current
Ba = Axial magnetic field
Br = Radial magnetic field

Fig. 4.2.5.5: Schematic of collector regions for the homopolar motor

4.2.5.1 Theory of the Hybrid Collector

4.2.5.1.1 Hydrostatics and Liquid Metal Flow

Consider the hydrostatically positioned pad in Figure 4.2.5.6. The liquid metal flows axially toward the rotor through the center of the pad and then, when it reaches the rotor, radially outward over the pad face. The liquid metal is then collected in the pad's circumferential annulus, and drained to a sump. The buffer gas flows radially inward over an outer circumferential containment labyrinth and is collected in the circumferential annulus with the liquid metal. The buffer gas is then drained to the sump with the liquid metal.

Assume:

1) Lift due to containment labyrinth is negligible, i.e., $p_3 << p_1$.

2) p_2 is approximately equal to atmospheric pressure and can be assumed equal to zero when all other pressures are gage pressures.

3) Pad face liquid metal flow velocity is greater than the rotor collector velocity.

4) The hybrid pad cross section is circular.

The lift force due to the pressure profile over the pad face is:[6]

$$F_L = \frac{P_1 A_L}{K_p}, \text{ N.} \qquad (4.2.5.1)$$

where:

p_1 = pocket pressure, N/m^2.

A_L = projected land area. For the case of the circular pad displayed in Figures 4.2.5.6 and 4.2.5.7, $A_L = \pi(D_2)^2/4$, m^2.

K_p = pressure factor. The pressure factor is a function of geometry, and for the circular pad

$$K_p = \frac{2 \ln (D_2/D_1)}{1 - (D_1/D_2)^2}, \text{ dimensionless.}$$

Dwg. 6354A39

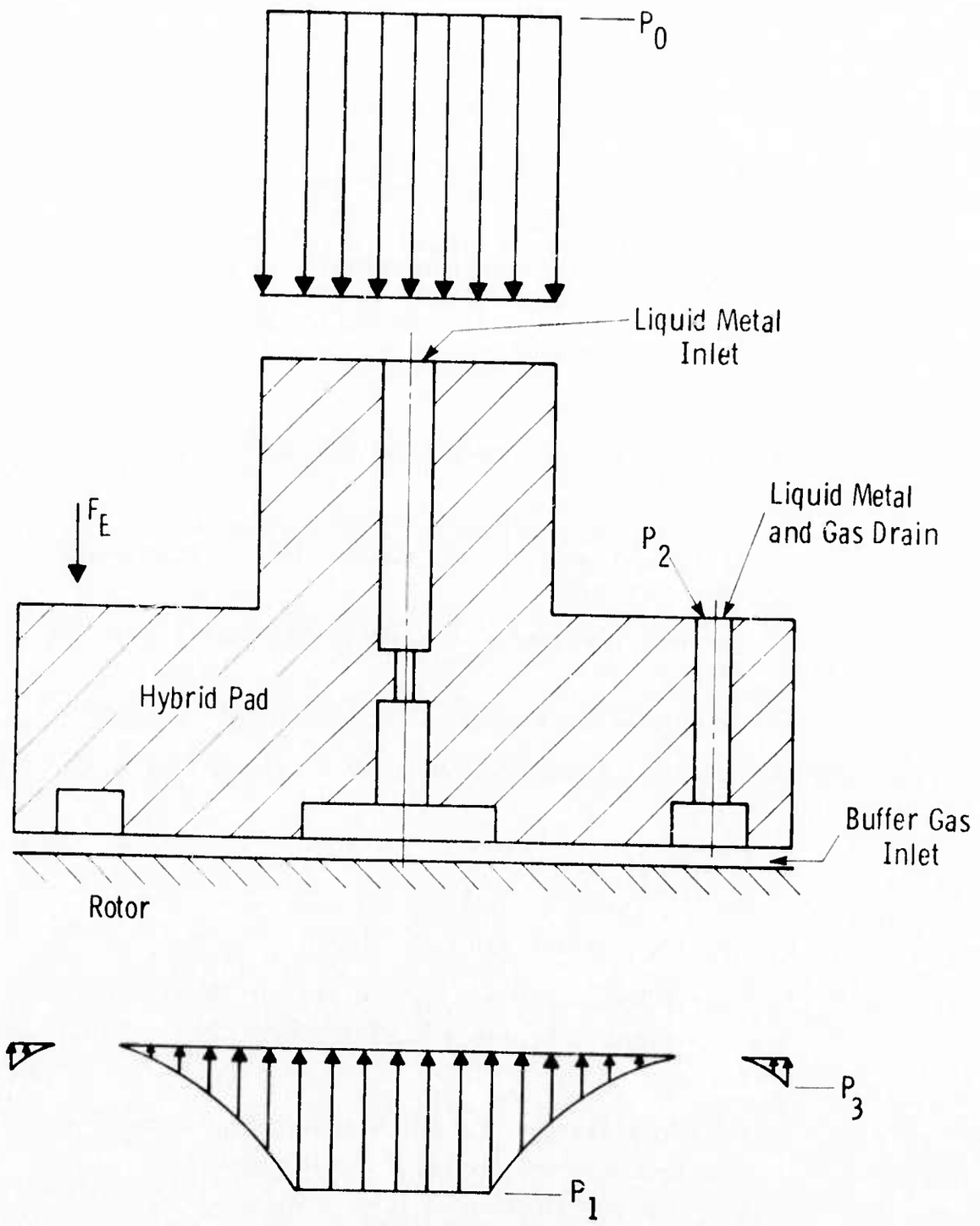

Fig. 4.2.5.6: Hydrostatically positioned pad

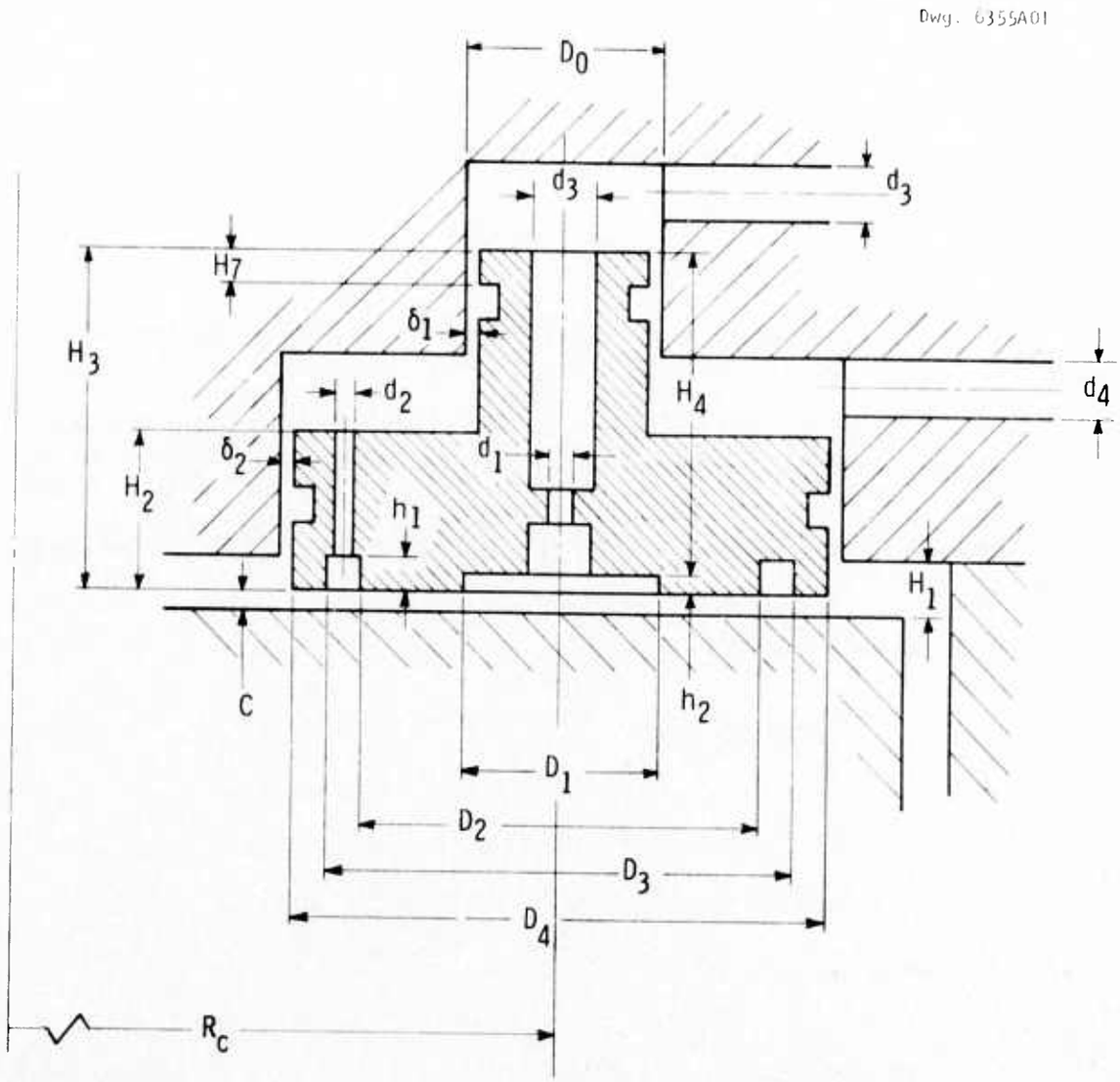

Fig. 4.2.5.7: Hybrid pad geometry

An outer stem force opposes the lift force. The outer stem force is given by the following expression.

$$F_o = P_o A_o, \text{ N} \qquad (4.2.5.2)$$

where:

P_o = liquid metal supply pressure, N/m^2.

A_o = pad stem area. For the circular pad $A_o = \pi(D_o)^2/4$, m^2.

Summation of the axial directed forces yields

$$F_E + P_o A_o = \frac{P_1 A_L}{K_p} \qquad (4.2.5.3)$$

where:

F_E = remaining extraneous pad forces parallel to the pad center line, N.

The flow rate of liquid metal through the hydrostatic pad is a function of the method of compensation and the pad face geometry. The most common methods of compensation are orifice, capillary and flow control value. For the present discussion, the orifice method of compensation is considered. The effects of other methods of compensation can be found in ref. 7.

The flow through the orifice is

$$Q_o = 0.661\, d_1^2 \left(\frac{P_o - P_1}{\rho}\right)^{1/2}, \text{ m}^3/\text{s} \qquad (4.2.5.4)$$

where:

ρ = mass density of liquid metal, kg/m^3.

d_1 = orifice diameter, m.

The flow over the pad land is[6]

$$Q_L = \frac{q_f}{12\, K_p} \frac{c^3 P_1}{\mu_L}, \text{ m}^3/\text{s} \qquad (4.2.5.5)$$

where:

q_f = flow factor. The flow factor is a function of geometry and for the circular pad

$$q_f = \frac{4\pi}{1 - (D_1/D_2)^2}, \text{ dimensionless.}$$

c = clearance, m.

μ_L = absolute viscosity, $\frac{N\text{-}S}{m^2}$.

Setting $Q_0 = Q_L$, equations 4.2.5.4 and 4.2.5.5, solving for P_1, and then substituting this expression for P_1 in equation 4.2.5.3 yields the following expression for clearance as a function of supply pressure.

$$c = \left[\frac{63\ \mu_L^2\ d_1^4\ A_L}{\rho\ q_f^2\ (A_o^2\ P_o^2 + 2A_o P_o F_E + F_E^2)}\ (P_o A_L - K_p A_o P_o - K_p F_E)\right]^{1/6}, \text{ m.} \quad (4.2.5.6)$$

Solving equations 4.2.5.4 and 4.2.5.5 for P_1, equating them to each other to eliminate P_1, and making $Q_0 = Q_L = Q$, yields the following expression for flow as a function of supply pressure and clearance.

$$Q = \frac{2.625\ N_p M d_1^4}{\rho}\left\{\left[\left(\frac{6.35\times10^{-2}\rho P_o}{d_1^4}\right) + \left(\frac{\mu_L K_p}{c^3 q_f}\right)^2\right]^{1/2} - \left[\frac{\mu_L K_p}{c^3 q_f}\right]\right\}, \text{ m}^3\text{/s/machine} \quad (4.2.5.7)$$

where:

N_p = number of pads per collector.

M = number of collectors per machine.

Thus, for a given geometry, fluid physical properties, and extraneous force, the clearance and flow can be found for various supply pressures.

The buffer gas flow equation is derived from the relationships presented in reference 8. Since the lift effect due to the buffer gas is small relative to the liquid metal lift, the clearance is determined by the liquid metal hydrostatic relationship in equation 4.2.5.6. For gas pressure drops across the confinement labyrinth of 6895 to 68,950 N/m^2 (1 to 10 psi), the buffer flow can be approximated by the expression:

$$Q_B = \left[\frac{(\Delta P)^{1/2} + 3.63}{1.086}\right] N_p McL, \ m^3/sec \qquad (4.2.5.8)$$

where:

ΔP = differential gas pressure across labyrinth, N/m^2.

c = clearance calculated by equation 4.2.5.6, m.

L = length of labyrinth tooth perpendicular to the flow per pad, (πD_4), m.

4.2.5.1.2 Power Losses

The power losses associated with the hybrid collector are:

P_Ω = Ohmic

P_V = Viscous on pad face

P_C = MHD and viscous core loss

P_E = Eddy current loss

P_P = Pumping power for hydrostatic fluid

P_B = Pumping power for buffer gas

Ohmic Loss

$$P_\Omega = I_p^2 \ R \ M \ N_p, \ watts/machine \qquad (4.2.5.9)$$

where:

I_p = load current per pad, amps.

R = pad resistance including contact potential resistance, ohms.

Viscous Loss on Pad Face

Assume: 1) $\delta << 1$, where δ is a dimensionless ratio of the Lorentz body force to the viscous drag force.[9]

2) Flow regime is turbulent.[9]

3) Viscous loss due to buffer gas is negligible.

$$P_V = \frac{\rho\, f_L (V)^3 A_L}{8} N_p M, \text{ watts/machine} \qquad (4.2.5.10)$$

where:

f_L = friction factor based on pad-to-rotor clearance, dimensionless.

V = collector rotor tangential velocity, m/s.

A_L = pad projected area, m^2.

Core Viscous and MHD Loss

The core MHD loss is based on an induced current due to the fluid velocity in the presence of a magnetic field.

$$P_C = (\pi/4)\, M\, N_p \left[(2f_c \rho V_c^3 d_3 H_4) + (\sigma_L B_r^2 V_c^2 d_3^2 H_4)\right], \text{ watts/machine} \qquad (4.2.5.11)$$

where:

f_c = friction factor based on core diameter.

V_c = fluid velocity through core, m/s.

d_3 = core diameter, m.

H_4 = core length, m.

σ_L = electrical conductivity of liquid metal, mhos/m.

B_r = radial component of collector magnetic field, T.

Eddy Current Loss[10]

Assume: 1) No load current.

2) No transverse current, i.e., no circulating current within the liquid metal.

$$P_E = M\, N_p\, A_p \left(\frac{\sigma V^2 B_a^2 W^2}{12\, c'} \right) \left(\frac{c'^2}{W^2} + 1 \right) \text{, watts/machine} \qquad (4.2.5.12)$$

where:

A_p = current transfer area per pad, m^2.

B_a = axial component of collector magnetic field, T.

W = collector width normal to B_a, m.

c' = effective clearance, m.

$c' = (c + \sigma\, \varepsilon_k + h_2)$, m.

ε_k = specific contact potential for each contact pair, Vm^2/A.

h_2 = current transfer pocket depth, m.

Hydrostatic Fluid Pumping Power

$$P_P = \frac{Q\, P_o}{\eta_L} \text{, watts/machine} \qquad (4.2.5.13)$$

where: η_L = liquid metal pump efficiency, %/100.

Buffer Gas Pumping Power

$$P_B = \frac{\gamma Q_B R(T+273)}{\eta_B} \left(\frac{k}{k-1} \right) \left[(r_p)^{\frac{k-1}{k}} - 1 \right] \text{, watts/machine.} \qquad (4.2.5.14)$$

where:

γ = mass density of buffer gas at drain, kg/m^3.

R = gas constant of buffer gas, $\frac{\text{watt-s}}{\text{kg } ^oC}$

T = buffer gas temperature at pad drain, ^oC.

η_B = buffer gas pump adiabatic efficiency, %/100.

k = Specific heat ratio of cover gas, dimensionless.

r_p = ratio of buffer gas supply pressure to drain pressure, absolute pressures.

The total collector loss is found by:

$$P_{tot} = P_{\Omega} + P_V + P_C + P_E + P_P + P_B, \text{ watts/machine} \qquad (4.2.5.15)$$

The relative loss is found by calculating the percent of machine power attributed to the total collector loss. The percent collector loss is found by the relationship:

$$LOSS = \frac{P_{tot}}{(POWER)} \times 100, \% \qquad (4.2.5.16)$$

where: POWER = total machine power, watts.

4.2.5.1.3 Expulsion Pressures

Pressures are developed in the liquid metal due to the MHD body forces. These MHD pressures are considered in order to determine if they are significantly large with respect to the hydrostatic control pressures. Figure 4.2.5.5 shows the direction of selected forces which upon integration yield eddy current ejection pressure, load current ejection pressure, pinch pressure and the pad face MHD pressure. The MHD pressure drop in the core is not shown on this figure, but it always works to retard the liquid metal flow.

Eddy Current Ejection Pressure

As reported in previous Semi-Annual Technical Report,

$$\Delta P_E = \frac{\mu\pi}{32}\left[\frac{\sigma_L R_c B_a \omega}{c'}\right]^2 W^4, \text{ N/m}^2, \qquad (4.2.5.17)$$

where:

μ = permeability of free space (10^{-7}, mks units)

ω = angular velocity, rad/s

R_c = average collector radius, m

Load Current Ejection Pressure

$$\Delta P_L = (2n-1)\mu\pi J^2 R_1^2 \left[(R_2/R_1)^2 - 2\ln(R_2/R_1) - 1\right], \ N/m^2 \qquad (4.2.5.18)$$

where:

n = number of series load circuits

J = collector average current density, A/m^2

R_1 = inner radius of current collector, m

R_2 = outer radius of current collector, m

Pad Pinch Pressure

$$\Delta P_p = \mu J I_p, \ N/m^2 \qquad (4.2.5.19)$$

Pad Face MHD Pressure

$$\Delta P_m = J B_r L_c, \ N/m^2 \qquad (4.2.5.20)$$

where: L_c = length of current transfer area in direction of rotor circumference, m.

Core MHD and Viscous Pressure

The core MHD pressure is based on the induced current due to the fluid velocity in the presence of a magnetic field.

$$\Delta P_c = \sigma_L V_c (B_r)^2 H_4 + 2\rho f_c V_c^2 \left(\frac{H_4}{d_3}\right), \ N/m^2 \qquad (4.2.5.21)$$

4.2.5.2 Discussion of the Hybrid Collector

A computer program was developed to evaluate different pad configurations. The program calculates pad performance based on the relationships presented in the previous section on theory. The following assumptions are inherent in the computer program:

1. The pad lift force at zero liquid metal flow equals the pad drive force at infinite flow. (That is, the hydrostatic force developed by the pad to move away from the rotor equals the hydrostatic force developed by the pad to move toward the rotor.)

2. The minimum allowable supply pressure is that value which, when integrated over the pad stem area, provides a force equal to the extraneous force. If the rotor moves away from the pad, the minimum supply (control) pressure corresponds to the minimum pressure required to force the pad to follow the rotor.

3. The electrical load current is transferred between the rotor and pad solely through the center pocket portion of the pad, with no transfer through the pad land portion.

4. The load current is transferred between the pad and stator through the circumferential area of the pad stem.

5. The hydrostatic flow velocity at any point on the hydrostatic land must be equal to or greater than the mean collector rotor tangential velocity.

6. The liquid metal and the buffer gas are constrained by seals such that no flow is allowed to bypass the pad. For convenience the bypass seals are assumed to be sliding O-rings.

Table 4.2.5.3 contains general information required to calculate the performance characteristics of a hybrid pad design collector and, with these results, permits assessment of how well it meets the restrictions or requirements outlined in Tables 4.2.5.1 and 4.2.5.2. The values shown in Table 4.2.5.3, although representative, are not intended to be taken as optimum values, but are merely to provide a reference frame for discussion.

Based on a total flow of 0.0314 m^3/s (500 gpm), see Table 4.2.5.3, the liquid metal flow per collector pad is 5.6×10^{-5} m^3/s (0.89 gpm). This flow appears to be excessive and should be reduced if possible. For the given pressure, the flow can be reduced by making the pad orifice and/or pocket diameter smaller. This, however, will reduce the hydrostatic flow velocity below the collector rotor tangential velocity. The result is that the pad lift force is impaired. In this situation, the fluid film

TABLE 4.2.5.3
TYPICAL DESIGN INFORMATION
(Also see Table 4.2.5.2)

General Collector Data	Value
1) Number of pads	90 (N)
2) Buffer gas flow per machine	.294 m^3/sec (624 ft^3/min) (Q_B)
3) Liquid metal flow per machine	.0314 m^3/sec (500 gal/min) (Q_L)
4) Buffer gas pump efficiency	50% (η_B)
5) Liquid metal pump efficiency	30% (η_L)
6) Extraneous force	39.14 N (8.8 lb) (F_E)
7) Pad spring constant with respect to rotor	2.92×10^6 N/m (16700 lb/in.) (K_S)
8) Hydrostatic fluid — Eutectic NaK 78	
a) Viscosity	540 Ns/m^2 ($.783 \times 10^{-7}$ lb-sec/in^2) (μ_L)
b) Mass density	858 kg/m^3 (.031 lb/in^3) (ρ)
c) Electrical conductivity	$.22 \times 10^7$ mhos/m (σ_L)
d) Specific contact potential	$.18 \times 10^{-8}$ Vm^2/A (ε_K)
9) Pad material — Copper	
a) Electrical conductivity	$.448 \times 10^8$ mhos/m
10) Buffer gas — Nitrogen	
11) Liquid metal supply pressure	345000 N/m^2 gage (50 psig) (P_0)
12) Liquid metal pocket pressure	172000 N/m^2 gage (25 psig) (P_1)
13) Buffer gas supply pressure	13800 N/m^2 gage (2 psig) (P_3)
14) Liquid metal and buffer gas combined drain pressure	0.0 N/m^2 (P_2)
15) Collector temperature	94°C (200°F) (T)

TABLE 4.2.5.3 (Continued)

	General Collector Data	Value
16)	Minimum allowable hydrostatic control pressure	245000 N/m^2 gage (35.5 psig)
17)	Flow factor	87.04 (q_f)
18)	Pressure factor	1.08 (K_p)

Collector Geometry (Refer to Fig. 4.2.5.7)

R_C = .442 m (17.4 in)

D_0 = .0143 m (.562 in)

D_1 = .0194 m (.763 in)

D_2 = .0210 m (.825 in)

D_3 = .0290 m (1.14 in)

D_4 = .0305 m (1.20 in)

$d_1 = 2.16 \times 10^{-3}$ m (.085 in)

$d_2 = 4.06 \times 10^{-3}$ m @ 12 holes (.16 in)

$d_3 = 6.10 \times 10^{-3}$ m (.24 in)

d_4 = .0140 m (.55 in)

$\delta_1 = 2.03 \times 10^{-5}$ m (.0008 in)

$\delta_2 = 2.03 \times 10^{-5}$ m (.0008 in)

$H_1 = 3.05 \times 10^{-3}$ m (.12 in)

H_2 = .0102 m (.40 in)

H_3 = .0297 m (1.17 in)

H_4 = .0282 m (1.11 in)

H_7 = .0130 m (.51 in)

$h_1 = 3.94 \times 10^{-3}$ m (.155 in)

$h_2 = 1.52 \times 10^{-4}$ m (.006 in)

$C = 2.72 \times 10^{-5}$ m @ $F_E = 0$
(.00107 in)

on the pad land cannot cover the full hydrostatic area because it is drawn away too fast by the rotor.[11-12] In regard to the sample operating conditions presented here, the pad land hydrostatic liquid flow velocity is equal to the mean collector rotor velocity.

A method for reducing the flow with only partial impairment of the lift force is to utilize pad geometries other than the circular cross section.[7] Future effort should be directed to find low-flow geometric configurations which impose minimal hydrostatic life impairment.

The extraneous force (F_E) listed in Table 4.2.5.3 is equal to 39.1 N (8.8 lb_f). This force should be reduced so that a lower minimum allowable hydrostatic control pressure can be used. The major portion of the extraneous force is attributed to O-ring friction. The O-rings could be replaced by controlled leakage seals which would offer essentially zero friction. Future effort in this area would be placed on finding the optimum bypass seal with respect to leakage and friction.

The pad spring constant, see Table 4.2.5.3, is a measure of stiffness with respect to the rotor. It is numerically equal to the change in extraneous force (from positive to negative) divided by the corresponding change in pad-rotor clearance. The spring constant is useful when making a mechanical response analysis of the rotor-pad-stator system. Future effort would determine the mechanical response of the pad with respect to the rotor and derive the current collector design relationships with respect to resonance.

The power loss associated with the hybrid current collector is given in Table 4.2.5.4 as 2.4% of the total machine output power. This is 0.4% greater than the design requirements (see Table 4.2.5.1, item 6). The major component of the collector loss is the ohmic loss, which is caused by the solid-liquid-solid interface contact resistances and the pad pocket liquid metal bulk resistance.

TABLE 4.2.5.4
SUMMARY OF CURRENT COLLECTOR COMPONENT POWER LOSSES

	Component	Power Loss kW	Power Loss %
1)	Ohmic loss, P_Ω	69.5	49
2)	Eddy current loss, P_E	22.9	16
3)	Core loss, P_C	0.9	1
4)	Viscous loss, P_V	6.6	5
5)	Liquid metal pump loss, P_P	36.3	25
6)	Buffer gas pump loss, P_B	5.4	4
7)	Total collector loss, P_{tot}	141.6	100
8)	Percent of total machine power		2.4% (LOSS)

One method considered for reducing the ohmic power loss is to reduce the current per pad by adding more pads. However, the present 90 pads employed per collector is the maximum that can be accommodated. Another possible method for reducing the ohmic loss is to increase the pad face area (i.e., effectively reducing the contact resistance). This event, however, also reduces the hydrostatic flow resistance which, in turn, results in an undesirable increase in fluid flow. By employing non-circular cross section pads, where lower flow velocities may be feasible, greater current transfer areas may be achieved.

Counter to the original design philosophy, a reduction in contact resistance may also be obtained by permitting the load current to be transferred between rotor and pad through the pad land area in addition to the pad pocket. Initially, current transfer was allowed only through the pocket area in order to avoid excessive eddy current power loss and ejection pressure. Although the eddy current induced loss will be increased as a result of the above suggested changes, it will likely be offset by reduced load current ohmic and liquid metal pumping power losses. Future effort should be placed on determining the optimum current transfer geometry with respect to losses.

Calculated MHD pressures for the sample pad collector design are summarized in Table 4.2.5.5. The liquid metal-load current ejection pressure reported here is of a significant magnitude, 6×10^4 N/m^2, when compared with the higher pocket pressure, 17×10^4 N/m^2 (see Table 4.2.5.3, item 12). The pressure profile through the liquid metal due to load current-self field effects is not known at this time, since pressure calculations using the derived expression only yield maximum values at one end of the collector. Future work is suggested to ascertain the disturbing effects of load current on liquid metal confinement, if any, through laboratory experimentation.

The pad face MHD pressure does not appear to be excessively large for the present hybrid pad collector design. If the pad geometry is changed from the circular shape, however, elongating the area of current transfer circumferentially would cause an increase in the pad face MHD pressure.

TABLE 4.2.5.5
SUMMARY OF CALCULATED CURRENT COLLECTOR MHD PRESSURES

Source of Pressure	Pressure N/m^2	Pressure (lb_f/in^2)
1) Eddy current ejection pressure, ΔP_E	2100	(0.30)
2) Load current loop ejection pressure, ΔP_L	60200	(8.7)
3) Pinch pressure, ΔP_P	2580	(0.37)
4) Pad face MHD pressure, ΔP_m	9020	(1.3)
5) Core MHD and viscous pressure, ΔP_C	380	(0.06)

At present no quantitative method has been developed to evaluate the collector's ability to confine liquid metal to the current transfer zone. Confinement of liquid metal is defined as the ability of the hybrid pad to transport liquid metal in and out of the current collection area in the presence of a moving rotor surface without liquid metal leakage beyond the outer confinement labyrinth. In general, the following qualitative statements may be made concerning confinement:

1. A reduction in the liquid metal supply flow will improve confinement ability.

2. An increase in the buffer gas flow will work to reduce leakage of liquid metal at the labyrinth location.

3. Certain MHD pressures may be utilized to aid confinement. In other cases, through design, the MHD expelling pressures can be reduced.

The above actions are intuitive and the degree to which confinement will be affected can only be determined through experimentation. This, again, is an area for future work in the development of a hybrid pad current collector.

Because of potential mechanical force couples, the circular geometry hybrid pad is undesirably susceptible to tilting. It appears that force couple compensation can be achieved by employing parallel flow restrictions.[7] This technique must be theoretically and experimentally studied in more detail.

4.3 REFERENCES

1. Warring, R. H., Seals and Packings, Trade and Technical Press Ltd., Morden, Surrey, England, 1967.

2. Chicago Rawhide Catalog No. 457013, Large Diameter Oil Seals.

3. Fuller, D. D., Theory and Practice of Lubrication for Engineers, John Wiley and Sons, 1956.

4. Shaw, M. C. and Macks, E. F., Analysis and Lubrication of Bearings, McGraw-Hill, New York, 1949.

5. Private communication with Dr. G. T. Hummert, Westinghouse Research Laboratories, April 29, 1975.

6. Loeb, A. M. and Rippel, H. C., Determination of Optimum Proportions for Hydrostatic Pads, ASLE Trans., Vol. 1, No. 2, p. 241, 1958.

7. Malanoski, S. B. and Loeb, A. M., The Effect of the Method of Compensation on Hydrostatic Bearing Stiffness, Journal of Basic Engineering, Trans. ASME, Series D, Vol. 83, No. 2, p. 179, June 1961.

8. Egli, A., The Leakage of Steam through Labyrinth Seals, ASME Paper No. FSP-57-5, 1935.

9. Rhodenizer, R. L., Development of Solid and/or Liquid Metal Collectors for Acyclic Machines, Final Report for Tasks 1, 2 and 3, Navy Ship Systems Command, Contract No. N00024-68-C-5414, February 27, 1970.

10. Hummert, G. T., Calculation of Eddy Losses in Liquid Metal Current Collectors, Westinghouse Memo 73-8G1-LIQMT-M1, November 20, 1973.

11. Boyd, J., Raimondi, A. A., and Kaufman, H. N., A Manual on Bearing Analysis, Westinghouse Research Laboratories, 1310 Beulah Road, Pittsburgh, Pennsylvania 15235, 1966.

12. Boyd, J., Kaufman, H. N., and Raimondi, A. A., Basic Hydrostatic Pad Design, Lubrication Engineering, Vol. 21, 1965 (Westinghouse Report 63-117-517R2).

SECTION 5
LIQUID METAL SUPPORT SYSTEMS

5.0 OBJECTIVES

The objectives of this Task are: 1) to investigate the compatibility of candidate machine materials with NaK and GaIn as well as with potential decontamination solutions; 2) to perform literature, analytical, and experimental studies to identify suitable materials and suggest alternate choices where necessary; 3) to design, fabricate, and test the liquid metal loop and cover gas systems that will be required in the SEGMAG generator; and 4) to establish the operating parameters and interactive responses of these systems.

During Phase I, the objectives were to identify the materials requirements and related problems for the segmented magnet homopolar machine, with particular emphasis to the long term compatibility problems between the selected liquid metal and the electrical conductors, insulation and structural materials in the system.

In Phase II, the objectives were: 1) to identify experimentally the SEGMAG machine materials that are compatible with NaK; 2) to provide a test facility to evaluate candidate current collectors under simulated machine environment; 3) to provide liquid metal and cover gas systems for the SEGMAG demonstration machine; and, 4) to provide test facilities for the SEGMAG and GEC machines.

During Phase III, the auxiliary equipment developed under Phase II was utilized in the SEGMAG test program. The SEGMAG liquid metal system was further developed and simplified. Support systems were considered for use in torque converter and motor applications where reversible and variable speeds are encountered. GaIn technology studies were pursued with respect to machine requirements.

5.1 PRIOR AND RELATED WORK

The work performed under this task is summarized below and is more fully described in our previous reports under this contract.

NaK was selected as the reference liquid metal, with GaIn as the alternate choice.

An extensive materials compatibility program was conducted, and the selection of materials for use in SEGMAG was based on their ability to withstand NaK exposure in a simulated machine environment.

Investigation was made of the chemical problems associated with wetting between NaK and copper or copper-based alloys.

Procedures were established for the disassembly and decontamination of machines using NaK and GaIn. Liquid metal recirculation and purification loops were designed, fabricated, tested, and employed in SEGMAG performance tests to maintain NaK in the current collectors. Cover gas recirculation, purification, and pressure maintenance systems were designed and constructed for SEGMAG performance tests. Full scale prototype current collectors were developed, tested and characterized prior to their employment in SEGMAG. The SEGMAG test bed, instrumentation, coolant system, and performance readout networks were developed and constructed for the machine evaluation tests.

During the design stage of the 3000 hp SEGMAG demonstration machine, great emphasis was placed upon developing the machine support systems since these were recognized to be necessary to successful, long term machine operation. An integrated design approach was employed, since many components were to be in contact with the liquid metal alloy (NaK) and also with the protective cover gas, nitrogen. To insure system compatibility many parameters and subsystem interactions were evaluated, including the following:

1. Effect of liquid metals on machine materials.
2. Contamination of liquid metal by out-gassing of machine materials.
3. Contamination of liquid metal by impurities in the cover gas or through atmospheric in-leakage.
4. Interference of NaK aerosols and oxides on current collector performance.

5.2 CURRENT PROGRESS

5.2.1 Machine Materials Selection

NaK is an alloy of sodium and potassium and is prepared by mixing these two elements in liquid form. Potassium and sodium are miscible in all portions, and the alloy in concentrations of 40 to 90 weight percent potassium is liquid at room temperature. The phase diagram for this system is given in Fig. 5.1. Eutectic NaK is characterized by its low density (0.867 g/cm^3 at 20°C), high electrical and thermal conductivity and low vapor pressure. It also reacts rapidly with oxygen to form Na_2O preferentially, and with water or water vapor to form the hydroxides of sodium and potassium. Thus, NaK systems must be protected by inert cover gas systems.

NaK is usually compatible with transition metals, but may show incompatibility with organic insulations and other materials because of its chemical reactivity.[1] Additionally, material incompatibility may result from materials outgassing and contaminating the liquid metal. Outgassing

Curve 649634-A

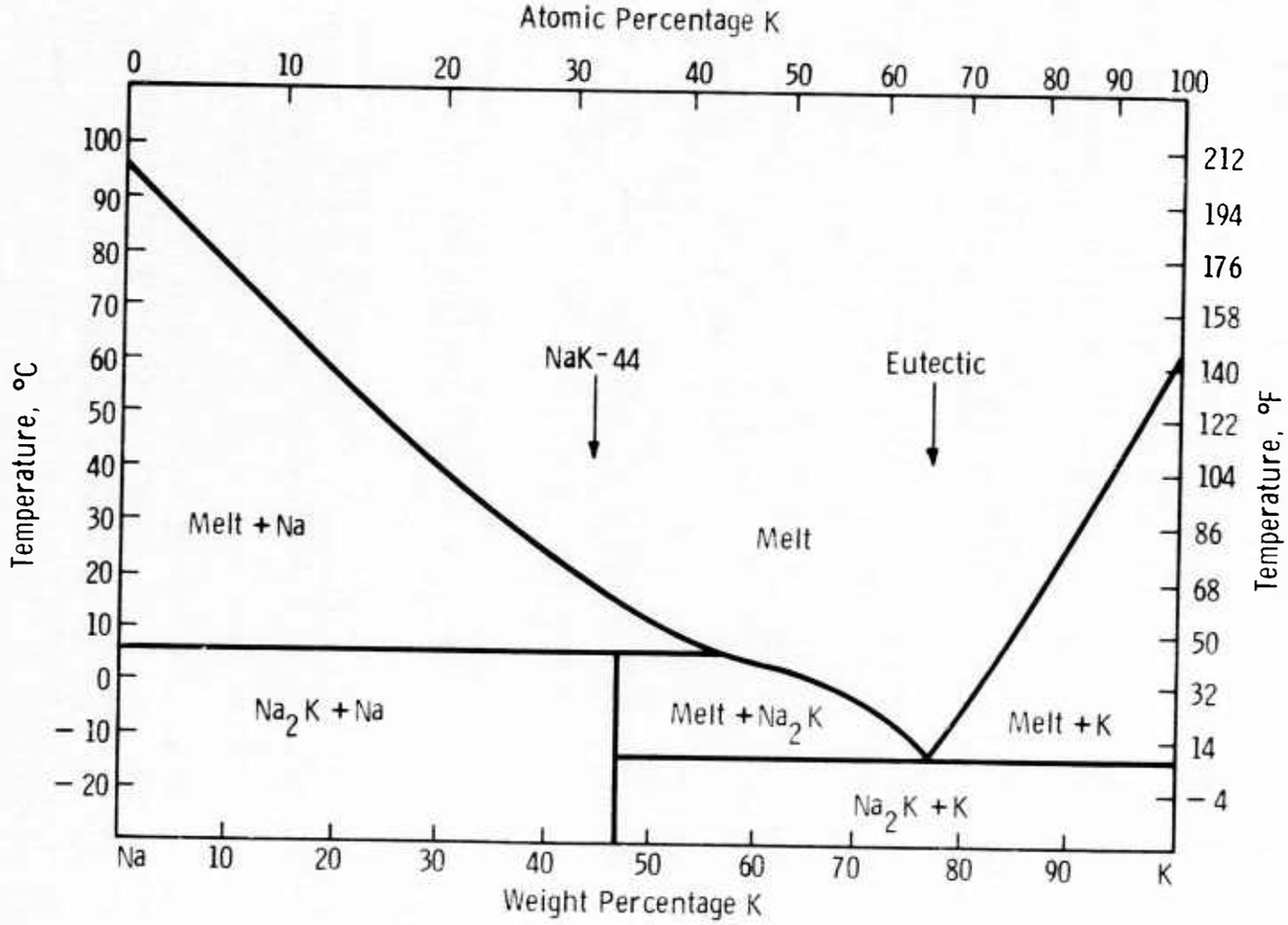

Fig. 5.1: Phase diagram for the NaK binary system.

problems may arise from structural, but more likely from organic insulation and materials. Outgassing may be due to either (1) absorbed gases on surfaces and in pores, or (2) reaction products from the polymerized organic insulating materials or solvents. In addition, local machine hot spots may be generated during machine operation which will cause thermal decomposition of organic materials.

A literature survey has indicated that most work dealing with liquid metals has involved their employment at elevated temperatures as heat transfer agents. In applications of this type, the liquid metal does not contact organic electrical insulation materials. A supplier's brochure[2] states that NaK is more reactive than either sodium or potassium at low temperatures, and that in reactions with organic materials, the potassium derivative is usually formed preferentially. NaK is particularly reactive with organic halides, and the use of halogen-containing polymers (PTFE or PVC for instance) for insulation applications in the homopolar machine appears to be precluded.[3] NaK reacts readily with all reactive hydrogens such as those in carboxyl, hydroxyl, amine, and even enolizable carbonyls. It also cleaves ether linkages. Although these considerations might appear to eliminate essentially all polymer systems from consideration except those of strictly hydrocarbon nature, other information[4] which tabulates data for exposure of certain polymer systems to NaK indicates that the lowered reactivities of these groups in large molecules may permit use of many polymer systems in contact with NaK. A phenolic laminate, for example, exposed to NaK at 384°K (250°F) for 336 hours did not appear to be damaged.[5] It is evident that all polymer systems proposed for NaK exposure applications must be verified experimentally. The literature survey did not reveal any information regarding contamination of NaK by outgassing products from polymeric systems.

Candidate insulating materials for each service category were defined by generic classification rather than by specific composition, and are listed in Table 5.1.

The design concept for the Westinghouse homopolar machine included an insulation hot spot temperature of about 403°K (130°C). The use of Class F (428°K, 155°C) insulation was therefore indicated in all service categories identified above except for the collector ring where Class A (378°K, 105°C) insulation was considered adequate.

Reaction of low molecular weight organic by-products with NaK constitutes a major problem area. Such compounds as water, carbon dioxide, carbon monoxide, and monomers which would contaminate the liquid metal can be given off by the insulation, either as a result of continuing cure during the operation of the machine or as a result of thermal pyrolysis.

Periodic cleaning of the machine is expected to involve exposure of the insulation to alcohol-water mixtures, and this necessarily will result in some absorption of both. Exposure of insulation to any sort of humid environment while the machine is not in operation must also

TABLE 5.1: TYPICAL ELECTRICAL MACHINE INSULATING SYSTEMS

Service Category	Candidate Materials
1. Conductor insulation	Kapton tape; glass-supported acrylic tape
2. Ground wall	Epoxy bonded mica tapes
3. Outer binder tape	Epoxy, acrylic or highly modified polyester tapes backed with glass and/or organic fabrics
4. Banding tape	Epoxy or acrylic pretreated glass tape
5. Collector ring	Polypropylene, polyethylene, epoxy laminated
6. Sealing compounds and connection seals	Mineral-filled epoxies
7. Coatings	Aminoformaldehyde epoxies or phenolic alkyds

result in some water absorption. In properly outgassing the insulation prior to returning the machine to operation would result in exposure of the liquid metal to both compounds.

Formation of an aerosol suspension of NaK in the confinement area during operation of the machine is believed to be unavoidable. In consequence, deposition of discrete droplets or possibly films of NaK on insulating surfaces is expected to occur. Since cleaning of these surfaces is anticipated not oftener than once every six months, the insulation must remain substantially unaffected by this environment.

Plastics and elastomers are usually considered for gasketing materials at low temperatures or for total containment of NaK. There is scarce, if any, room temperature data as to the compatibility of plastics and elastomers in NaK. However, a number of tests were conducted at 394°K - 450°K (250°F to 350°F).[2] This data eliminates some of the low melting plastics, and some of these can be ruled out due to their chemical composition. It is known that room temperature NaK will dissolve Teflon; tests have been made with Viton, a fluorinated material, with unsatisfactory results.

The Liquid Metals Handbook[5] discusses the compatibility of plastics with alkali metals based on work performed at NASA. In part it concludes that from the standpoint of weight loss of the plastic and contamination of the metal, the materials that demonstrated the most acceptable behavior were Kel-F3700 and Buna-N in 394°K (250°F) sodium for 9 days and neoprene and Buna-N in 450°K (350°F) sodium for 7 days. Neoprene

and Kel-F are halogenated, and therefore it is recommended that these not be used with alkali metals because of the potential of an explosion hazard associated with their use. Polyethylene has been tested at room temperature in NaK for 3½ years with no visible change.[2]

With the definition of candidate homopolar machine materials, experimental verification of NaK compatibility was initiated. More than 1000 hours of cumulative NaK exposure time has been attained on more than 120 individual samples. These include: (1) rotor banding materials, (2) rotor bar insulation, (3) laminate composites, (4) potting compounds, (5) Silastic elastomers, (6) coatings and paints, (7) seal materials, (8) cooling fluids, (9) braze alloys, and (10) structural metals. The evaluation of candidate materials has proceeded through a defined test plan which has been so designed as to incorporate the material exposure sequence which will be followed during actual machine start-up, operation, machine decontamination, and requalification of components after decontamination and subsequent reassembly. Proposed materials have been exposed to commercial grade NaK in test canisters heated isothermally in a constant temperature oil bath. Figure 5.2 illustrates the glove box facilities which were utilized to prepare and handle candidate materials and to charge them into test canisters with NaK.

All compatibility studies were performed at 140°C for defined time intervals. This temperature was selected because in all instances, it represented the most severe condition that any one machine component was expected to encounter (machine hot spot temperatures were calculated to be 130°C max). Therefore, it was assumed that materials which survived this condition in liquid NaK would be prime candidates for the demonstration machine. In addition, materials were evaluated at NaK exposure intervals of 100, 500, and 1000 hours by defined physical measurements. Water was employed as the NaK decontamination fluid. The antechamber of the sample preparation glove box served as a sample baking chamber, simulating machine pre-start up conditions of roughing pump vacuum at 100°C for a fixed time interval of 24 hours.

Physical testing for material evaluation included: weight changes, dimensional changes, hardness, electrical resistivity, flexural properties, tensile properties, infrared spectroscopy, and scanning electron microscopy (SEM).

Figure 5.3 illustrates the flow sequence of selected materials during the NaK compatibility studies. This program has provided quantitative information on the compatibility of materials with eutectic NaK.

1. Rotor Banding Material. An epoxy Novalac/glass fiber was selected as the rotor banding material. Since this material was expected to serve as both insulation and a NaK barrier to the rotor bar system in the Westinghouse design, it was important that NaK compatibility be established. Selected material specimens were exposed to NaK and

Fig. 5.2: Glove box facilities utilized for the preparation and handling of materials being evaluated for NaK compatibility

material compatibility established by tensile testing and scanning electron microscope (SEM) examination. Table 5.2 lists the tensile test data for this material.

Since the ultimate strength remained essentially unchanged after more than 1000 hours of NaK exposure, as compared with air aged specimens, and no material degradation had occurred, as shown by SEM examination, this banding material was selected as a prime condidate for use in the demonstration machine.

2. Electrical and/or Rotor Bar Insulation. Electrical insulation systems were evaluted for NaK compatibility. Since no reported literature values could be found for NaK compatibility of materials of this type, insulation packages were defined from the NaK chemistry of organic systems. Test specimens were prepared and exposed to liquid

TABLE 5.2

ROTOR BANDING MATERIAL 431-S-2 (EPOXY NOVALAC RESIN/GLASS FIBERS) TENSILE TEST DATA

Specimen I.D.	Specimen No.	Ultimate Strength (ksi)
Archieves - as prepared	1	122.9
	2	116.9
Air aged (180°C) 250 hours	3	150.1
	21	157.8
Air aged (180°C) 998 hours	5	163.5
	17	154.3
NaK Exposed (140°C)	7	142.8
99.5 hours	9	139.3
NaK Exposed (140°C)	8	132.2
507.5 hours	10	132.2
NaK Exposed (140°C)	11	150.9
1009.5 hours	12	149.2

Dwg. 7238037

FIG. 5-3—SIMPLIFIED FLOW CHART OF MATERIALS COMPATIBILITY TEST PLAN

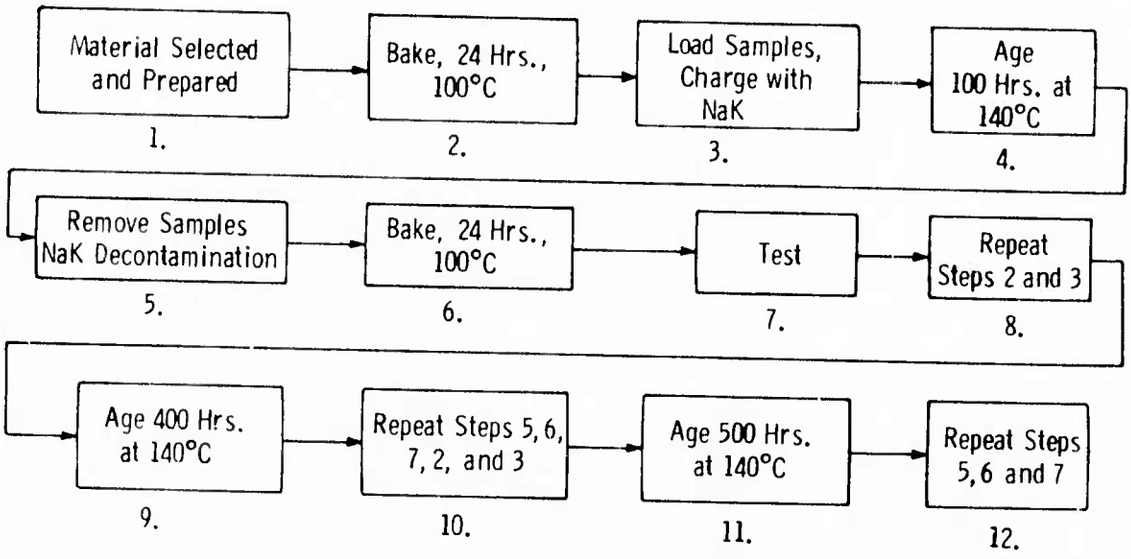

Fig. 5.3: Simplified flow chart of materials compatibility test plan

and vapor eutectic NaK at 140°C. Surface and volume resistivity measurements for these insulation systems have shown that these selected materials qualify as NaK compatible, see Fig. 5.4. Since these specimens were also decontaminated prior to electrical measurements, they also qualified as being compatible with the anticipated machine decontamination scheme. These results indicated that when little or no information is available for NaK compatibility, basic alkali metal chemistry can provide reliable guidelines in the selection of candidate materials.

3. Silastic Elastomers. Early in this study silastic elastomers, 116 RTV and RTV 732, were selected as probable sealing materials for use in the demonstration machine. Compatibility studies have shown that although these materials are compatible with NaK at room temperature, severe degradation occurs at elevated temperatures (140°C). As a result of this study, silastic elastomers have been found to be incompatible with the NaK environment and are not recommended for machine applications in which NaK exposure may occur.

4. Machine Laminates. A number of laminate composite materials have been evaluated for NaK compatibility. In addition to noting weight

MATERIALS COMPATIBILITY STUDY
ELECTRICAL INSULATION SYSTEMS

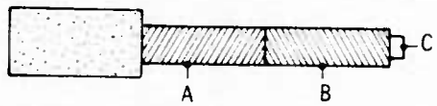

Insulation System	Electrodes	Resistivity, Megohms Archives	Heat, 112 Hrs.	Heat, 1156 Hrs	NaK 112 Hrs.	NaK, 449 Hrs.	NaK, 1156 Hrs.
1. Kapton Film 1/2 Lapped, Mica Bonded to Kapton Tape, Polyester on Dacron	A-C (Vol)	∞	∞	∞	5×10^5	∞	∞
	B-C (Vol)	–	–	–	5×10^5	∞	∞
	A-B (Surface)	∞	5×10^5	∞	5×10^5	∞	∞
2. Kapton Film 1/2 Lapped, Mica Bonded to Kapton Tape, Epoxy on Dacron and Glass	A-C (Vol)	∞	10×10^5	∞	5×10^5	∞	∞
	B-C (Vol)	–	–	–	5×10^5	∞	∞
	A-B (Surface)	∞	∞	∞	10×10^5	∞	∞
3. Kapton Film 1/2 Lapped, Mica Bonded to Glass Tape, Polyester on Dacron	A-C (Vol)	∞	10×10^5	∞	9×10^3	37×10^3	4×10^5
	B-C (Vol)	–	–	–	22×10^3	∞	∞
	A-B (Surface)	∞	∞	∞	1×10^5	∞	∞
4. Kapton Film 1/2 Lapped, Mica Bonded to Glass Tape, Epoxy on Dacron and Glass	A-C (Vol)	∞	∞	∞	∞	∞	∞
	B-C (Vol)	–	–	–	10×10^5	∞	∞
	A-B (Surface)	∞	10×10^5	∞	∞	∞	∞

Note: ∞ > 10^6 Megohms
Ageing Temperature = 140°C

Fig. 5.4: Surface and volume resistivity values obtained on heat aged and NaK exposed electrical insulation systems.

and dimensional changes, flexural properties were also determined. From these measurements, trends were established for the ultimate stress and elastic modulus of these materials as a result of NaK exposure. Figures 5.5 and 5.6 note the changes in maximum stress and elastic modulus of selected candidate laminate materials as a result of NaK exposure at 140°C.

5. Braze Alloys. It has been known for some time that microbraze alloys are compatible with NaK. On the other hand, soft solders of tin/lead composition are incompatible even for very short periods of time.[1] Silver solders may be employed, but little quantitative information is available concerning the compatibility of these braze alloys with NaK. This study determined whether or not selected silver braze alloys could be employed in the SEGMAG demonstration machine. Since all the braze joints were to be protected from the NaK environment by the rotor banding material in the Westinghouse design, total braze alloy compatibility was not essential. However, in the event that NaK did penetrate the protective barrier of the rotor banding material, the most compatible alloy had to be selected. A total of five silver braze alloys were evaluated for eutectic NaK compatibility at 140°C to a maximum exposure time of >500 hours. Table 5.3 summarizes the various alloys studied and the weight changes which were observed at exposure times of 112 and 592.8 hours.

Note that two (BCup-5 and BAu-4) of the five braze alloys completely failed in 112 hours. SEM studies performed on these materials have indicated that the failure mechanism is by way of the selective leaching of precious metals (silver or gold) from the alloy matrix. The three remaining materials have also lost weight due to the removal of silver from the alloy matrix, but these small losses occur only under the most severe NaK exposure conditions.

A summary of the materials compatibility program is presented in Table 5.4. This table lists the generic classification of all the candidate materials which were evaluated for NaK compatibility at a temperature of 140°C. This table also lists the quantitative physical measurements which were carried out for each of the materials specified and indicates whether or not each material may be employed for use in the SEGMAG machine. In general, as noted in Table 5.4, almost all of the candidate materials were found to be acceptable for the machine environment thus indicating that our initial assumptions concerning the chemical reactivity of NaK with various organic systems were valid. In addition, Table 5.4 also shows that reported NaK incompatible seal materials (graphite base) may be employed provided that a protective supporting matrix, such as a polyimide, is employed when formulating seal materials.

5.2.2 Liquid Metal Systems

Successful operation of a homopolar machine employing a liquid metal as the electrical current transfer media requires intimate and continuous

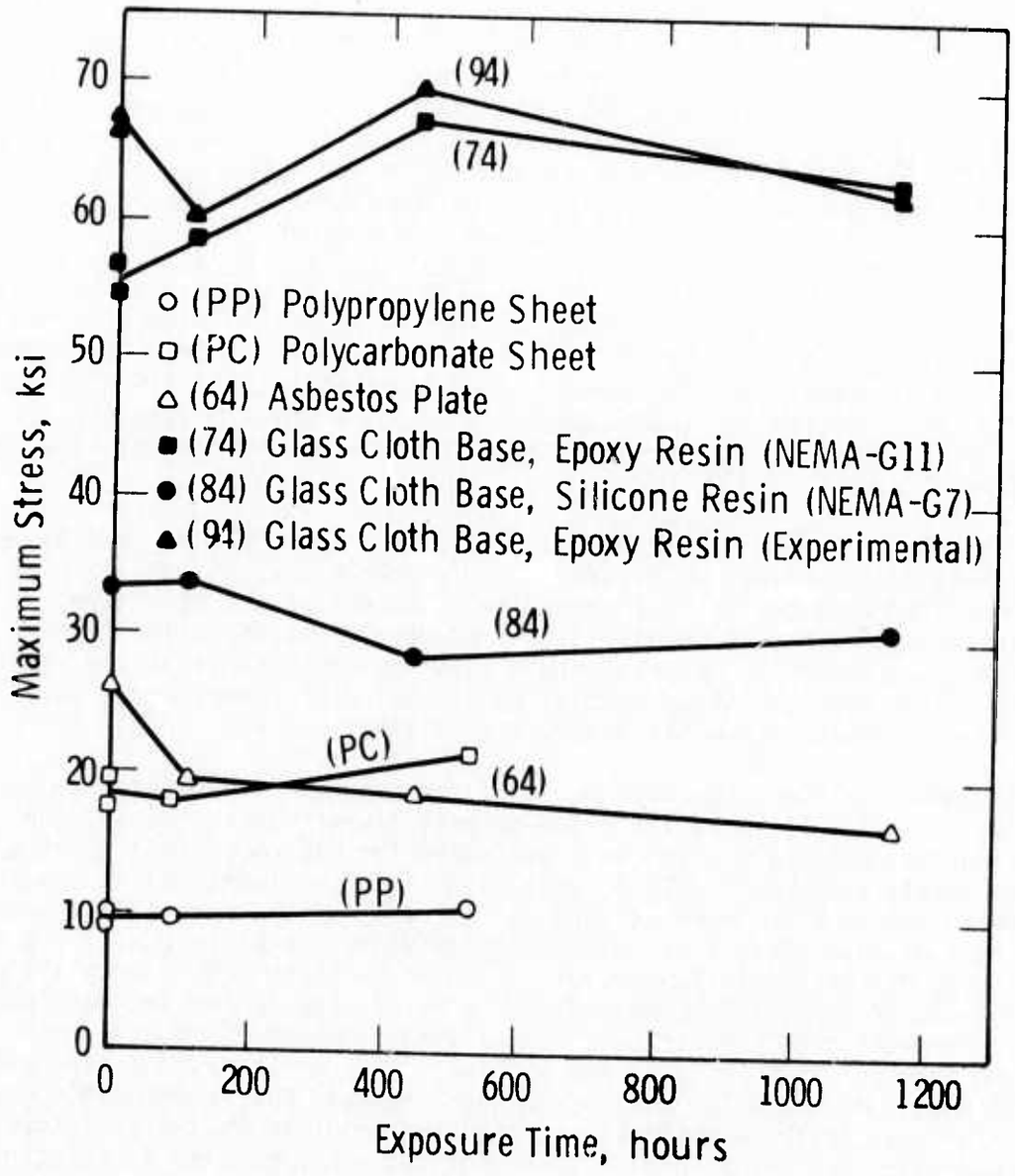

Fig. 5.5: The change in maximum stress of candidate laminate materials as a result of NaK exposure at 140°C

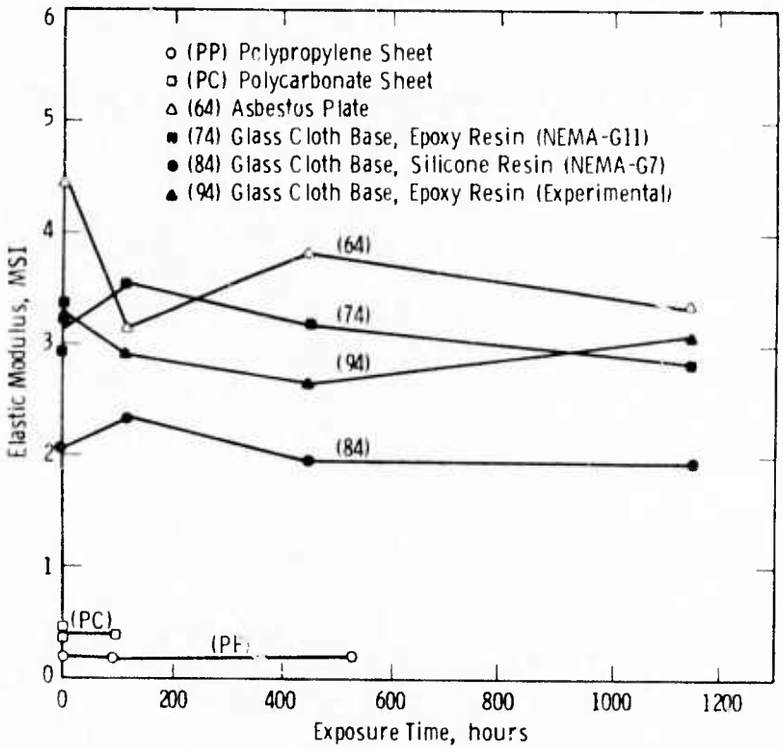

Fig. 5.6: The change in elastic modulus of candidate laminate materials as a result of NaK exposure at 140°C

TABLE 5.3

BRAZE ALLOYS EVALUATED FOR NaK COMPATIBILITY AT 140°C

Sample I.D.	Composition	% Weight Change 112 Hrs	% Weight Change 593 Hrs	Visual Observation
BAg-8	72% Ag, 28% Cu	-1.5	-4.03	OK
BAg-18	60% Ag, 30% Cu, 10% Sn	-0.6	-0.44	OK
BT-Li	71.8% Ag, 28% Cu, 0.2% Li	-0.4	-0.69	OK
BCup-5	15% Ag, 80% Cu, 5% P	+2.1	-4.25	Severe Attack
BAu-4	81% Au, 18.5% Ni	-71.0	--	Sample Dissolved

TABLE 5.4 - MATERIALS COMPATIBILITY SUMMARY

CANDIDATE SEGMAG ORGANIC BASE MATERIALS
EVALUATED FOR NaK COMPATIBILITY (140°C)

Material		Type	NaK Compatibility	Preliminary Screening Experiments	Weight Changes	Dimensional Changes	Hardness	Electrical Resistivity	Elastic Modulus	Maximum Stress	Tensile Properties	Mass Spectrometry	Infrared Spectroscopy	Scanning Electron Microscopy	Friction and Wear Studies
Banding Tapes	1.	polyester on glass	A	✓	✓	✓	✓						✓		
	2.	acrylic modified epoxy on glass	A	✓	✓	✓	✓						✓		
	3.	polyester on experimental fibers	A	✓	✓	✓	✓								
	4.	epoxy Novolac resin on glass	A	✓	✓	✓					✓				✓
Banding Pads	1.	epoxy on glass	A	✓	✓	✓	✓								
Laminates	1.	glass cloth base, silicone resin	A	✓	✓	✓			✓	✓					
	2.	glass cloth base, epoxy resin	A	✓	✓	✓			✓	✓					
	3.	asbestos plate	A	✓	✓	✓			✓	✓					
Rotor Bar Insulation	1.	Kapton film 1/2 lapped, mica bonded to Kapton tape, polyester on dacron	A	✓			✓	✓							
	2.	Kapton film 1/2 lapped, mica bonded to Kapton tape, epoxy on dacron and glass	A	✓			✓	✓							
	3.	Kapton film 1/2 lapped, mica bonded to glass tape, polyester on dacron	Q	✓			✓	X							
	4.	Kapton film 1/2 lapped, mica bonded to glass tape, epoxy on dacron and glass	A	✓			✓	✓							
	5.	Kapton film, type H (2-3 mil)	U	X	X	X									
Coatings	1.	epoxy enamel	A	✓	✓										
	2.	electrostatically deposited epoxy coatings	A	✓	✓										
Silastic Sealants	1.	116 RTV	Q	✓	X	X									
	2.	732 RTV	U	X	X	X									
	3.	892 RTV	U	X	X	X									
Miscellaneous	1.	cooling fluid - Wemco C	A	✓											
	2.	adhesive - (Eastman 910 MHT)	U	X											
	3.	potting compound - silica filled epoxy	A	✓	✓	✓	✓								
	4.	polyethylene sheet	U	✓	✓	X									
	5.	polypropylene sheet	A	✓	✓	✓	✓								
	6.	polycarbonate sheet	A	✓	✓	✓	✓								
CANDIDATE SEGMAG INORGANIC BASE MATERIALS EVALUATED FOR NaK COMPATIBILITY (140°C)															
Seals (125°C)	1.	99.9% graphite	U	X											
	2.	carbon-graphite + MoS_2	U	X											
	3.	carbon-graphite + MoS_2 (>SK-235)	U	X											
	4.	similar to above with phenolic impregnation	U	X											
	5.	straight carbon-graphite	U	X											
	6.	bronze matrix + carbon	A	✓											
	7.	polyimide matrix + 15% graphite + 10% Teflon	A	✓											✓
	8.	polyimide matrix + 15% MoS_2	A	✓											✓
	9.	80% tungsten diselenide - 20% gallium-indium	U	X											
	10.	WSI + oxide coating	U	X											
	11.	90% WSI - 5% Ag - 5% CaF_2	U	X											
	12.	tungsten diselenide	U	X											
	13.	carbon-graphite, density = 1.8 gms/cc	U	X											
	14.	carbon-graphite, density = 1.9 gms/cc	U	X											
	15.	pyrographite	U	X											
	16.	impervious pyroimpregnated graphite	U	X											
	17.	boron nitride + 3 w/o boric oxide	A	✓											
Structural Metals	1.	copper PD135 (rotor)	A	✓											
	2.	copper OFHC (stator)	A	✓											
	3.	rotor steel	A	✓											
Braze Alloys	1.	nicrobraze	A	✓											
	2.	precious metal	U	X										X	
	3.	soft solder	U	X										X	

A = acceptable for use in both NaK liquid and vapor.
Q = questionable NaK compatibility - may be used at lower temperatures (50-100°C).
U = unacceptable - adequate protection from NaK must be provided.
✓ = passed test.
X = failed test.

contact of the fluid with rotating and stationary members. Ideally, this fluid would be hermetically sealed in the current collector zone, thus preventing contaminants from reacting with the liquid metal and the liquid metal from escaping. However, rotating seals, for large diameter high speed machines that are also compatible with candidate fluids are not technically feasible at this time.

Other current collection techniques which employ a batch process without adequate sealing must overcome severe obstacles for long term operation. These include:

- Loss of fluid through aerosol and droplet migration.
- Oxide and reaction product buildup due to contaminants reacting with the fluid.
- Compositional changes because of selective oxidation.
- Flow instability because of inadequate supply during some operating conditions.

The most practical method for overcoming these obstacles is through the use of a recirculating system. Such a system was selected to service the Westinghouse 3000 Horsepower Prototype Homopolar Generator (SEGMAG). Figure 5.7 schematically presents a loop design to service each of the six SEGMAG current collectors. Eutectic NaK, the SEGMAG current transfer fluid, is circulated by a centrifugal pump through a high resolution electromagnetic flowmeter, through a water cooled cold trap, and into the current collector annulus. Drain channels collect NaK overflow from the current collector and return it to the sump tank and back to the pump inlet. Gravity drainage of the NaK to the sump tank is assisted by a recirculating gas system. Original design plans considered one large NaK loop with six parallel feed-drain legs for current collection fluid circulation. Problems were apparent when the I^2R losses were considered for common NaK current collection lines. Losses of over 40 kW were predicted. A technique of breaking the NaK flow through insulated connections and utilizing one NaK loop demonstrated that electrical isolation of the current collectors could be maintained. However, verification of this novel NaK recirculation technique for extended, unmanned operation was considered too time consuming to contract schedules, and the more secure, individual loop approach was followed.

Each NaK loop was designed to service one current collector and was completely isolated electrically from other loops and ground. The sump tank contains approximately two liters of eutectic NaK which is sufficient to maintain long term compositional stability and replace that which may be lost by aerosol formation and fling-out. Level probes in the sump tank indicate whether NaK levels are becoming unacceptably high or low. The sump tank also provides the first stage

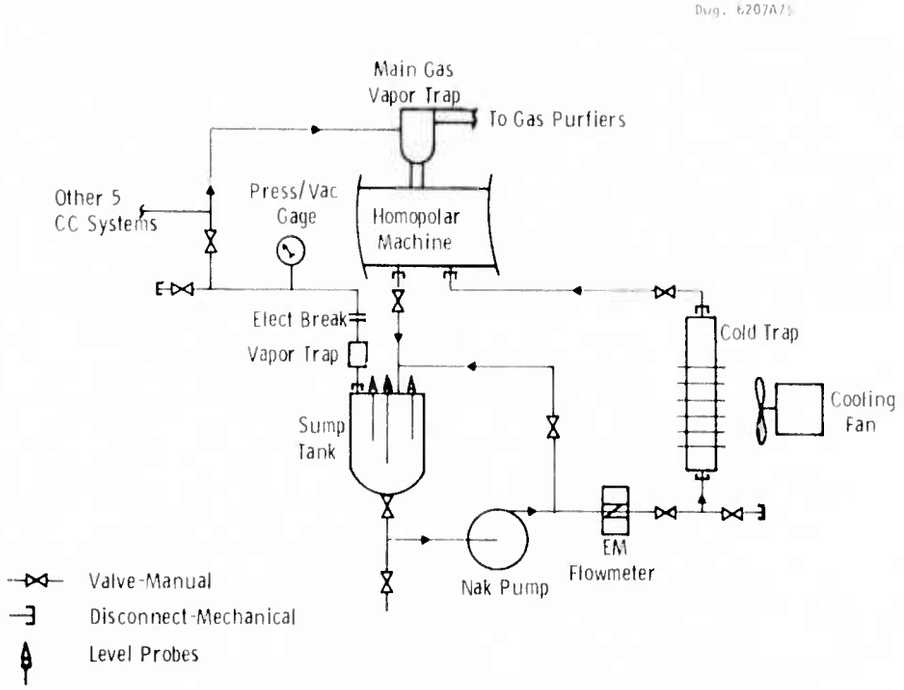

5.7: Small NaK loop concept for servicing each current collector independently

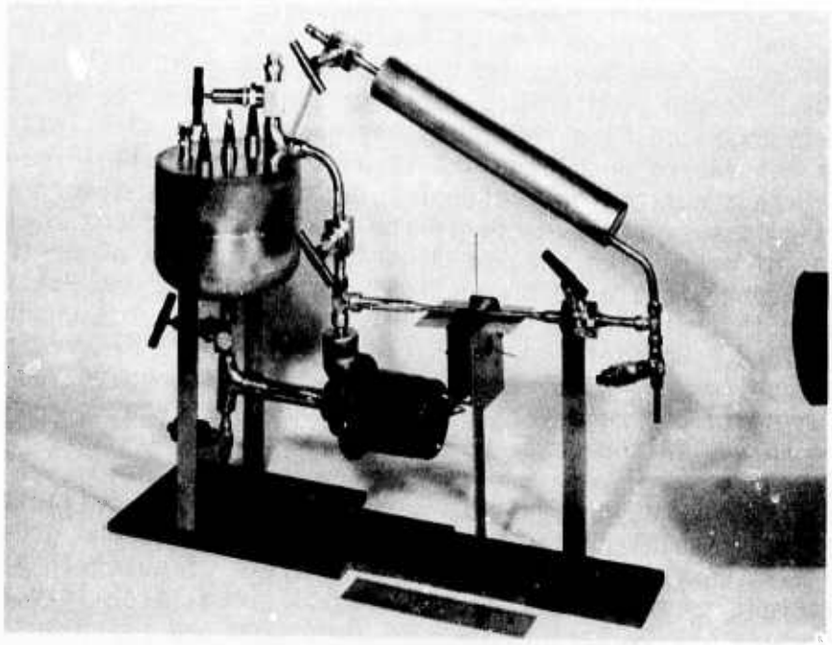

Fig. 5.8: Assembled NaK loop for current collector service in prototype SEGMAG machine

of NaK purification where by insoluble or precipitating oxides and impurities float to the surface of the NaK pool.

In the loop, the NaK flows from the flowmeter up through a cold trap, which removes soluble impurities and oxides by a precipitation process and particulates by a filtering process, before returning NaK to the current collector. Figure 5.8 presents one of the SEGMAG NaK loops; components can be identified from Fig. 5.7. The loops are of type 304 stainless steel, and consist of all welded, inspected construction, employing liquid metal bellows seal valves. Loop capabilities are presented in Table 5.5. As demonstrated in Fig. 5.9 the six NaK loops are placed beneath the SEGMAG unit.

The NaK pump was selected after evaluating electromagnetic (EM), gear, bellows, and centrifugal pumps. It is a canned rotor, inductively coupled, centrifugal pump and was qualified for over 1000 hours in NaK prior to its selection. The flowmeter is electromagnetic, and was designed by Westinghouse for low temperature low flowrate NaK service. A calibration curve presented in Fig. 5.10 demonstrates the meter's accuracy to ± 5 cc/min in the 0-800 cc/min range. The NaK system proved to be entirely satisfactory for SEGMAG operation. Each of the six loops operated for hundreds of hours without major problems, and a prototype loop has operated for more than 9000 hours continuous operation.

Recent work with one loop systems to service multiple current collection sites has been performed. Multiple current collector homopolar machines equipped with common liquid metal recirculating or supply systems are faced with the problem of electrical short circuits through the liquid metal. Electrically isolating each current collector with an independent liquid metal system is a viable solution for machines with six or less collectors but is not feasible for machines with a large number of collectors.

Electrical losses of several kilowatts can be expected from low voltage machines (<100 V) and typical $\frac{1}{4}$" feed lines. The problem is compounded by the necessity to cool these liquid metal lines to prevent overheating and possible line failure. Also complicating the problem is the different requirement for current collector inlet flow compared with outlet flow. Inlet flow is clean purified liquid metal under controlled pressure and flowrate conditions, while outlet flow may be sporadic, contaminated, and drained by gravity. For these reasons, techniques for electrically isolating a flowing liquid metal stream were investigated and were found to vary in approach for inlet and outlet lines. Two general approaches may be used in electrically isolating multicollectors from a common supply. One method is to increase the resistance of the NaK line to the extent that losses are no longer a problem. The other method is to physically separate the liquid metal with an insulating material such as gas as it flows into a tank or insulated pipe section.

TABLE 5.5 - NaK Loop Capabilities

1.	Temperature:	Max. 250°C loop, 150°C pump Min. 0°C loop and pump
2.	Flowrate:	0-800 cc/min
3.	Inventory:	Sump tank volume - 2700 cc NaK charge in system - 2000 cc Total working Nak - 850 cc
4.	Physical size:	Each loop 2' x 2' x 7" wide Six loops fit into 2' x 2' x 3' long
5.	Pressure:	Max. 50 psig loop, 15 psig pump Min. high vacuum loop, 0 psig pump
6.	Material:	All 304 s/s or 316 s/s Valves - Metal bellows seal welded All welded, inspected construction
7.	Purity control:	Two stages First stage - Sump tank, oxides float Second stage - Cold trap, filter
8.	Level control:	Sump tank - Three electrical continuity probes

The first method can be accomplished by making the liquid metal line small in diameter and long in length. For example, a 304 stainless steel tube 1/8 OD x .028 wall 100 ft. long filled with NaK 78 at 100°C has a total resistance of approximately 2.3 ohms. This resistance is reasonable and would result in a power loss of approximately 10 kw based upon a 20 collector, 100 V, 20,000 horsepower machine with one line to each collector. Several problem areas would have to be investigated before utilizing this technique. These include:

- Susceptibility of the line to plugging
- Heat buildup as a function of current and NaK flow
- Pressure drop as a function of NaK flow
- Arrangement of (20) 100 ft long tubes on the machine

This method would only be applicable to the inlet flow which would be clean liquid metal at controlled pressure and flow conditions. The other approach, physically separating the flowing liquid metal, can be accomplished by various techniques. One technique utilizes receiver tanks with a liquid/gas interface for each collector and is illustrated

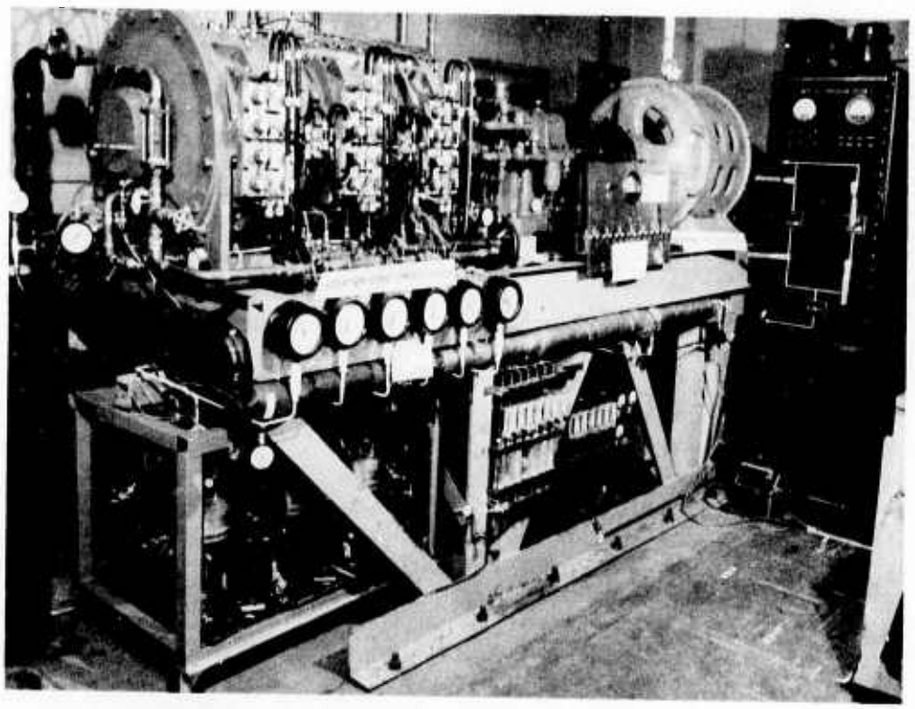

Fig. 5.9: 3000 HP Segmented Magnet Homopolar Generator (SEGMAG) on test bed. The NaK loops are located below the SEGMAG and the diagnostic dials. The gas systems are to the lower right and far right of the test bed.

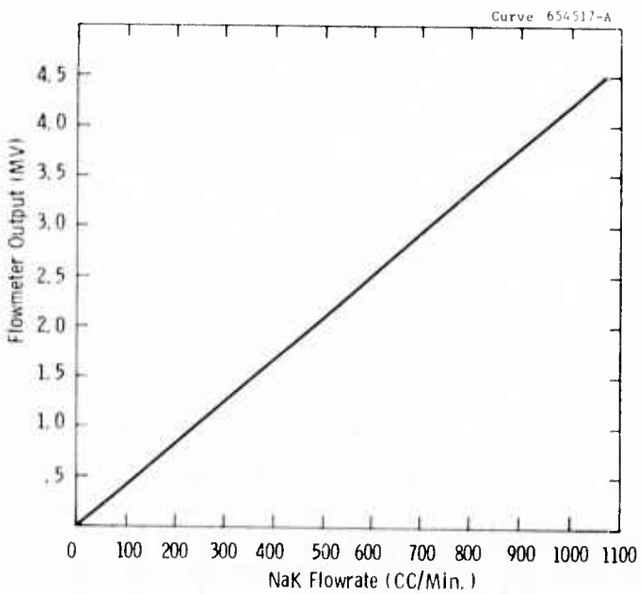

Fig. 5.10: Calibration of NaK flowmeter.

in Fig. 5.11. Level probes in the supply tank would automatically maintain the correct liquid level by actuating a solenoid valve to fill the supply tank and at the same time empty the drain tank. A logic system would prevent more than one current collector being connected to the common header at one time. This system should operate well in the short term, however over the long term it would probably be unreliable because of the large number of valve operations required.

Another technique (Fig. 5.12) relies on a bubble of gas injected into the liquid metal stream to separate the liquid into slugs as it flows through an insulated pipe section. This method has been proven in small scale laboratory operations, but long term trouble free operation has yet to be demonstrated. Also the problem of removing the gas before it enters the current collector would have to be solved.

Figures 5.13, 5.14, 5.15 represent other techniques for breaking the liquid metal into electrically isolated slugs or drops. Each has merit but has to be proven experimentally and judged against the following desirable qualities:

- Workability
- Reliability
- Simplicity
- Long Life
- Cleanliness (non-contaminating)
- Predictability

Work is continuing in this area toward developing a method with the above qualities that can be proven for both the inlet flow and the outlet flow.

5.2.3 Cover Gas Systems

An automated cover gas handling system was fabricated for the demonstration SEGMAG machine. The gas system consisted of three subsystems: 1) Main gas recirculation and purification unit; 2) Gas pump and supply for tandem gas circumferential seals; and 3) Intercollector gas system. These are illustrated in the schematic in Fig. 5.16.

The main gas recirculation and purification system consists of a commercial unit which Westinghouse designed and contains tandem (parallel) towers of Dow resin and molecular sieve materials. Dry nitrogen is thus circulated through the machine, and through one tower at a time. The tower removes oxygen and moisture to levels of 1 ppm and below. Refrigerant-cooled heat exchangers were added to remove condensible vapors (NaK vapor, organic compounds) that could leave the machine and affect the active resins. One tower may be automatically regenerated

Dwg. 6355A18

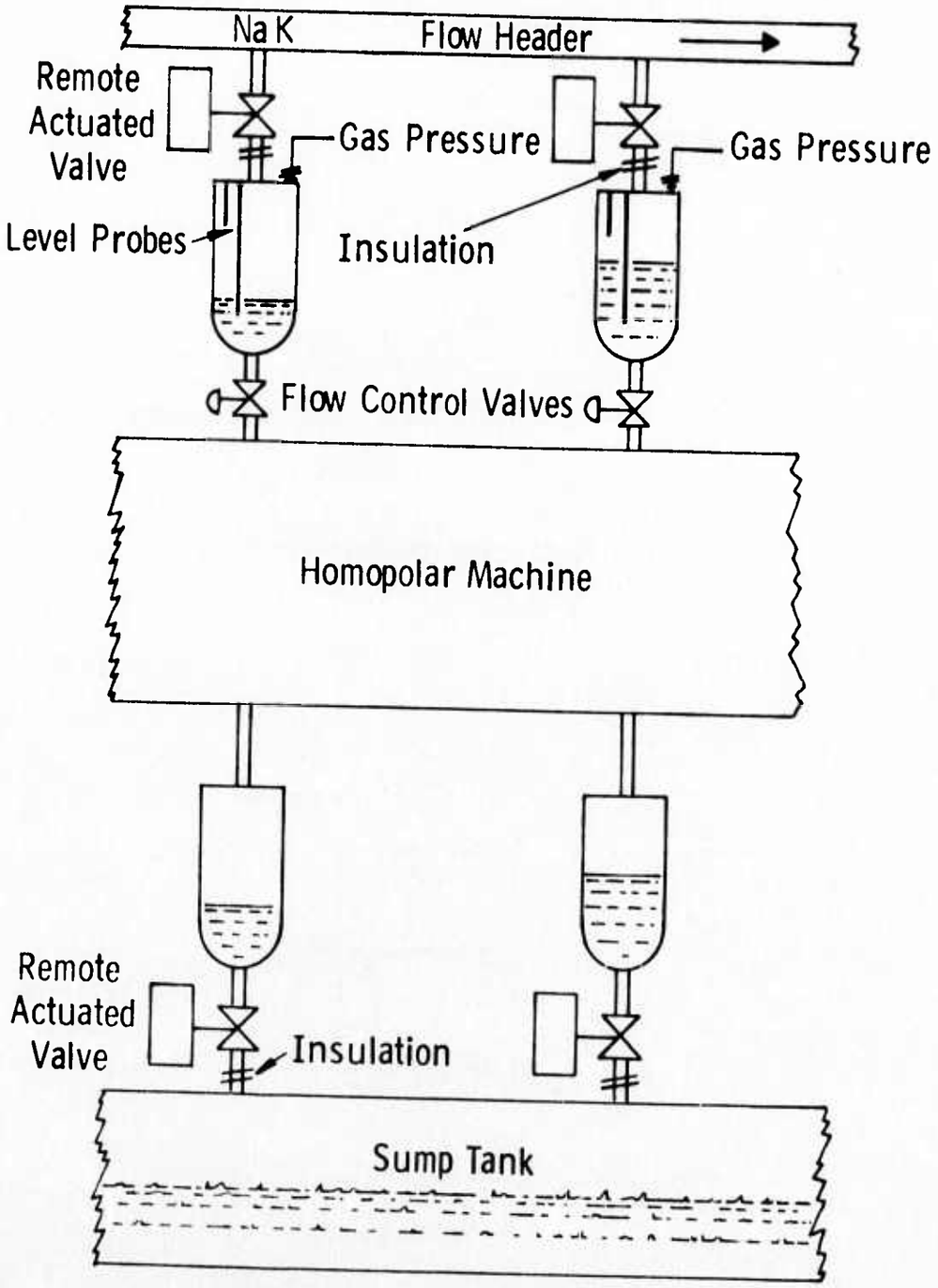

Fig. 5.11: Valve and tank system

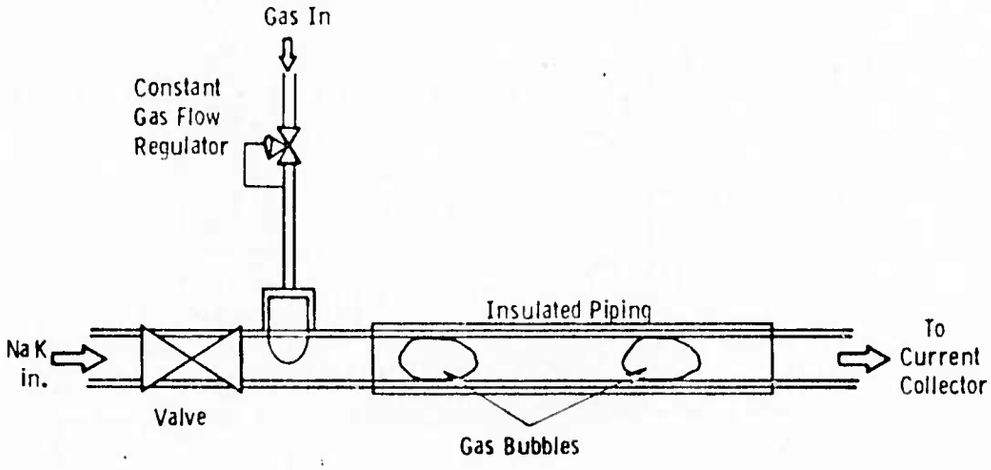

Fig. 5.12: Gas bubble injection

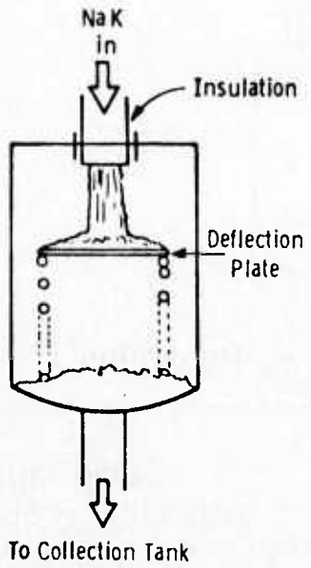

Fig. 5.13: Splash plate technique

Dwg. 6355A19

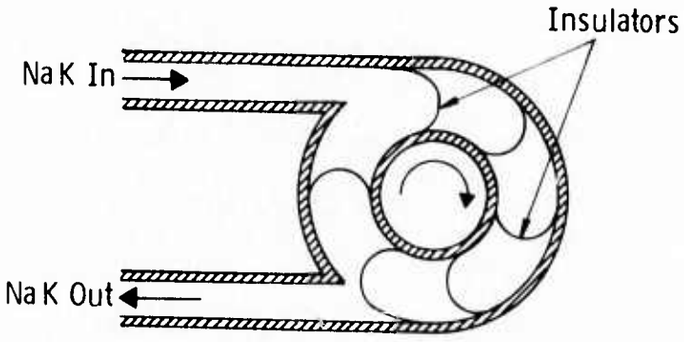

Fig. 5.14: Rotating vane isolator

Dwg. 6355A17

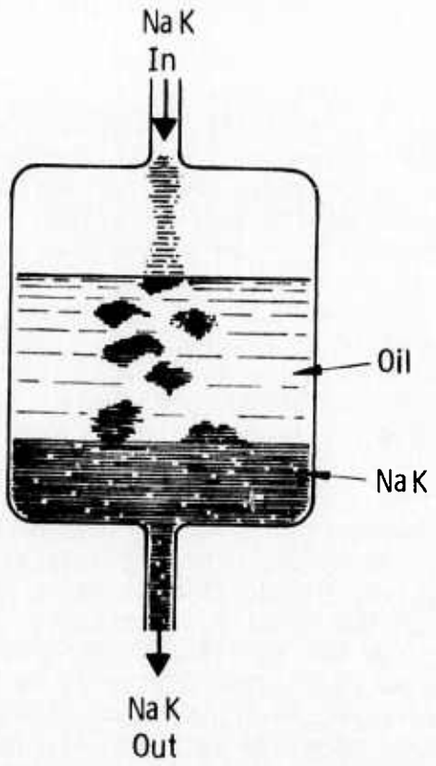

Fig. 5.15: Oil insulator technique

while the other is on-line. Flowmeters and control valves balance the flow and circulation of dry nitrogen through the machine housing. The pressure is maintained at 4 psig and high and low pressure alarm interlocks are provided. A continuous sample of gas is drawn and sampled for oxygen and moisture purity, and a trace recorder is employed to indicate oxygen levels. An alarm interlock is provided for the detection of oxygen levels above 10 ppm (V). Cover gas can be circulated through the system at 0 to 35 SCFM. Experimental operation of this unit with the SEGMAG showed it to perform better than expected, and to maintain machine cover gas purities at 1 ppm (V) for oxygen and even better for moisture during machine temperature excursions reaching 90-115°C. Thus the NaK inside the machine was not subject to oxidation and oxide formation problems.

A second gas system operates from the main gas system to distribute the nitrogen. A mechanical, bellows pump is employed to extract gas from the main gas system recirculation lines and to raise the pressure to 5-7 psig for insertion into the tandem circumferential shaft seals. Dry nitrogen is thus supplied to the seals at 1-2 SCFH. Half of the gas is lost to the environment, half returns to the machine housing for recirculation and purification. A gas pressure controller automatically supplied cover gas makeup for losses, as well as maintaining system pressure.

A third gas system, also illustrated in Fig. 5.16, called the intercollector gas system, is employed. A mechanical, bellows gas pump is employed to pull cover gas down the NaK drains of each current collector (gravity drains to a sump tank) and thus assist drainage. This gas is removed from each loop at the sump tank (the void space above the NaK level), drawn through a vapor trap, and then forced by the gas pump through six flowmeters, and reinjected into the intercollector gas gaps between the rotor and stator. Once in the gas gap, the gas divides and flows into the adjacent current collectors, sweeping aerosol and NaK vapor. The gas then exits via the NaK drains and repeats the cycle. Contaminants which enter the gas are removed by reaction with the NaK, the reaction products floating on the NaK surface in the sump tank.

Trial operation of the cover gas system, first with the glove box (100 CF), and subsequently with the SEGMAG machine (less than 1 CF), have confirmed its operation. For the initial startup, a roughing pump vacuum was applied to the machine while it was heated to 70-80°C. Following removal of the volatiles, moisture, etc., in this fashion, a dry nitrogen gas purge was initiated. Monitoring of the effluent purge gas for oxygen and moisture showed both to be below 100 ppm (V), and the main cover gas recirculation system was started. This system operated continuously once the machine was clean of oxygen and moisture. The shaft seal system was activated only prior to and during rotation. The intercollector gas network was only active during NaK circulation through the machine. The on-line oxygen and moisture monitors operated continuously.

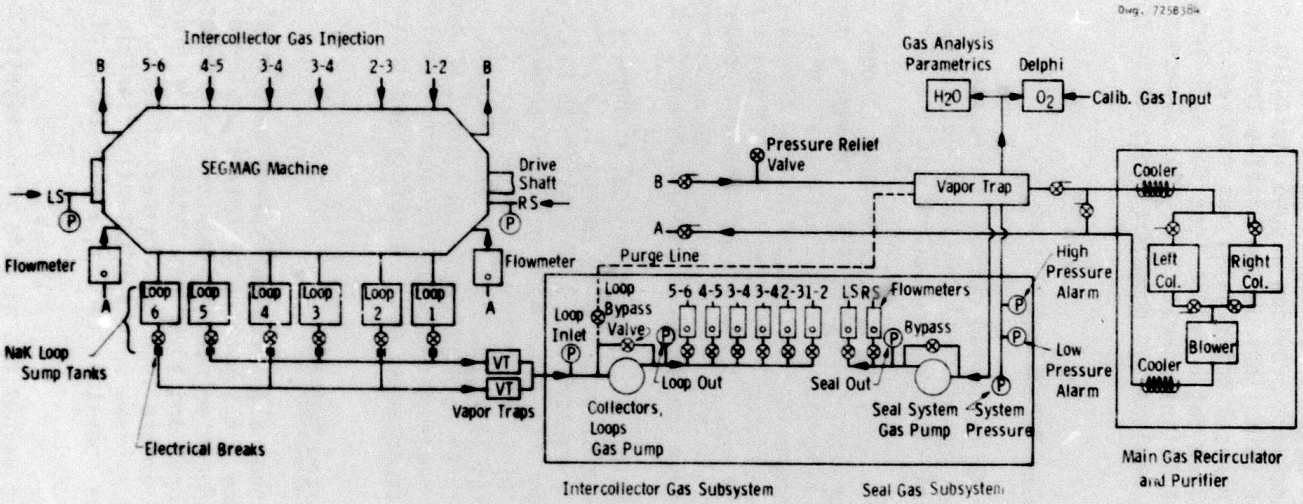

Fig. 5.16: SEGMAG cover gas systems

A fourth cover gas system, not illustrated in Fig. 5.16, provided an auxiliary blow-down network for NaK which collected between current collectors. This network provided a good indication of collector performance (i.e., NaK retention) during machine transient conditions. NaK, lost to the intercollector gaps, was removed from the machine and collected in graduated catch basins (one for each intercollector zone). Continuous or intermittant operation of this blowdown network could be selected, and a bellows gas pump was provided to assist lost NaK removal.

5.2.4 Gallium-Indium Technology

Although NaK_{78} is the preferred current collection fluid for constant, high speed machines (generators), eutectic Gallium-Indium, 14.2-16.5 at % Indium,[6,7] may be the more suitable fluid for slow, variable speed machines (motors). The primary reasons being: (1) eutectic Gallium-Indium is inherently easy to handle, because it does not react violently with water vapor or oxygen as does NaK_{78} (however, care must be exercised because of its toxicity[8]); (2) it has a higher density[9] than NaK_{78}, it is therefore less influenced by MHD forces; (3) it is easily purified by simple electrolysis[10]; and, (4) it has a higher electrical conductivity than NaK_{78}.[11] Thus, since viscous losses are less important in low speed machines than in high speed machines, eutectic Gallium-Indium may be the more desirable current collection fluid.

In an effort to aid the electro-mechanical engineers in designing homopolar machines that will employ eutectic Gallium-Indium as a current collection fluid, a machine designer's guide to Gallium-Indium technology is being prepared. This guide is intended to cover the following aspects of Gallium-Indium technology: (1) physical and chemical properties; (2) compatibility with organic, inorganic, and structural metals; (3) machine degass and start-up procedures; (4) decontamination and clean-up schemes; (5) current collector wetting; (6) purification techniques; and (7) safety and toxicity.

5.2.5 Support System Summary

As can be envisioned, all three subsystems were vital to successful machine performance. All machine materials employed were compatible with NaK and NaK decontamination products and processes. The materials, NaK loops, and cover gas systems all interacted in a viable fashion to ensure long term operation of the machine. The NaK and cover gas systems were sufficiently flexible to allow fine tuning the machine operation through a wide range of performance testing.

The following conclusions can be made with respect to the homopolar machine liquid metal support systems. Long term homopolar machine

operation will require a design incorporating: (1) selection of proven NaK compatible materials; (2) a liquid metal recirculation and purification system; (3) a cover gas network which can remove degas as well as inleakage contaminants to provide for clean NaK environments. The materials selected by this study have exhibited NaK compatibility, and show trends for continued long term compatibility. The NaK recirculation and purification loop (prototype) now has over 9000 hours continuous operation with various contamination levels of cover gas. The cover gas system is a modified commercial unit which has typically operated many months without maintenance.

5.3 REFERENCES

1. O. J. Foust, Ed., Sodium-NaK Engineering Handbook, Gordon and Breach, Science Publishers, Inc., New York, 1972.

2. MSA Research Corporation Technical Bulletin, NaK and Potassium, Bull. No. MD-70-1, MSA Research Corporation, Evans City, PA 16033.

3. C. G. Allan and J. L. Drummond, The Reaction of PTFE with Liquid Sodium, Potassium, and NaK Alloy, TRG Report 2104(D), National Technical Information Service, Springfield, VA 22151, 1970.

4. MSA Research Corporation Publication, Introduction to NaK and BZ Alloys, MSA Research Corporation, Evans City, PA 16033.

5. C. B. Jackson, Ed., Liquid Metals Handbook, Sodium (NaK) Supplement, July, 1955.

6. Hayes, F. H., and O. Kubaschewski, "A Reassessment of the System Indium-Gallium," Journal of the Institute of Metals, 97, 381-383, (1969).

7. Svirbely, W. J., and S. M. Selis, "The Gallium-Indium System," J. Phys. Chem., 58, 33-35, (1954).

8. Sax, N. I., Dangerous Properties of Industrial Materials, third edition, Van Nostrand Reinhold Company, New York (1968).

9. Suzuki, K., and O. Uemura, "Knight Shift, Magnet Susceptability and Electrical Resistivity of Pure Gallium and Gallium-Indium Eutectic Alloy in the Normal and the Supercooled Liquid State," J. Phys. Chem. Solids, 32, 1801-1810, (1971).

10. Walkden, A. J., British Patent 1317478, (1971).

11. Zrnic, D., and D. S. Swatik, "On the Resistivity and Surface Tension of the Eutectic Alloy of Gallium and Indium," J. of the Less - Common Metals, 18, 67-68 (1969).

SECTION 6

SEAL STUDY

6.0 OBJECTIVES

A study of the sealing problems between the liquid metal, bearing oil system, and the environment shall be conducted. Seal system designs will be evolved for both the SEGMAG and SMHTC machines.

There are two subtasks to the seal study:

1) Confinement of liquid metal to the current collection zone. This work is reported in Section 4, "Current Collection Systems".

2) Development of the seal systems for the primary rotor shafts of the homopolar machines. This work is reported in Section 6, "Seal Study".

During Phase I of this program, our objectives were, 1) to review the state-of-the-art of seal technology as applicable to homopolar machines, 2) design a test apparatus capable of evaluating the performance of various seal concepts under operating conditions anticipated in homopolar machine applications.

During Phase II our objective was to develop a shaft seal system for homopolar generator applications, where the mode of operation is both unidirectional and continuous. In particular, the goal was a shaft seal for the SEGMAG generator.

In Phase III, the seal technology is to be extended to, 1) torque converter and motor applications where reversible and variable speeds are encountered , and 2) unidirectional high speed (96 m/s collector speed) generators.

6.1 PRIOR AND RELATED WORK

Studies performed during Phase I indicated that a tandem circumferential seal, or bore seal, was the prime candidate for satisfying the requirements imposed on the primary rotor shaft. The circumferential seal not only exhibits the ability to withstand high velocity rubbing at its primary sealing surfaces, but also the ability to provide a high degree of sealing effectiveness. Its design conserves weight and space, provides virtually unlimited shaft travel, and is easily assembled. Figure 6.1 is a schematic of this seal type.

With regard to material selection for use in these seals, care was exercised to insure that the self-lubricating composite employed retains its lubricating ability in a no-moisture, inert gas environment. Standard grades of carbon-graphite seal materials exhibit extremely poor

friction-wear characteristics in dry argon. Face seal screening tests on candidate seal materials for use in the primary rotor shaft seals of homopolar machines indicated that two polyimide matrix composites exhibit satisfactory friction-wear characteristics in the inert, no-moisture environment required for these machines. The composites contain solid lubricants, such as molybdenum disulphide, Teflon, and graphite, as fillers. Both materials were also found to be compatible with NaK at a temperature of 108°C. Seal segments suitable for use in tandem circumferential seals were fabricated from these materials.

A seal test stand was designed and constructed. Through the use of a 2:1 pulley ratio, the test stand is capable of performing experiments on various seal configurations over a 7000 rpm speed range in inert, bone-dry environments. Leakage rates, operating speed, and seal and bearing temperatures are continuously monitored. The test stand is capable of evaluating seals for shafts ranging in diameters from 2 to 6 inches.

Tandem circumferential seals were purchased for functional testing purposes as well as for use on the SEGMAG machine. Testing results on these units indicated that seal leak rates can be held to 0.02 cfm or less and that the use of carbon-graphite seal materials in these units is unsatisfactory when they are applied in dry, inert gas environments.

The test program for functional seal testing consisted of three phases:

1) Candidate seal materials were evaluated with regard to their ability to operate effectively in an inert, no-moisture environment.

2) Concurrently, these materials were evaluated with respect to their compatibility with NaK at room temperature and, where appropriate, at elevated temperature.

3) Finally, the most promising materials were fabricated into actual seals and tested extensively with respect to operating speed, runner design and material, and load pressure. The results were compared against those obtained on units employing standard carbon-graphite materials. Parameters monitored during these tests included seal wear, leakage, and operating temperature.

All face seal screening tests on candidate seal materials were completed and the results were previously reported. NaK compatibility studies on these materials were also completed and reported.

Three functional tests were performed on tandem circumferential seals designed by the Stein Seal Company. The first two experiments were performed on seals equipped with USG-67 carbon-graphite segments in

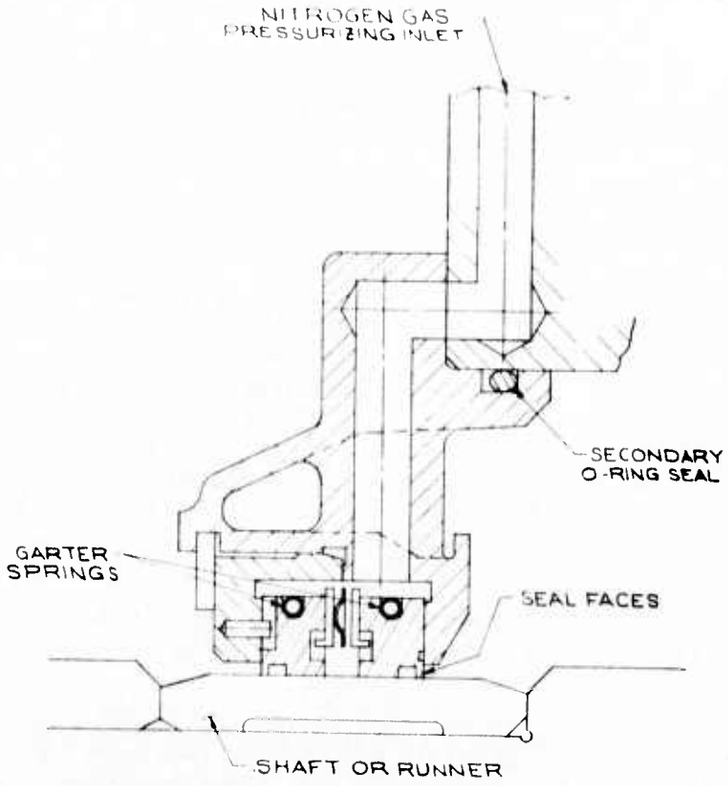

Fig. 6.1: Schematic of typical tandem circumferential seal

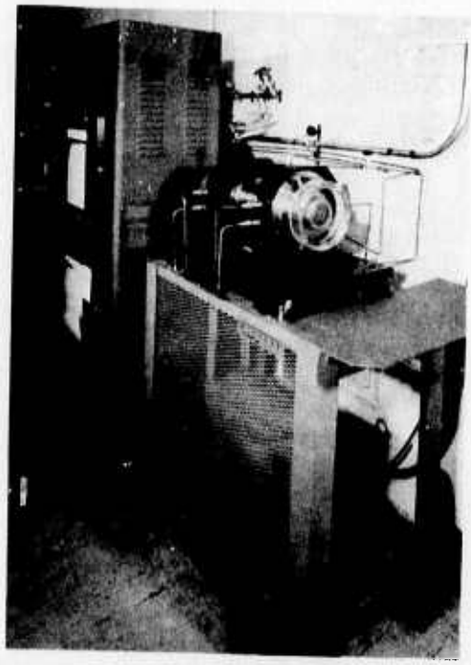

Fig. 6.2: Tandem circumferential seal test rig

order to obtain bench mark performance data on standard seal designs. The third experiment was performed on a seal of identical design but equipped with segments fabricated from Vespel SP-211.

The first two seal tests resulted in excessive wear of the seals after 25 hours of operation in the test rig. Figure 6.2 shows this test rig.

The final test performed during this period utilized a Stein circumferential seal equipped with segments fabricated from the Vespel SP-211 polyimide-matrix composite. After an initial run-in of 10 hours, the seal was thoroughly inspected, reassembled, and then operated at 3600 rpm while being fed dry nitrogen (dew pt < - 45°C) at a feed pressure of 5 psig. A total, accumulated life of 800 hours was achieved on this seal with no segment dusting or significant wear, and with measured leak rates of 0.005 to 0.01 cfm. This seal was then inspected, reassembled and stored as a spare for SEGMAG.

The SEGMAG seals were assembled and tested for 150 hours to insure performance similar to the endurance test units.

Seal performance of the SEGMAG shaft seals was monitored during the test program. The seal leakage measured during SEGMAG operation was similar to that measured during the seal run-in period. The seals were not disassembled during SEGMAG rework since there was no evidence of damage during the test program.

A state-of-the-art review has been initiated to evaluate potential reversing seal concepts for the SMHTC shaft seals. The seals used on the SEGMAG generator are essentially a unidirectional design. The shaft seal for the SMHTC motor shaft will be designed for low leakage and wear at operating speeds from zero to 500 rpm in either direction.

6.2 CURRENT PROGRESS

No work was scheduled for this reporting period.